

614977394

**Design of Air Cushion Vehicles Using Artificial Intelligence:  
Expert System and Genetic Algorithm**

by

Tae-Cheol Jung, B.Eng

Ryerson University

Toronto, 2002

A thesis

presented to Ryerson University

in partial fulfillment of the

requirements for the degree of

Master of Applied Science

in the program of

Mechanical Engineering

Toronto, Ontario, Canada, 2003

©Tae-Cheol Jung 2003

PROPERTY OF  
RYERSON UNIVERSITY LIBRARY

UMI Number: EC53446

### INFORMATION TO USERS

The quality of this reproduction is dependent upon the quality of the copy submitted. Broken or indistinct print, colored or poor quality illustrations and photographs, print bleed-through, substandard margins, and improper alignment can adversely affect reproduction.

In the unlikely event that the author did not send a complete manuscript and there are missing pages, these will be noted. Also, if unauthorized copyright material had to be removed, a note will indicate the deletion.

UMI<sup>®</sup>

---

UMI Microform EC53446  
Copyright 2009 by ProQuest LLC  
All rights reserved. This microform edition is protected against  
unauthorized copying under Title 17, United States Code.

---

ProQuest LLC  
789 East Eisenhower Parkway  
P.O. Box 1346  
Ann Arbor, MI 48106-1346

## **AUTHOR'S DECLARATION**

I hereby declare that I am the sole author of this thesis.

I authorize Ryerson University to lend this thesis to other institutions or individuals for the purpose of scholarly research.

I further authorize Ryerson University to reproduce this thesis by photocopying or by other means, in total or in part, at the request of other institutions or individuals for the purpose of scholarly research.

## **BORROWER'S PAGE**

Ryerson University requires the signatures of all persons using or photocopying this thesis. Please sign below, and give address and date.

## ABSTRACT

In the thesis, initial design of an Air Cushion Vehicle (ACV) is performed with the expert system and its skirt system is further optimized with the genetic algorithm. Both the expert system and genetic algorithm are advanced computerized design techniques of artificial intelligence. Those techniques are specifically developed for the ACVs with programming codes in this thesis. Then the main objective is to show the successful implementation of those techniques in the design of ACVs.

The thesis work is divided into two parts. In the first part, the general configuration of ACVs, including the overall dimensions, weight distribution, parametric properties, and several subsystems, is studied and designed by the expert system as an initial design phase. In the second part of the thesis, the skirt system of ACVs is further optimized. In particular, the properties of the bag and finger skirt are optimized for improved ride quality and stability by the genetic algorithm. For the validation of these two artificial intelligence techniques, the CCG (Canadian Coast Guard) 37 ton Waban-Aki and U.S. Navy's 150 ton LCAC (Landing Craft Air Cushion) are selected for the tests. The results of the tests proved that the expert system was successfully implemented and was a powerful tool for the initial design of ACVs. Furthermore, the genetic algorithm optimized the skirt system with significantly improved ride quality and stability. It was also shown that the skirt mass was an important design factor in the heave response of the bag and finger skirt. Hence, this thesis work opened the new possibility of designing ACVs with artificial intelligence techniques.

## ACKNOWLEDGEMENTS

The author would like to acknowledge Dr. Joon Chung for his constant help and guidance. He is the one who introduced the interesting and fascinating topic to the author and furthermore showed generosity for the use of his valuable literatures and resources. Without his great advice and intuition, this thesis would not be successful.

The author also would like to thank professors in Ryerson University. Valuable lessons and insight about the mechanical system and its control could be achieved through their lectures. Moreover when the author faced difficulty understanding and analyzing thesis work, they provided assistance without any hesitation. Their great support was greatly appreciated.

Finally, my family and friends have provided a constant encouragement and inspiration whenever the author was experiencing a difficult time. They deserve my gratitude without any doubt.

# TABLE OF CONTENTS

Author's declaration	ii
Borrower's page	iii
Abstract	iv
Acknowledgements	v
Table of Contents	vi
List of Tables	ix
List of Figures	x
Nomenclature	xiii
<b>1. INTRODUCTION</b>	<b>1</b>
1.1 Background of Air Cushion Vehicle	1
1.2 Background of Expert System	7
1.3 Background of Genetic Algorithm	11
1.4 Objectives	16
<b>2. INITIAL DESIGN OF ACVs WITH EXPERT SYSTEM</b>	<b>19</b>
2.1 Overview of Initial Design Process	19
2.2 Code Development for Expert System with MATLAB	22
2.3 Implementation of Expert System	25
2.4 Input Parameters	31
2.5 Determination of Principal Dimensions	33

2.6 Main Subsystem Design	41
2.7 Tests of Expert System	48
2.8 Discussion and Recommendation	52
<b>3. OPTIMIZATION OF SKIRT SYSTEM WITH GA</b>	<b>54</b>
3.1 Overview of Skirt Optimization with GA	54
3.2 Code Development for GA and Skirt System with MATLAB	57
3.3 Model of the Bag and Finger Skirt	61
3.4 The Linearized Equations of Motion	69
3.5 Parameter Estimation	74
3.6 Implementation of GA	77
3.7 Results of Experiments	89
3.7.1 Optimization of Waban-Aki Skirt	89
3.7.2 Optimization of LCAC Skirt	94
3.7.3 Effect of various skirt masses on optimization	98
<b>4. CONCLUSIONS</b>	<b>103</b>
<b>REFERENCES</b>	<b>106</b>
APPENDIX A. Codes for Linearized Equations of Motion of a Bag and Finger Skirt System	112
APPENDIX B. Codes for Parameter Estimation	118

APPENDIX C. Codes for Genetic Algorithm	123
APPENDIX D. Codes for Expert System	135
APPENDIX E. CCG WABAN-AKI	143
APPENDIX F. LCAC	144

## LIST OF TABLES

2.1 Sample data set for ACVs	33
2.2 Weight distribution of ACVs in SWBS	35
2.3 Results of expert system on Waban-Aki	48
2.4 Results of expert system on LCAC	49
3.1 Sample individual with binary coding	78
3.2 Parameters used in the GA on skirt optimization problem	88
3.3 Properties of the original and optimized skirt system in Waban-Aki	90
3.4 Properties of the original and optimized skirt system in LCAC	96
3.5 Second peak magnitude and percentage of reduction for each system	102

## LIST OF FIGURES

1.1 Development of skirts in ACV	2
1.2 Basic concept of the bag and finger skirt	3
1.3 Elements of the bag and finger skirt	4
1.4 Structures of the finger element	5
1.5 Structure of expert system	10
1.6 Infeasible region in the search space	12
1.7 Multiple local optimums	13
1.8 Flow chart of simple genetic algorithm	15
2.1 Initial design process for ACVs	20
2.2 Expert system for initial design of ACVs	21
2.3 Flow chart of program codes for expert system	24
2.4 Forward-chaining and backward-chaining mechanisms	26
2.5 Rule-based knowledge representation	27
2.6 Frame-based knowledge representation	28
2.7 General procedure for knowledge acquisition	29
2.8 Input parameters on expert system	32
2.9 Approximated curve in the relation of craft's weight and length	34
2.10 Approximated curve in the relation of craft's weight and width	34
2.11 Approximated curve in the relation of craft's weight and total power	39
2.12 Design progress with determination of principal dimensions	40
2.13 Lift fan selection process	44

2.14 Design progress with main subsystem design	47
3.1 Design restrictions for ACVs	54
3.2 Design parameters to be optimized	55
3.3 Overall process of the GA on skirt optimization	56
3.4 Flow chart of program codes for the GA and skirt system	60
3.5 Two dimensional section of the bag and finger skirt	62
3.6 Parameters used for the skirt geometry	65
3.7 Parameters used for the finger geometry	65
3.8 Parameter estimation	76
3.9 Frequency response curve for original skirt system	79
3.10 Constraint conditions in penalty function	81
3.11 Single point crossover	83
3.12 Two point crossover	84
3.13 Random crossover	85
3.14 Single bit mutation	86
3.15 Two bit mutation	87
3.16 Overall performance of the GA on Waban-Aki skirt optimization	89
3.17 Frequency response curves for the original and optimized skirts of Waban-Aki	93
3.18 Phase shift curves for the original and optimized skirts of Waban-Aki	93
3.19 Physical shapes of the original and optimized skirts of Waban-Aki	94
3.20 Overall performance of the GA on LCAC skirt optimization	95
3.21 Frequency response curves for the original and optimized skirts of LCAC	97

3.22 Phase shift curves for the original and optimized skirts of LCAC	97
3.23 Physical shapes of the original and optimized skirts of LCAC	98
3.24 Frequency response curves for different skirt mass condition on Waban-Aki	99
3.25 Phase shift curves for different skirt mass condition on Waban-Aki	100
3.26 Frequency response curves for different skirt mass condition on LCAC	100
3.27 Phase shift curves for different skirt mass condition on LCAC	101

## NOMENCLATURE

$A$	System dynamic matrix
$A_b$	Effective area of bag to cushion feed hole orifices, $m^2$
$B$	System input matrix
$B_b$	Width of the vehicle base, m
$B_c$	Width of the cushion footprint, m
$B_f$	Finger width, m
$b$	Inner bag chord length, m
$C$	System output matrix
$c$	Outer bag chord length, m
$C_b$	Pneumatic capacitance of bag volume
$C_c$	Pneumatic capacitance of cushion volume
$D$	Fan maximum diameter, m
$D_b$	Length defining craft base geometry, m
$D_s$	Specific diameter of fan
$g$	Gravitational acceleration, $m/s^2$
$H_b$	Length defining craft base geometry, m
$H_f$	Total pressure rise across fan, Pa
$h_c$	Height of craft base, m
$h_e$	Hover gap, distance from the ground to the finger tips, m
$h_f$	Effective cushion leak height, m
$h_g$	Height of ground measure from datum, m

$h_s$	Height of skirt, m
$I_s$	Moment of inertia about center of skirt mass, $\text{kg}\cdot\text{m}^2$
$L_1, L_2, L_3, L_4$	Lengths defining geometry of finger and inner bag, m
$L_b$	Length of vehicle base, m
$L_c$	Length of cushion footprint, m
$L_D$	Length defining craft base geometry, m
$L_M$	Distance from center of mass of the skirt to inner bag joint, m
$L_m$	Length of model, m
$L_{ob}$	Length of outer bag, m
$L_p$	Total peripheral length of skirt, m
$M_c$	Total mass of craft including skirt, kg
$M_s$	Mass of skirt, kg
$N_s$	Specific speed of fan
$n$	Fan rotational speed, rpm
$P$	Total power, kW
$p_b$	Bag pressure, Pa
$p_c$	Cushion pressure, Pa
$Q$	Flow rate, $\text{m}^3/\text{s}$
$Q_a$	Volume flow from cushion to atmosphere, $\text{m}^3/\text{s}$
$Q_b$	Volume flow from fan to bag, $\text{m}^3/\text{s}$
$Q_c$	Volume flow from bag to cushion, $\text{m}^3/\text{s}$
$Q_i^{NC}$	Non conservative forces acting on skirt due to bag and cushion pressures

$q_i$	Generalized coordinates
$S_c$	Cushion footprint area, m <sup>2</sup>
$U$	System input vector
$V_b$	Volume of bag, m <sup>3</sup>
$V_c$	Volume of cushion, m <sup>3</sup>
$W$	Total craft weight
$W_1$	Structure weight
$W_2$	Propulsion weight
$W_3$	Electrical weight
$W_4$	Command surveillance weight
$W_5$	Auxiliary system weight
$W_6$	Outfit and furnishing weight
$W_7$	Armament/Equipments weight
$W_E$	Empty craft weight
$W_L$	Load weight
$W_{ls}$	Lift system weight
$x_s$	Lateral skirt deflection, m
$X, Y$	System variable and system output
$\eta_l$	Lift system efficiency
$\eta_t$	Total fan efficiency

# 1. INTRODUCTION

## 1.1 Background of Air Cushion Vehicle

Air Cushion Vehicle (ACV) is one of the advanced marine vehicles that provide versatile utilization and superior performance. It is a unique transportation vehicle based on air cushion support. Since ACVs have shown the ability to operate over rough surfaces such as water, ice, forest, and other terrains, they have been developed for practical application in a relatively short period of time. The early concept about ACVs was started from Sir Christopher Cockerell's experiment in England, 1955 [1]. Then many forms of design and construction were continuously developed for better performance and real world application.

As an amphibious vehicle, ACVs not only offer excellent performance on rough surfaces, but also provide the high speed that other conventional marine vehicles could not easily achieve. These unique abilities have attracted many researchers, military agencies as well as commercial transport companies. For example, in North America, the U.S. Navy's 150 ton landing crafts (LCAC) are now in service where other vehicles are difficult to operate such as on-water operations and in amphibious assault warfare. Canada also utilized ACVs (CCG Waban-Aki) for search-and-rescue missions, navigational aids, and ice-breaking service. Besides, many commercial and sport/utility ACVs have been manufactured and provided the services in many countries.

The skirt system is one of the important components consisted in ACVs. Thus the effort to develop a good skirt system had been started from the early time of ACV history. A good skirt should provide excellent performance in terms of power consumption, ride

quality, stability, maneuverability, and so on. Figure 1.1 describes the development of skirt in ACVs. The shapes of skirt of early ACVs were as simple as the plenum or periph-

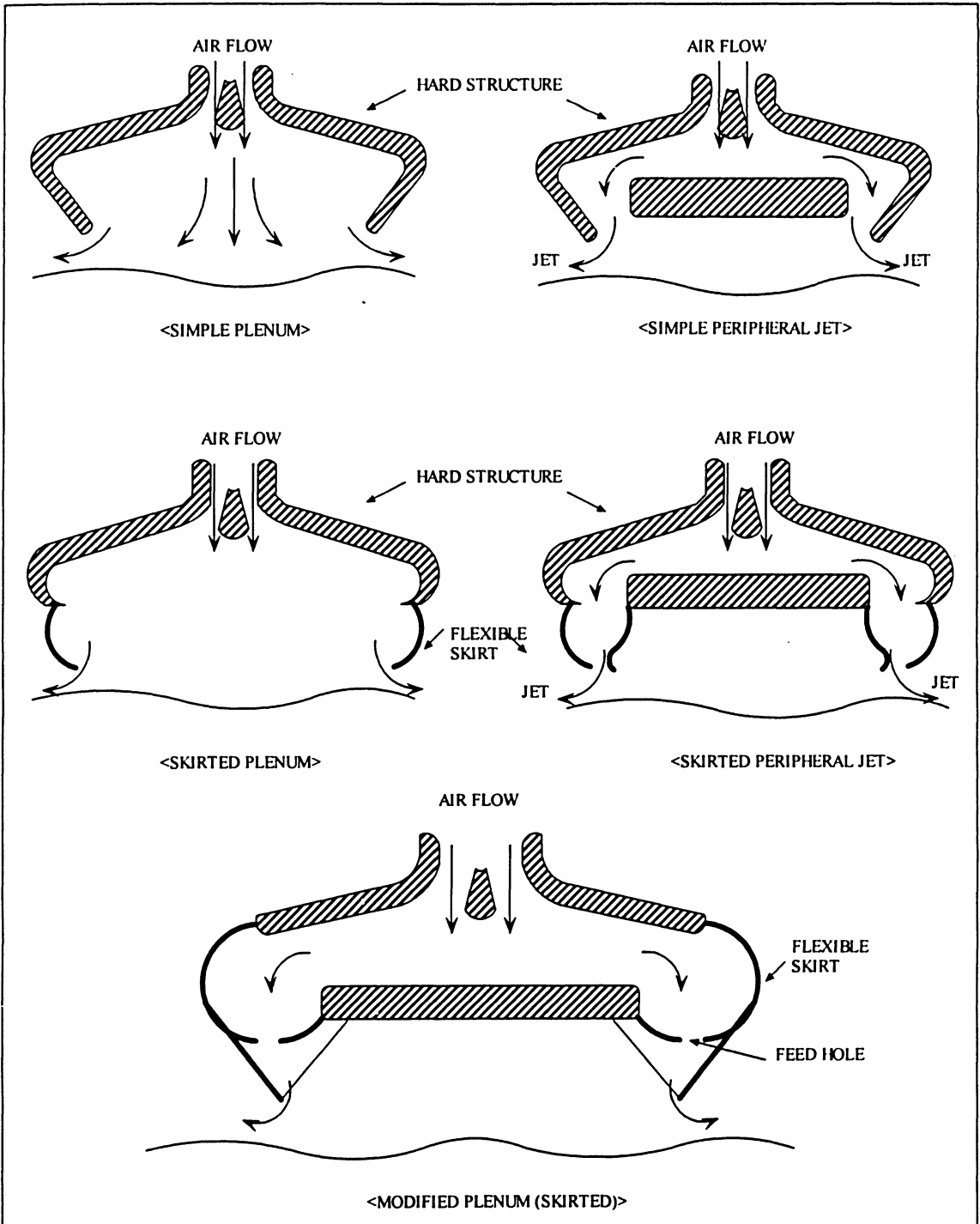


Figure 1.1: Development of skirts in ACV (Mantle P.J., 1980)

eral jet forms. However, through further development, they could be shaped in the form of the bag and finger skirt. The bag and finger skirt, as the most updated and advanced shape, provides the outstanding performance [2]. First of all, it has shown a quite significant reduction in the power requirement for the lift. Secondly, the hover-gap, which is the gap between the bottom of the skirt and the ground, of vehicles has been maintained reasonably well, so that it has shown real amphibious characteristics. Furthermore the maneuverability and stability have been greatly improved in comparison with the earlier skirt models. Finally, the skirt elements have become easily replaceable due to the use of detachable finger elements.

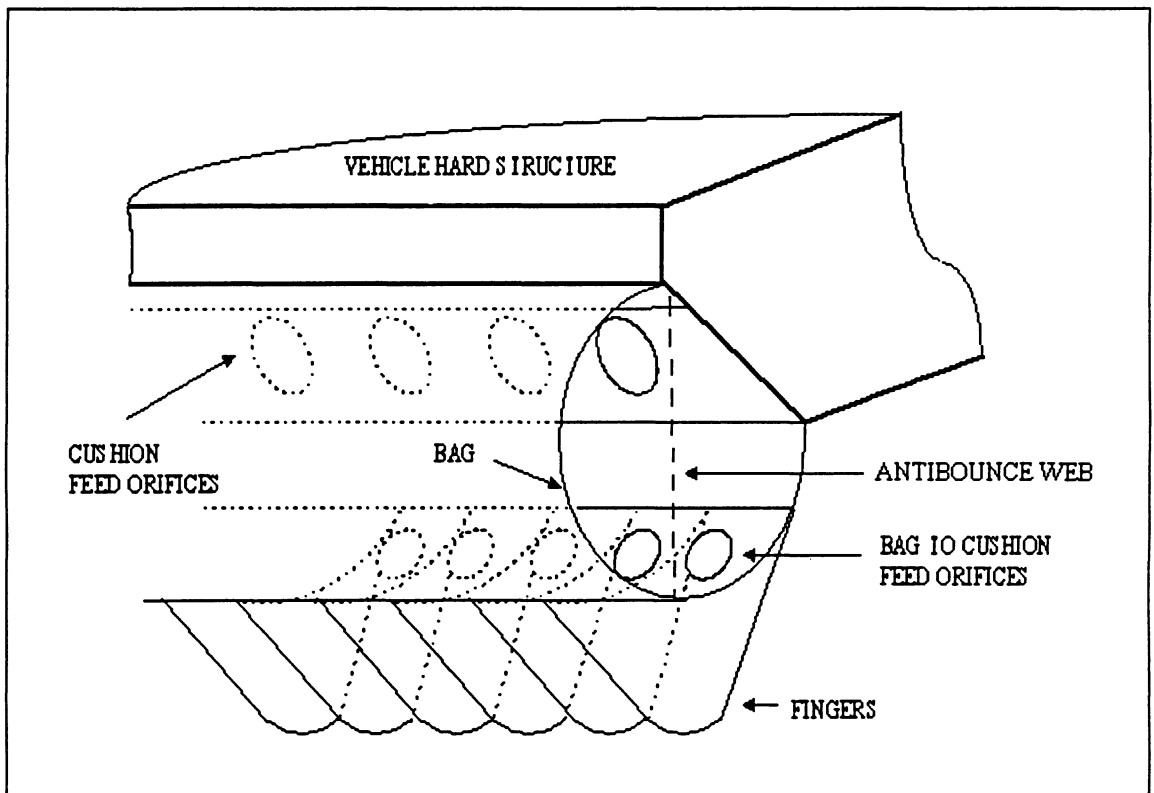


Figure 1.2: Basic concept of the bag and finger skirt (Sullivan et al, 1994)

The air flow paths and pressures in a typical bag and finger skirt system are described as follows. The air for cushion lift is provided by centrifugal or mixed-flow

fans. The lift fan system thus provides the required pressure to support the vehicle, and accommodates the changes in cushion volume as the vehicle passes over various terrains. The fans deliver air directly into a plenum chamber of which the bag volume forms a part. In most craft, the front and side bags form a single volume with only the rear bag being separately fed. From these bags, air passes through a number of orifices located on the bottom portion of the bag as depicted in Figure 1.2 to the main cushion. Once in the cushion the air pressure should be sufficient to support the craft. From the finger the flow exits to the atmosphere through the hover-gap. The cushion equilibrium flow  $Q_e$  is determined by the nature of the surface over which the vehicle operates. Also, the equilibrium value of the bag pressure  $p_{be}$  is determined from the considerations of vehicle responsiveness and stability. The size of the feed orifices located in bottom portion of the bag is then chosen to obtain the required pressure ratio,  $p_b/p_c$  [3]. Figure 1.3 depicts the air flow paths and pressures in the bag and finger skirt for ACVs.

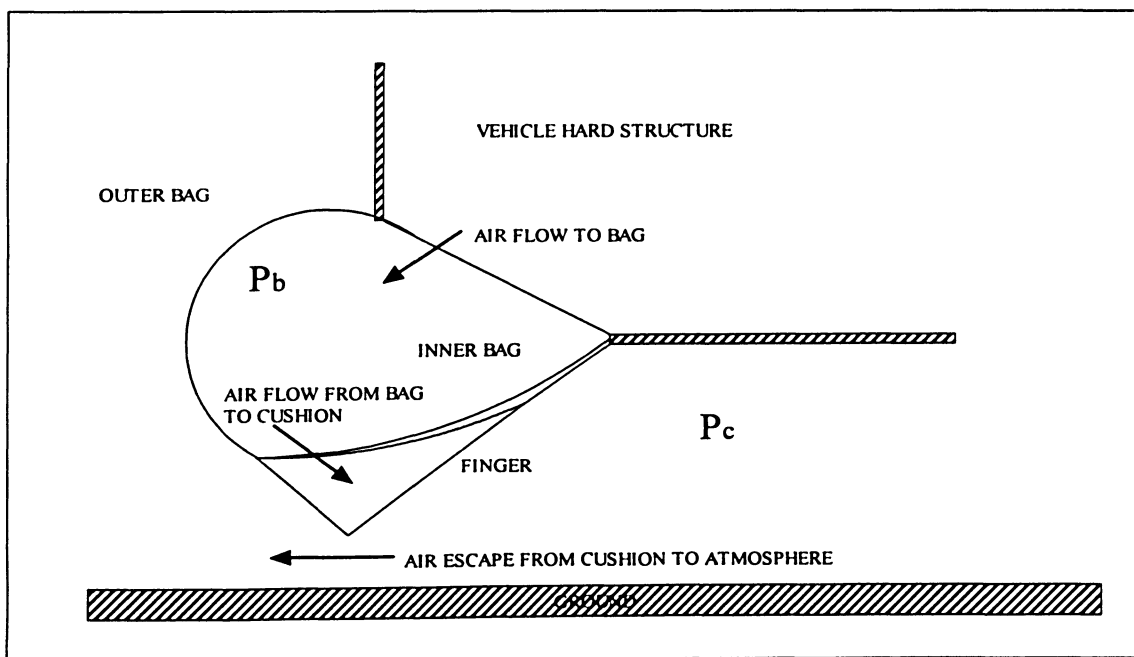


Figure 1.3: Elements of the bag and finger skirt (Chung J., 1997)

The bag and finger skirt is mainly composed of the bag section and finger section. There are bags underneath of the vehicle's hard structure. These develop different pressure to help vehicle's stability. The bag acts as a filter for long wavelength disturbances by changing its shape in response to changes in both bag and cushion pressures induced by vehicle motion. The fingers provide the continuous surface seal by keeping the effective hover-gap to a minimum in the presence of short wavelength disturbances. The structure of finger element is illustrated in Figure 1.4 and this can be easily replaceable due to wear with use.

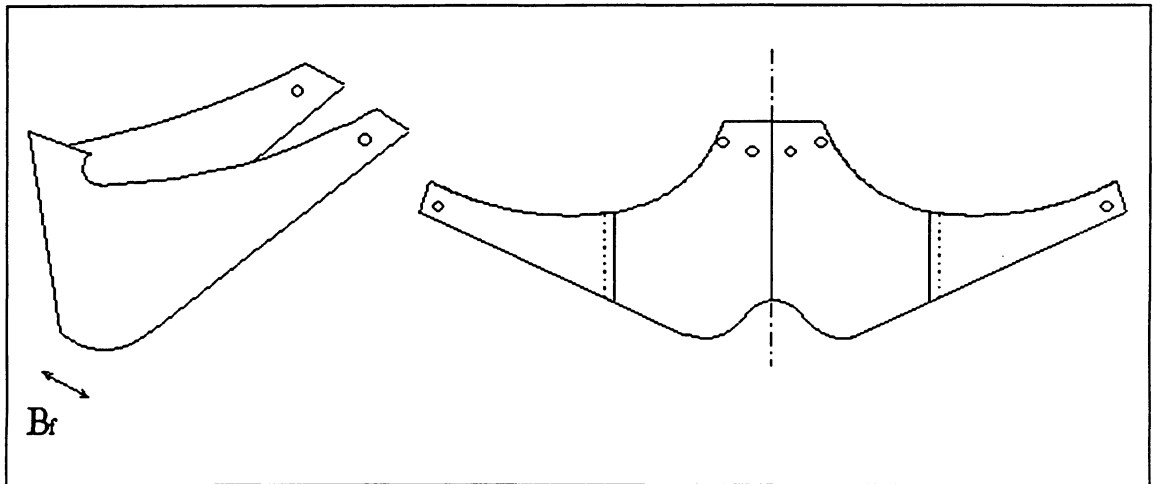


Figure 1.4: Structures of the finger element (Chung J., 1997)

Along the development of such an incredible shape of skirt, advanced material must also be involved in order to sustain all the frictions and forces applied on it. The wide choices for its material were developed ranging from chain mail to glass-reinforced plastics, sheet rubber, etc. In the end, elastomer-coated fabrics proved to be the most advanced and successful material for the skirt of ACVs [4].

Although the bag and finger skirt provides such an incredible performance as described earlier, its behavior is still not completely understood and it is not free of

problems. One such problem is its tendency to produce a rough ride and another is its susceptibility to an instability known as *skirt bounce*. The skirt bounce is the dynamic instability of the skirt-cushion system under the interaction of pressure flow variation and skirt deformation. It becomes a particular problem when the skirt oscillation frequency excites the natural frequency in heave of the craft. Those problems will be minimized with the optimized skirt geometry and system properties in the later part of the thesis. Then the optimized bag and finger skirt will eventually produce improved ride quality and stability.

## 1.2 Background of Expert System

An expert system is defined [5] as “A high performance problem solving computer program, capable of simulating human expertise in a narrow domain”. It is also referred as computer software which can perform human reasoning and judging for the specific areas such as engineering design, control system, biology experiment, and many other domains. In general, human experts store the specific knowledge and facts in computer’s memory, and set the logical relationship in the particular domain. Then the expert system is used by beginners for that domain or experts of different fields.

Expert system has been used in a wide area of applications related to design, interpretation, prediction, planning, monitoring, and control systems. One example of a design application, the marine propeller, was designed based on the expert system [6]. It initially starts with the known facts such as performance of ship and specified mission, and then it designs the dimensions and other characteristics of propeller for the given goal. Beside the marine propeller design, initial design of aircraft and UAV (Unmanned Aerial Vehicle) [7,8] were also carried out by the expert system. Control system based on the expert system can interpret the current situation of a system and predict the possible outcomes, and then it controls the problems with the necessary acts and it continuously monitors the system. As an example of such a system, an automated instructor assistant, called Minerva-DCA, has been utilized at the U.S. Navy’s Surface Warfare Officer School in Newport, Rhode Island [9]. Expert system can also be used for handling of medical problems. For instance, it was applied to make a decision in treatment selection for congenital heart disease [10]. Furthermore, the specific program codes for the design of ACVs were developed with expert system [11]. Beside the above examples, expert

system has been used for many other applications such as repair, debugging, instruction, diagnosis, decision making process and so on.

Humans become experts in a certain narrow area after they are educated for a long time and achieve a great deal of experience in the real world. Once they become experts, they are capable of providing high efficiency so that they can solve problems in a fast and reliable manner. Moreover they can start problem solving activity from vague data with limited known resources. Thus human experts are especially able to provide great help on problems which require complicated procedures and fall into newly explored domains. However they do have drawbacks due to limitations on the amount they can learn. Knowledge covers a wide range and its amount is huge, so that humans can learn only a certain portion of it. Hence, they need to co-operate with each other to thoroughly satisfy certain requirements in a given domain.

On the other hand, expert systems are built based on the behaviors of human experts in order to overcome the difficulties human experts face in reality. Expert systems are capable of providing *availability*. Availability is that the systems could be utilized under any situation even if human experts are not presented. Thus this characteristic of expert system is suitable for emergency cases or hazardous environments where humans cannot directly be present. Another aspect of expert systems is a combined knowledge. Once all the knowledge is stored in computer's memory from human experts of all fields, then the system can handle any problem by itself as long as the stored knowledge is related to the problem. This characteristic can save a tremendous time consumption and effort that human experts should spend in order to solve the problems. There are however some disadvantages of expert systems. It is hard for them to start from vague data.

Furthermore it is not easy to build the complete knowledge about a particular domain. Hence it is generally recommended to use expert systems in order to help humans and their decision making processes.

Expert system is consisted of three main components such as an inference engine, a knowledge base, and a working memory [5]. An inference engine performs the analysis and interpretation of given problems and solves them with the stored facts and specific knowledge in knowledge base. Inference engine also records the status of system or the errors occurred at every step of solving procedure in working memory. The working memory could also be used as the module for a reasoning explanation [12]. Among these three components, the knowledge base is the most important and essential part of expert system. The reason is that expert system is built based on the structure of knowledge base and it spends most of time in searching the solution. Hence the right method for knowledge base structure could produce high efficiency in computation.

The procedure that expert system pursues for the final goal is described as follows. At starting point, users describe the problem in computer's language with the given initial conditions or known facts related to that problem. Then inference engine will produce more data or estimations based on those inputs. At that moment, it will also search the solution path or particular knowledge stored in knowledge base. The working memory saves all the procedures and paths which inference engine uses. Finally expert system obtains the result or solution for the problems and shows how it reaches the final step with the short explanations. The overall flow or procedure of how expert system performs and interacts with users in specific domain is described in Figure 1.5.

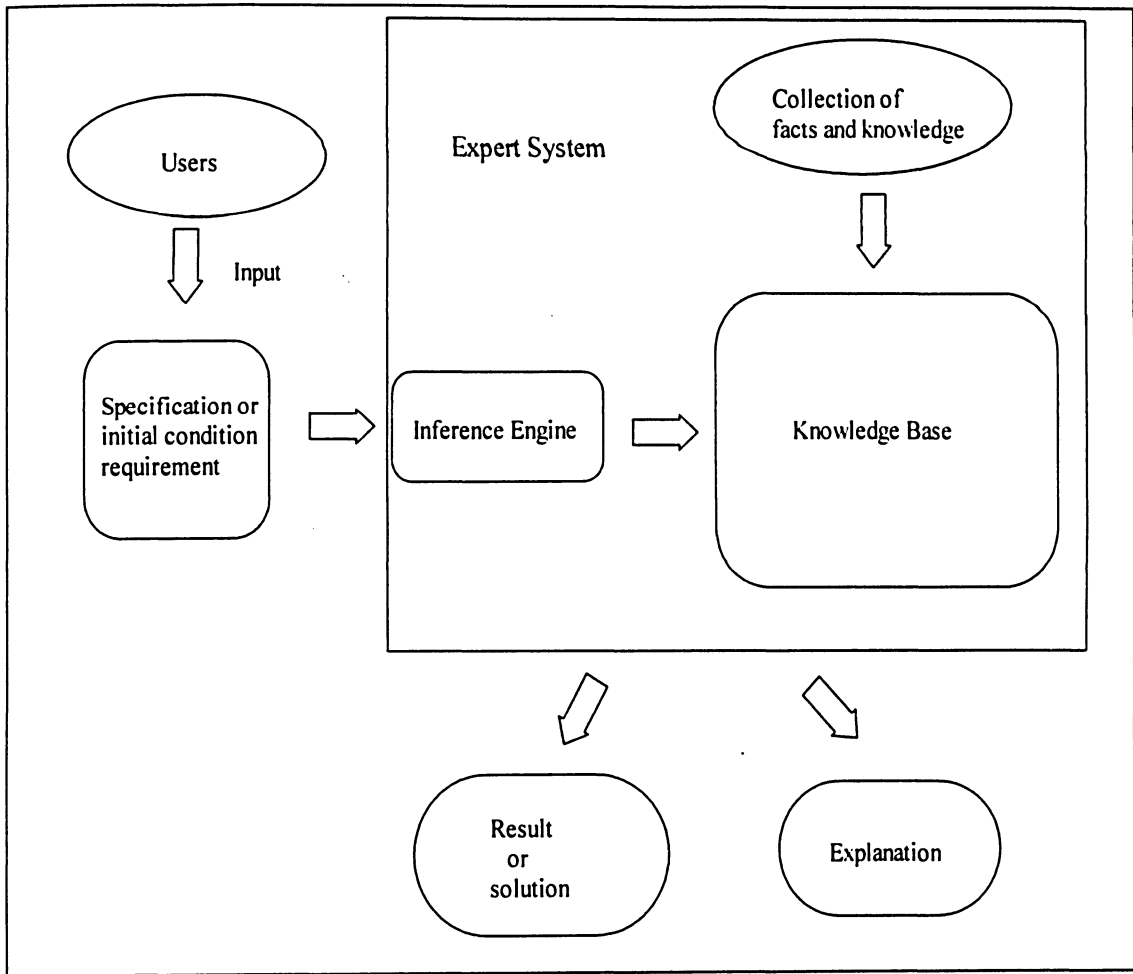


Figure 1.5: Structure of expert system

### 1.3 Background of Genetic Algorithm

In nature, all species have to go through an evolution process in order to fit the given environment. Evolutionary process means any change or modification in their genes so that they can have a better chance to survive for the given environment. For the past several hundred years, it has clearly been seen that strong species mostly survive compared to weaker ones. The term, *strong*, here indicates how reliable or suitable their genes are for a particular environment. Since there have been many changes in the environment, modifications in the genes of species have also been made through the various forms of evolutionary process. Then, the last survivor in the given environment can be seen as the one, who possesses the best genes as well as experiences the most advanced form of evolution process. Genetic algorithms are built on this natural evolution process in order to find the best solution for the given environment or problem condition.

Genetic algorithm (GA) is the search algorithm based on the mechanics of natural selection and natural genetics [13]. Since the GA is a powerful and broadly applicable stochastic search and optimization technique, the attention to the GA has grown rapidly by many researchers and designers. GA was developed originally as a technique of function optimization derived from the principles of evolutionary theory. In recent years it has been found very useful for problem solving in the fields such as biology, computer science, engineering, etc. For example, it was used to find the optimized dimensions of aircraft structure for specified missions [14]. Wing airfoil was also developed based on the GA technique for specific characteristics including desired lift, moment, and drag properties [15]. Furthermore it was used in biology application to predict the protein

tertiary structure and interpret the electrical spiking behavior of neurons. It has been applied to computer science including parallelizing and scheduling programs on multi-computers, distributed database design, and others [16]. Airline fleet assignment and optimization of an air cushion vehicle's bag and finger skirt were also performed using the GA technique [17,18].

Using the GA technique provides unique advantages compared to other conventional techniques. For example, most engineering optimization problems have unevaluated and infeasible regions. Some points evaluated from the search techniques can correspond to these unrealizable regions [19]. These points should be avoided during the search process and the optimal solution point must be within the feasible region for the realistic application. This could be done by the GA optimization. Figure 1.6 describes the possible regions in which the solution point might be found by search techniques.

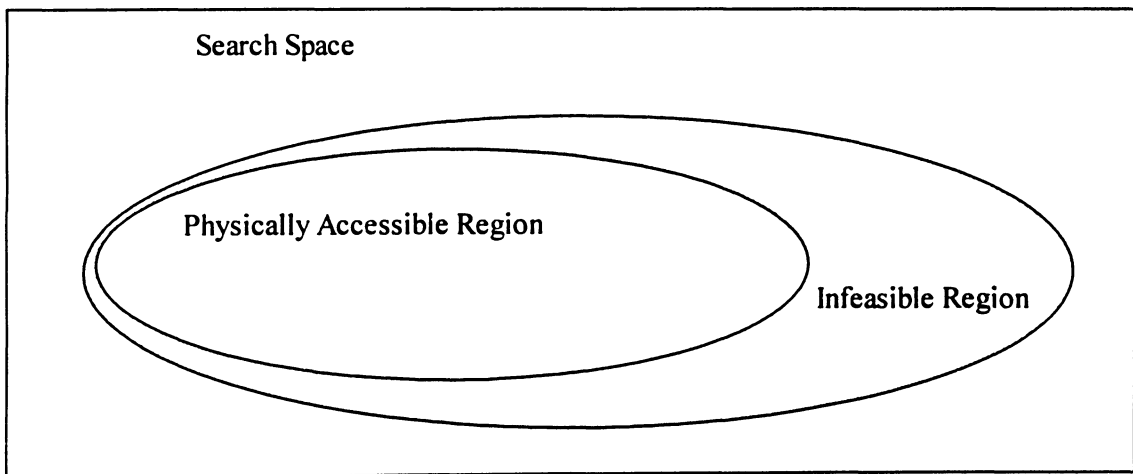


Figure 1.6: Infeasible region in the search space

The search space may also have a large number of local optimums. The conventional search methods such as calculus-based, enumerative, and random techniques can be trapped in one of these local optimums which is not desirable. This

problem can be prevented using the GA technique. Figure 1.7 shows several local optimums in the domain.

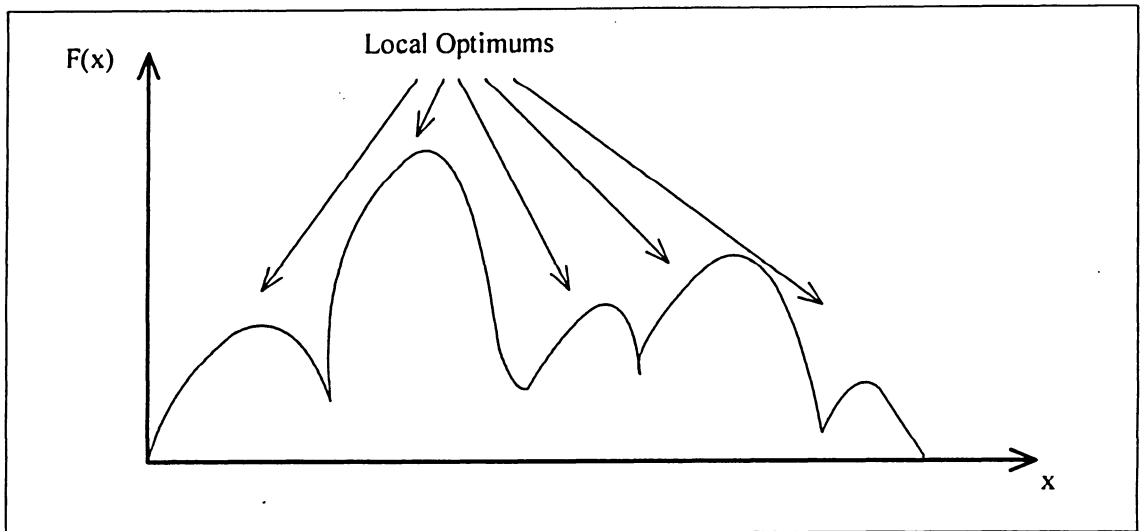


Figure 1.7: Multiple local optimums

The GA has its own characteristics, which are different from other conventional search techniques in some principles [13,20].

- 1) It works with a coding of the parameter set, not the parameters themselves.
- 2) It searches from a population of points, not a single point.
- 3) It uses payoff (objective function) information, not derivatives or other auxiliary knowledge.
- 4) It uses probability transition rules, not deterministic rules.
- 5) It uses commonly bit operators which require much less memory and are computationally more efficient.

The GA starts from generating random initial population which is consisted of potential solution points. In this step the evaluation of each individual in the population is also included with objective function [21]. Then the initial population is going through

the first genetic operator, selection process. The purpose of this operator is to give more chances of survival for strong individuals and to die off the weakest ones. After this process, the population enters the crossover operator. Crossover operator is performed to build the new individuals. This process can be compared to the natural evolution process generating new children from the parents. Crossover process is the main and essential part of genetic algorithm because it can produce better genes for the given environment or problems being optimized. Finally, the mutation operator follows the crossover. The main role of mutation process is to provide the diversity in the population. Without the mutation, it is hard to reach the solution point which is located far from the current direction of search. It insures that the probability of reaching any point in the search space never go to zero [22]. This operator also prevents the premature convergence of the GA to one of the local optimal solutions.

Once all the main operators are performed on the initial population, new population is developed. This new population is genetically superior to the previous one and has better chance to survive for the given environment. Then this whole procedure will be continued until the satisfaction is met or it reaches the maximum number of generations which is pre-set by user. The above description of the GA is a simple general flow of the optimization procedure. This algorithm can be built with more advanced components such as elitist replacement, remainder stochastic sampling method, penalty function, etc. They are actually used in this thesis work for better performance of optimization process, and their descriptions will be addressed in the later chapter. Figure 1.8 shows the general flow chart of simple GA.

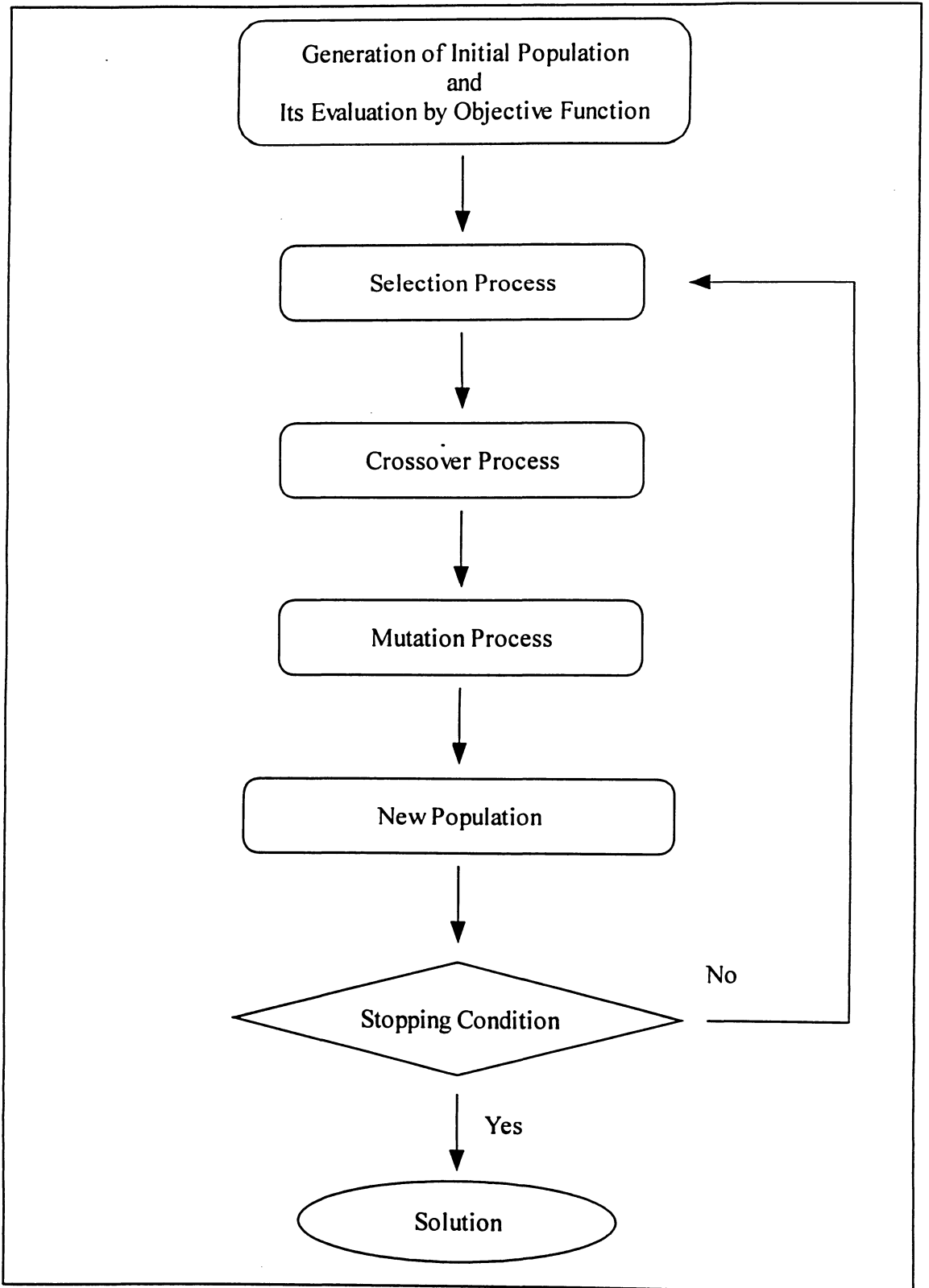


Figure 1.8: Flow chart of simple genetic algorithm

## 1.4 Objectives

The main objectives of this thesis are to build the expert system for initial design of ACVs and to find the optimal properties of bag and finger skirt for better ride quality and stability using the genetic algorithm. Hence the work presented in this thesis is divided into two parts. It should be noticed that optimization of skirt system with the GA is more emphasized than initial design of ACVs by the expert system. The reason is that the expert system needs a tremendous amount of database and resources related to ACVs, so that it requires long term research to complete the system. This system should continuously be studied, up-dated, and built. Hence only the initial stage of designing is simply carried out by the limited level of expert system. However the skirt optimization by the GA is processed in depth.

The motivation for the expert system is to help beginners who want to design ACVs and to provide an opportunity for human experts to approach different design concepts without spending too much time and effort. It is really difficult for new designers to know where they should start from and how to proceed toward the final goal. Thus the expert system guides and advises them toward the goal they want to achieve. Furthermore this expert system can also help the real experts with showing the results of various configurations and systems, so that they can understand the different approaches and concepts which they cannot directly demonstrate due to a lack of time and financial affordability. Expert systems will start to design ACVs with the given desired initial conditions such as craft weight and maximum velocity inputted by users. Then it will decide the overall dimensions and other properties of ACVs according to the knowledge base stored in computer's memory. Finally the expert system will find the general

configurations and characteristics of the subsystems. For the knowledge base, various works of literature, statistical data, common trends from historical examples, etc. are collected and summarized. Further details about the procedures of how the expert system establishes the initial design of ACVs and the knowledge base will be addressed in the following chapter. For the validation of program codes and their successful implementation, the results of the experiments will be compared with the existing vehicles.

In the second part of the thesis, the bag and finger skirt is optimized with the GA technique for better ride quality and stability. Design variables of the bag and finger skirt will be the dimensions of the bag and finger, and pressure ratio of the bag and cushion areas. The mathematical model for the skirt system will be studied and it will be linearized at the equilibrium conditions. The ride quality can be defined from the amplitude of craft heave frequency response. Typical ACV's heave amplitude response for small ground input as a function of frequency shows a characteristic double-peak with the lower frequency peak being associated with the craft mass and the higher frequency peak associated with the skirt mass [23]. This second peak is very large due to the large motion of the skirt interacting with the non-linear characteristics of flow escape between the bottom of the fingers and the ground. This large resonance peak is undesirable since its frequency is very close to the range of 25 rad/s to 50 rad/s where most people feel the maximum sensitivity for the vertical vibration [2,24]. Thus for better ride quality, the second peak of frequency response curve should be outside of this frequency range and its magnitude must also be reduced as much as possible. This condition will improve comfortable ride.

The optimized bag and finger skirt must produce the proper eigenvalues of system matrix for the stability of vehicles. Instability of ACVs is also coming from the *skirt bounce*. Skirt bounce is the dynamic instability of the skirt-cushion system under the interaction of pressure flow variation and skirt deformation. The current method of suppression of skirt bounce is to use an element known as anti-bounce web (shown in Fig. 1.2) that interferes with the ability of the skirt to filter out surface irregularities. In order to reduce skirt bounce without using anti-bounce web, a higher pressure ratio is necessary, but it will also increase the lift power requirement for the system. Thus Mantle [4] suggests the proper pressure ratio between the bag and cushion ranging from 1.0 to 1.6 in order to minimize the instability from skirt bounce. Hence, the GA will find the best dimensions of skirt and pressure ratio by examining the frequency response curve, system matrix, and pressure ratio of the bag and cushion predicted by linearized equations.

For the validation of expert system and GA on the design of ACVs, the CCG (Canadian Coast Guard) 37 ton Waban-Aki and U.S. Navy's 150 ton LCAC (Landing Craft Air Cushion) are selected and compared with the experimental results. All program codes including the expert system, genetic algorithm, and simulations for behavior of vehicles are developed in the MATLAB software. The tests, validation, and debug for the codes have also been done to produce the accurate and fair results for the thesis work. Details of these programmings are presented in this thesis and some of them are shown in appendices.

## **2. INITIAL DESIGN OF ACVs WITH EXPERT SYSTEM**

### **2.1 Overview of Initial Design Process**

Initial design process for ACVs by the expert system is described in this chapter. Since the complicated processes and many trade-offs among the several subsystems involve in the design process, some of design procedures are simplified and limited in order to avoid the complexity in this work. Hence the subsystems of ACVs are designed in a limited range such that it only includes the lift system, propulsion system, and skirt and cushion system.

The design procedure is commonly separated into the two categories such as “Determination of principal dimensions” and “Main subsystem design”. In the section of “Determination of principal dimensions”, the expert system will find the main dimensions of vehicle such as craft length and craft width with the given craft total weight. Then it will analyze the detailed weight distribution of vehicle with relations and facts stored in the knowledge base. At last, it will perform the parametric study. In the section of “Main subsystem design”, three main subsystems will be designed with the expert system. The expert system will decide the properties and performance of these subsystems according to the knowledge base containing facts and equations. Those facts and equations are acquired from the literatures, statistical data, common trends, and the collection of manufactured ACV data sheets. In knowledge acquisition process, more than 70 existing ACV data sheets are collected in order to obtain the valid relationship among the several elements and design factors. Figure 2.1 illustrates the initial design process for ACVs and Figure 2.2 describes the expert system for initial design of ACVs.

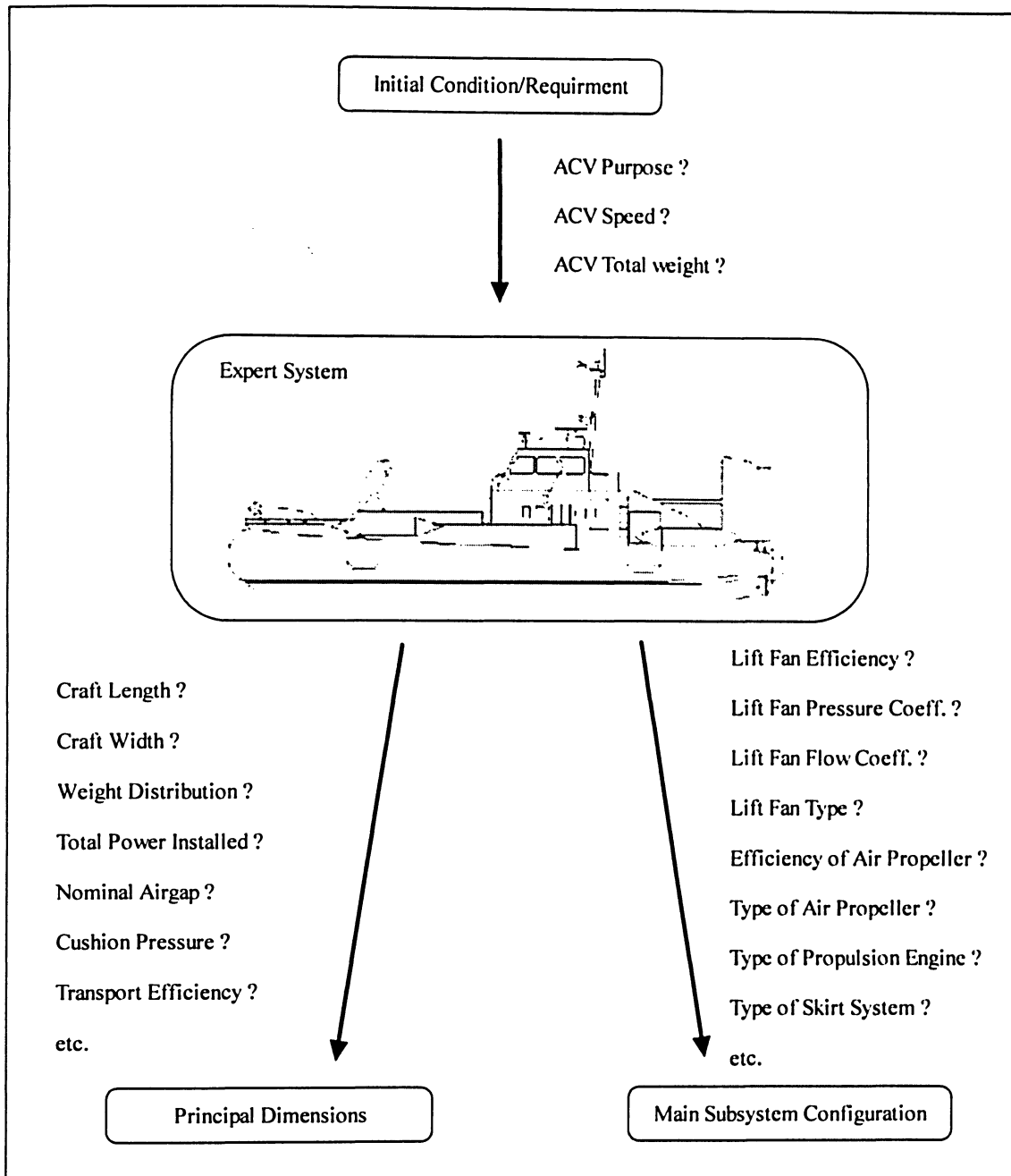


Figure 2.1: Initial design process for ACVs

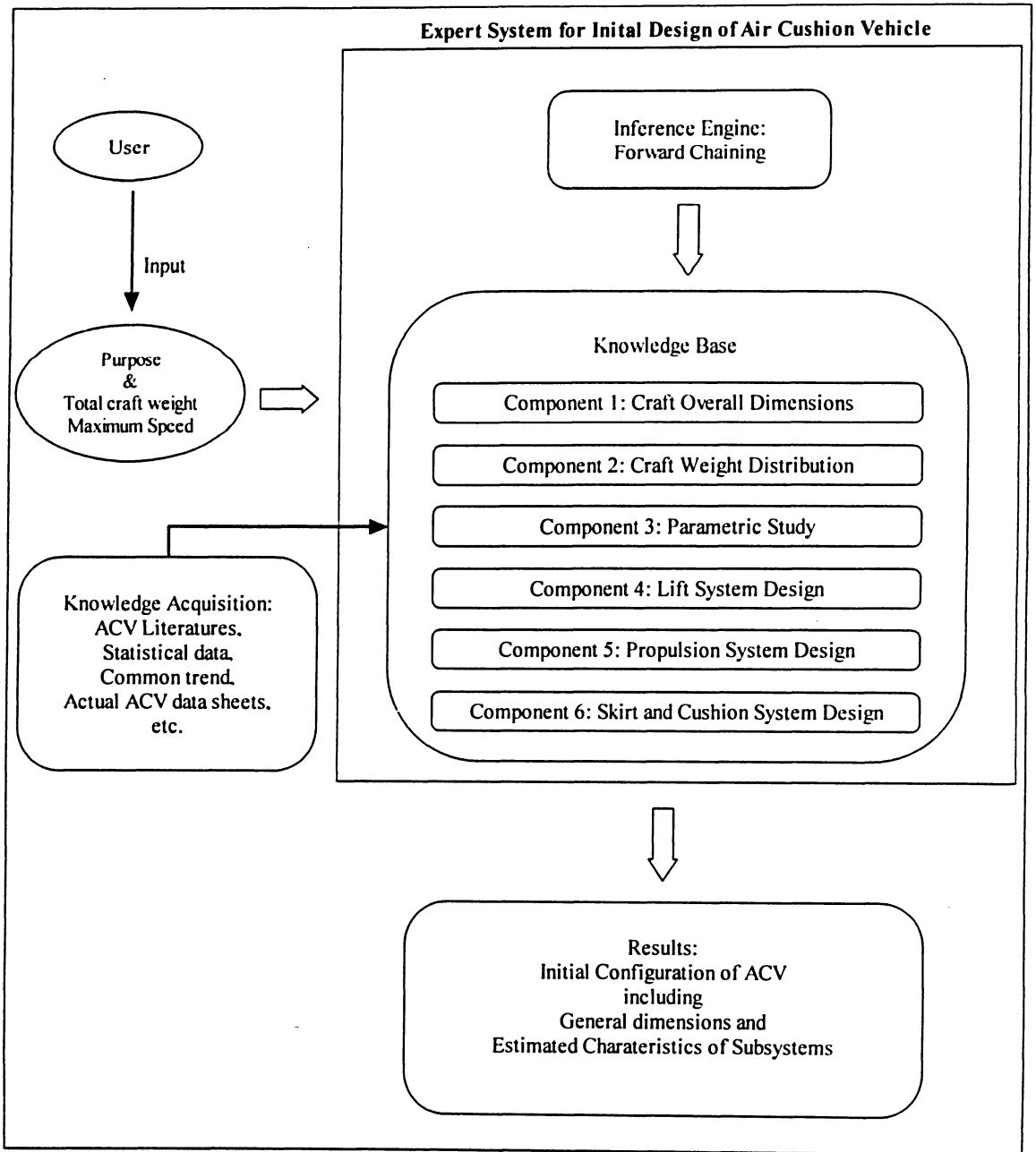


Figure 2.2: Expert system for initial design of ACVs

## 2.2 Code Development for Expert System with MATLAB

The codes were developed in MATLAB in order to implement the expert system for initial design of ACVs. Since the design process for ACVs is quite complex, the codes were developed as the main source and other calling sources. Thus the user needs to run only the main source code in the MATLAB software with the given constraint conditions. Then it will produce the initial configuration of ACVs with other calling source codes. The followings are the list of codes built and applied for the initial design of ACVs.

### Main Source Code

ES.m                      Expert system is initiated and inference engines are activated

### Calling Source Codes

inference\_engine1.m      Inference engine related to the design process, “Determination of Principal Dimensions”

inference\_engine2.m      Inference engine related to the design process, “Main Subsystem Design”

input\_file.m              Initial condition and requirement are inputted

output\_file.m             Results are recoded in this file

speed\_category.m         Vehicles are categorized by its speed limit

OD.m                      Knowledge base component related to “Overall Dimensions”

WD.m                      Knowledge base component related to “Weight Distribution”

PS.m                      Knowledge base component related to “Parametric Study”

LS.m	Knowledge base component related to “Lift System Design”
ProS.m	Knowledge base component related to “Propulsion System Design”
SCS.m	Knowledge base component related to “Skirt and Cushion System Design”

**Other Source Code**

ACV_Database.xls	Over 70 ACVs Data sets are stored and Correlations are acquired
------------------	---

As mentioned earlier, the codes for Expert System have not been built for complete initial design process of ACVs, but they still provide the rough estimations and general configurations related to the vehicle’s main parameters and subsystems. These codes show possibility of the Expert System on initial design of ACVs. The more detailed and complete codes will be developed in future research work as a long term project. The second part of the thesis work which is about the skirt optimization with the GA will present more complicated and satisfactory codes, and their capability is much more sophisticated and fully satisfies the expected level of development in terms of completeness. The following sections will describe each component of expert system. Figure 2.3 illustrates the flow chart for the interaction of these program codes.

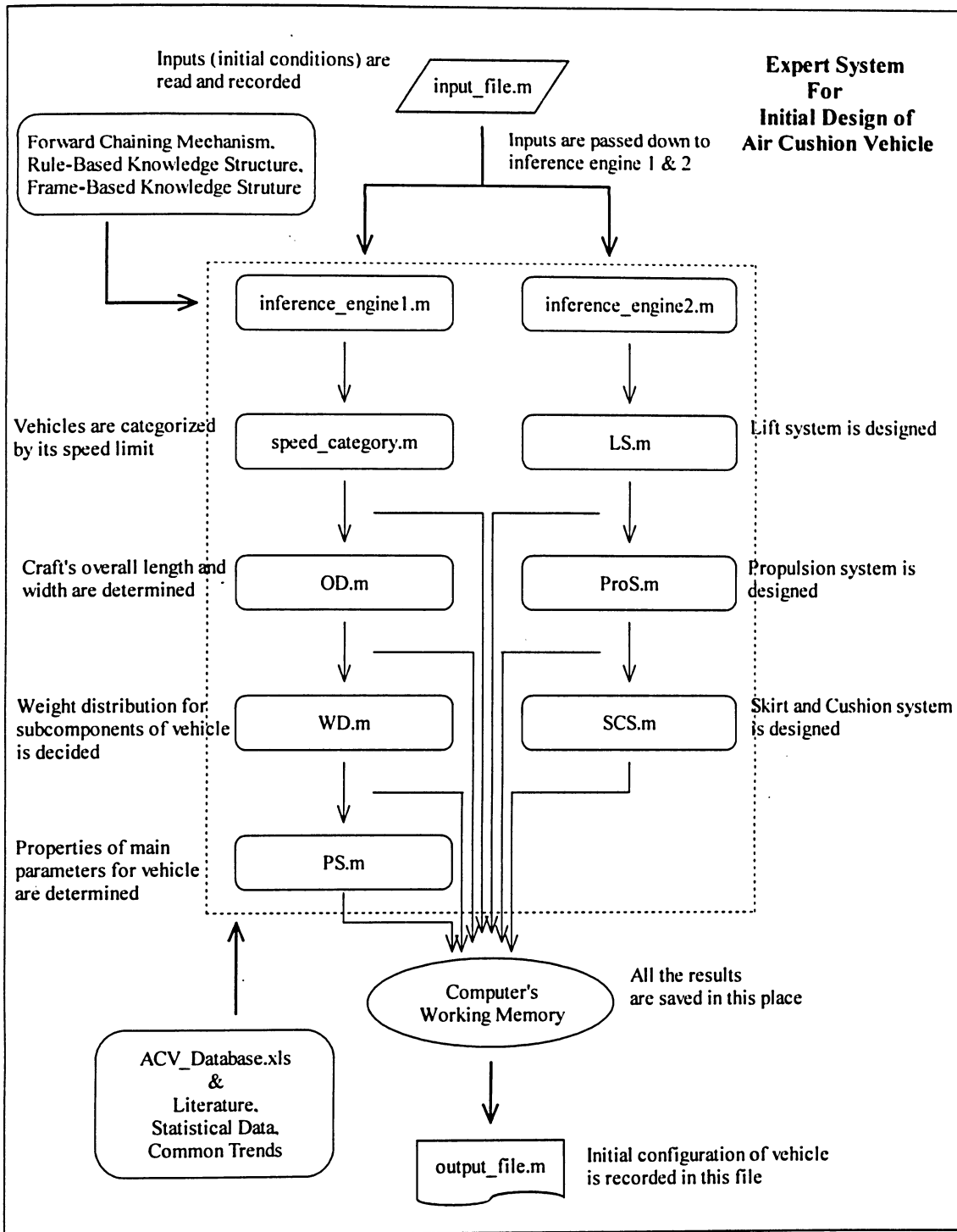


Figure 2.3: Flow chart of program codes for expert system

### **2.3 Implementation of Expert System**

In order to successfully implement the expert system, the three main components of system need to be defined and constructed in a specific way for the initial design of ACVs. In this section, those components specifically built for the initial design of ACVs are described.

Inference engine is the heart of expert system since it controls all the important functions. It is capable of extracting the reasoning from how it reaches the goal, and it controls the flow of problem solving procedures. Moreover it can directly interfere with the decision making steps and simulate the results. Thus the inference engine could be considered as a human brain, because it can artificially do what humans do for the problem solving activity. There are two common methods available for inference engine to search the rules and to determine the solutions. They are the Forward-Chaining and Backward-Chaining. The forward-chaining is the mechanism that starts to solve the problem with the known facts or given conditions. Then it searches forward for the solutions or final goals. The backward-chaining is the mechanism that starts to search from the final goal and conclusion. Then it determines whether a conclusion or final solution is valid or not, when it goes through every sub structures of problem solving activity. In this thesis, the forward-chaining is utilized to apply the inference engine. The reason is that the overall design process starts from the initial conditions inputted by users and final solution is obtained through the problem solving activity. Hence the forward-chaining mechanism is more appropriate for initial design process of ACVs. Figure 2.4 describes a simple example of two mechanisms of inference engine.

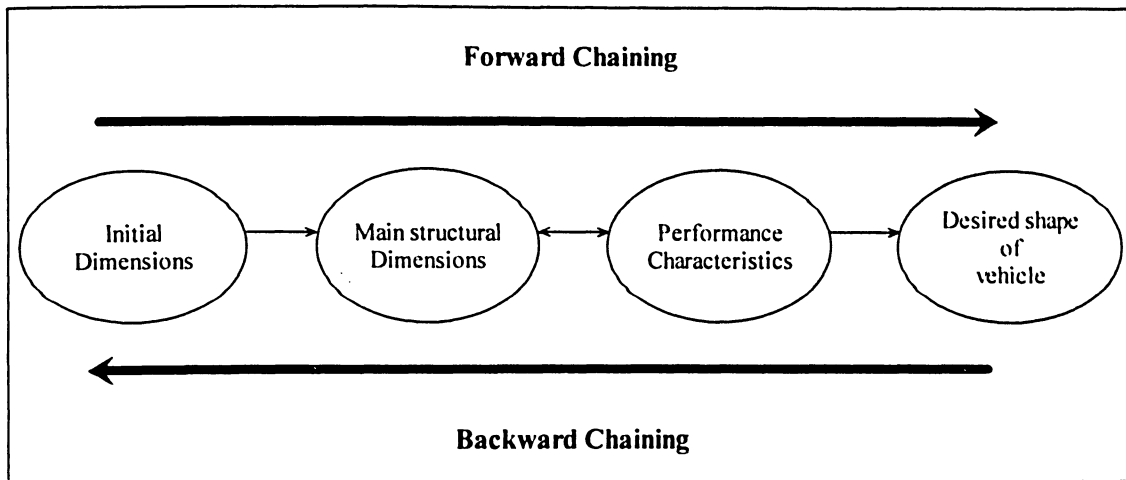


Figure 2.4: Forward-chaining and backward-chaining mechanisms

Knowledge should be stored in a form that computer can access, understand, and use for the problem solving activity. This could be done by specific structures of knowledge base. The most common structures of knowledge base are the Rule-based system and the Frame-based system [7,25,26].

In the rule-based knowledge representation a component, called 'rule interpreter', examines the problem condition and executes the proper action according to the matching rules which stored in a component called 'rule memory'. Those two components are the essential parts of rule-based knowledge representation and they work together. The rules are basically consisted of two main parts: *IF* and *THEN*. In the statement of *IF* part, some conditions are written and they should be satisfied by the rule interpreter in order to carry on the action specified in the statement of *THEN* part. For example, the condition could be set like "if the vehicle is a truck" for the *IF* part and the action specified in the *THEN* part will be "then the number of wheels is four". If there is more than one rule that satisfy the condition, then the rule interpreter selects only one of them and executes it. There are several ways how to determine the right one among some choices such as methods of

*refractoriness, recency, and specificity* [5]. Figure 2.5 illustrates the Rule-based structure and *fire* in the figure means the execution of the action.

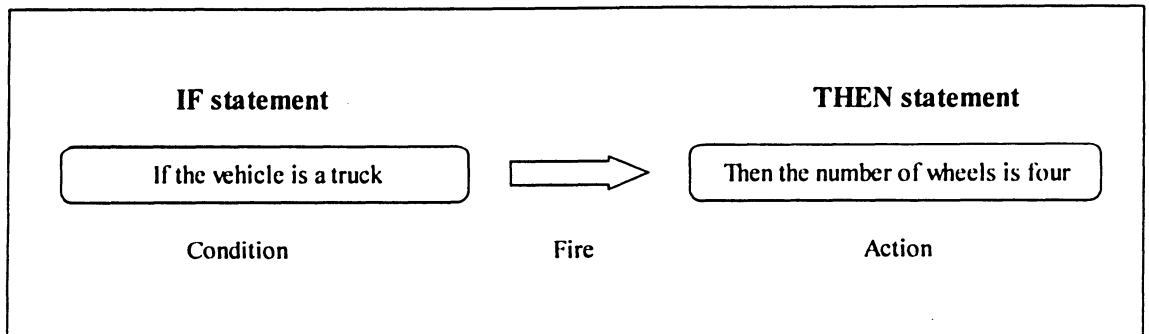


Figure 2.5: Rule-based knowledge representation

In Frame-based knowledge representation, knowledge is represented in data structures called frames. Frames are created based on the mechanism of hierarchical structure and all the important information previously decided is passed down to the end of decision process. In other words, the frame at the top level of structure is considered as *superclass*, while the frame at the bottom level of structure is called as *subclass*. Thus the relationship among elements basically lies on vertical bonding.

Since frame-based system uses the structural representation, they are very useful and powerful in applications that require the logical reasoning and procedures from the initial step to the final goal for the problem solving. However it is usually difficult and complicated to construct such knowledge system based on the frame itself. On the other hand, rule-based system is easier to implement and has powerful algorithm in each problem solving step. Hence in the thesis it uses a combined rule-based and frame-based knowledge structure in order to represent the system in a structural point as well as in a sub-structural point. This particular structure represents knowledge efficiently. Figure 2.6 shows a simple example of Frame-Based Knowledge Representation.

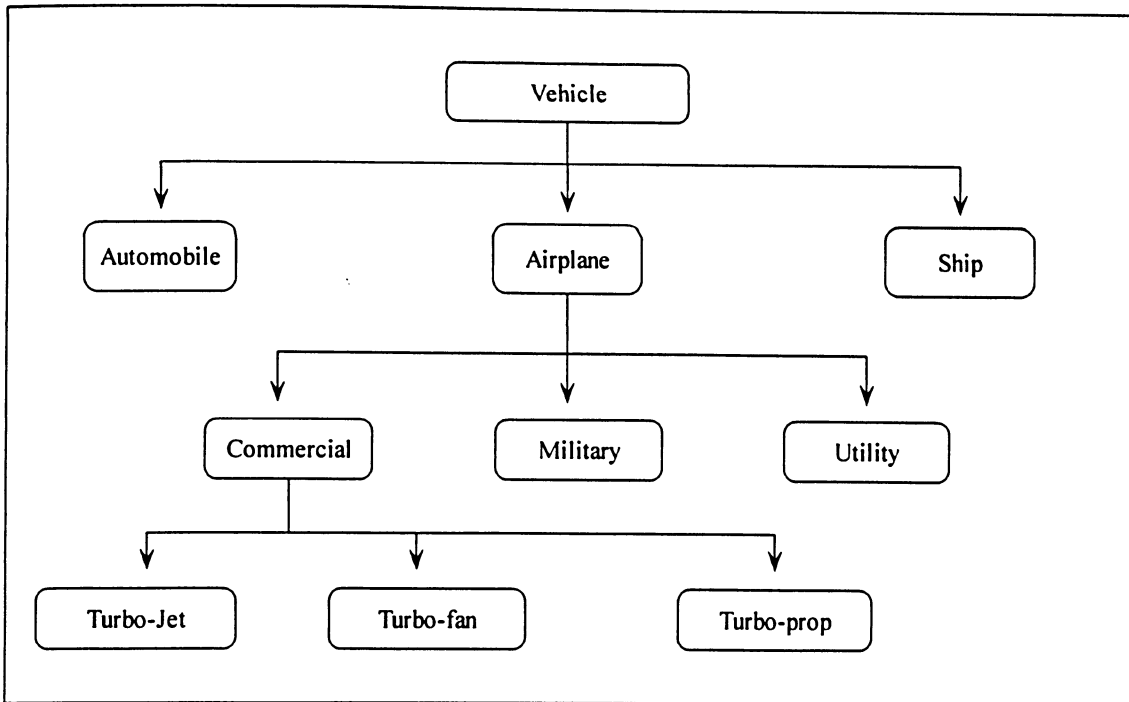


Figure 2.6: Frame-based knowledge representation

Another important feature of expert system is the knowledge acquisition [27,28]. It is often considered as the bottleneck, because knowledge itself has not been defined clearly and many difficulties rise when knowledge engineers try to obtain and construct it. Here the knowledge engineers are the ones whose expertise is about the knowledge construction and interpretation. Thus, this is the component of expert system which delays the most of time in building the system and is identified as the major obstacle.

General questions are the most typical method of getting knowledge from human experts. This method is usually applied at the beginning of knowledge acquisition process. The knowledge engineers usually start from the simple and general questions in order to provide the opportunity for experts to understand the topic and characteristics of problem. Then they move to more specific types of questions related to the topic. Focused discussions are another method of knowledge acquisition. They are used for deeper and

more specific questions than the general questions. Figure 2.7 describes the general procedure for knowledge acquisition.

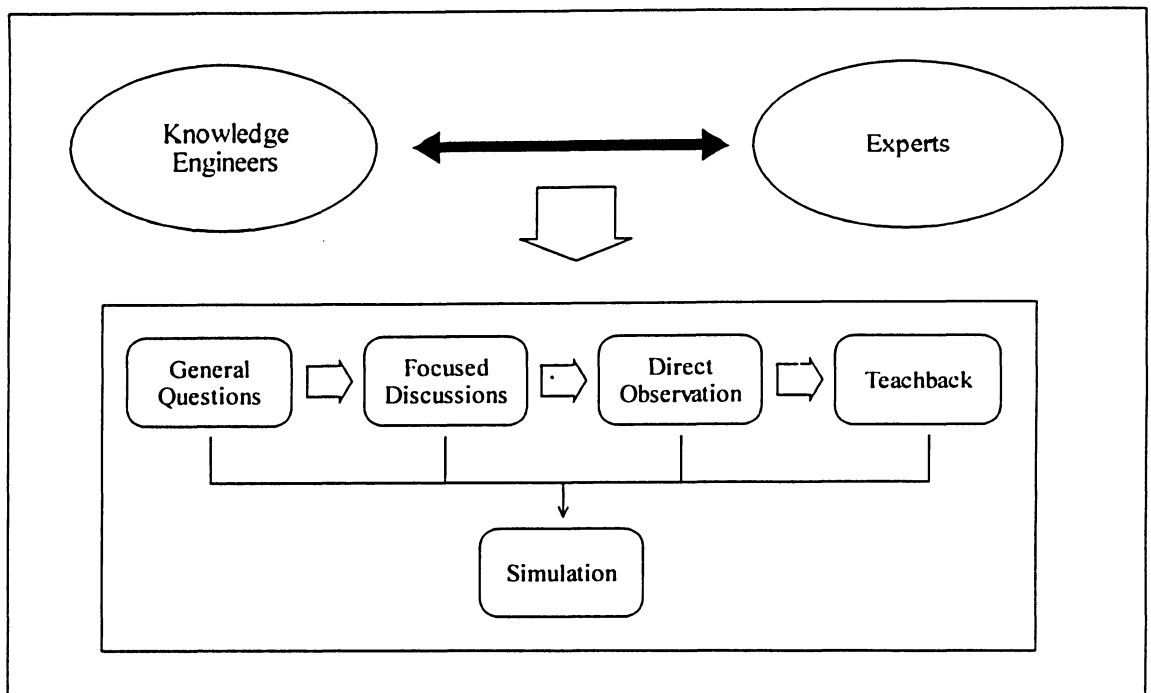


Figure 2.7: General procedure for knowledge acquisition

Observation is the technique that obtains the specific knowledge through the direct monitoring during the performance of experts. This method is required the knowledge engineers to spend the time with experts. Thus the more involved the knowledge engineers become, the better knowledge they could produce. The knowledge engineers might get the answers during the observation which they could not obtain during the general questions or focused discussions. Teachback is another technique for knowledge acquisition. When the knowledge engineers have completed the general questions, focused discussions, and observation, then they teach the experts what they have learned during those knowledge acquisition methods. The purpose of this technique is to verify the knowledge the knowledge engineers obtained and not to miss any

important information during the previous knowledge acquisition steps. There are also several other methodologies available such as questionnaire, feedback, and statistical analysis [29]. In this thesis work, statistical analysis of past data sets on ACVs was mainly used to build the knowledge base. The general guidance and advice from the experts also contributed to the knowledge base. The more details about this statistical analysis and general guidance applied in this thesis will be explained in the following sections.

## 2.4 Input Parameters

The users need to specify the initial conditions and requirements for the initial design of ACVs, before the expert system initiates the design process. In this thesis, those input parameters are limited to the vehicle's purpose, maximum speed, and total weight. The purpose of ACV is generally categorized into the three branches such as commercial purpose, military purpose, and sport/utility purpose.

1. The commercial purpose is to deliver a given number of passengers or amount of cargo between two specified points at highest possible transport efficiency considering the lowest cost and best profit.
2. The military purpose needs the similar requirement to commercial transport but applies different speed and travel time consumed.
3. The sport and utility purpose, transport efficiency is not so important factor but a simple structure and less effort for the vehicle maintenance are preferred. The cases of public services such as ice breaking and search-and-rescue are also included in utility purpose.

The next input parameter is vehicle's maximum speed. This parameter helps to define the speed category according to knowledge base. Each ACV can be categorized into the three different speed ranges such as low speed, medium speed, and high speed. This speed range is defined [4] as follows. The low speed range is from 0 m/s to 13.4 m/s, while the high speed range is from 44.7 m/s to the higher speed. The medium range is the speed between low and high speed categories.

Once the users specify the purpose and maximum speed of the vehicle, then they need to input the total vehicle weight. The total vehicle weight is very important and essential element of initial design process, because the expert system starts to design based on this given condition and seeks further the main dimensions such as craft length and craft width. Then all the characteristics of subsystems of ACVs are established from these main dimensions. Figure 2.8 depicts the initiation of expert system with input parameters.

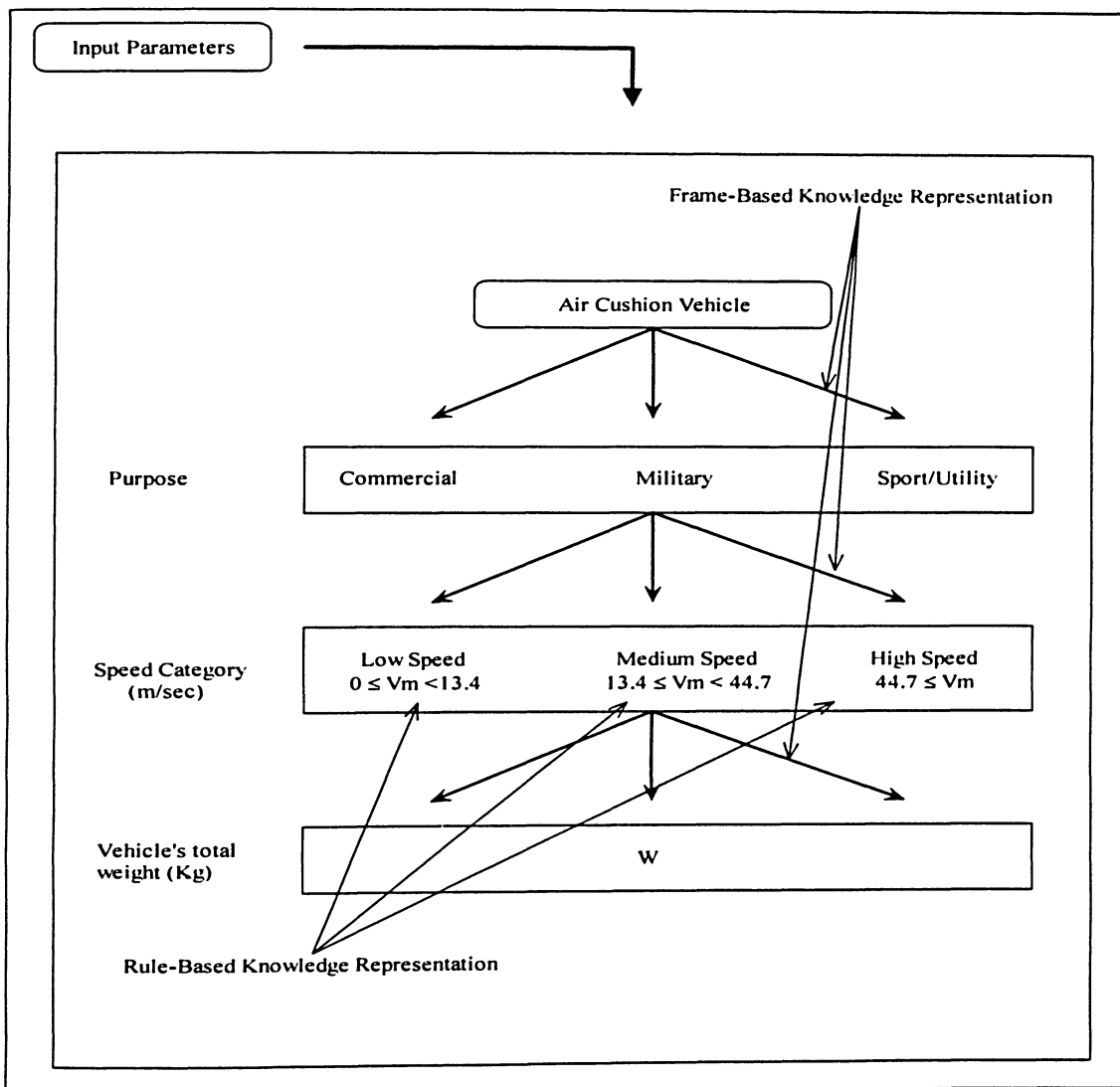


Figure 2.8: Input parameters on expert system

## 2.5 Determination of Principal Dimensions

Expert system starts to design the initial configuration of ACVs by obtaining the craft overall dimensions from the knowledge base. For the overall dimensions of vehicle, the knowledge base contains several data sheets of ACVs which describe the properties or general characteristics. Then inference engine tries to find common trends or common design rules from this knowledge base set. Thus once user inputs the total craft weight, then expert system obtains the matching overall dimensions of craft from the common trends in the data sheets of ACVs manufactured in the past. The following table shows a sample data set for ACVs collected during the research period of time.

Table 2.1: Sample data set for ACVs

Name	Builder	Purpose	Power Plant	Length(m)	Beam(m)	Mc(kg)	Vcru(m/s)	Vmax(m/s)	Payl.(kg)
Saint-Michel	Ackerman I.	Public Ser.	37kW	5.9	2.3	600	13.9	n/a	600
Baroudeur	Ackerman I.	Public Ser.	37kW	3.7	2.2	200	11.1	n/a	n/a
Adoc 4	Ackerman I.	Public Ser.	37kW	4.6	2.3	200	13.9	n/a	n/a
Adoc 3S	Ackerman I.	Sport/Util.	37kW	3.6	1.8	200	11.1	n/a	n/a
Garonne	Ackerman I.	Public Ser.	63kW	7.0	3.0	1100	16.7	n/a	500
Canair 300	ACV D.	Sport/Util.	1 Piston engine	3.8	2.2	182	9.7	12.5	182
Canair 500	ACV D.	Sport/Util.	1 Piston engine	5.0	2.2	237	11.1	13.3	295
AH560P	Airlift H.	Comm.	2 Piston engines, 77kW	6.1	4.0	830	15.3	16.4	550
AH560U	Airlift H.	Sport/Util.	2 Piston engines, 77kW	6.1	4.0	759	15.3	16.4	650
AH1160	Airlift H.	Comm.	2 Diesel engines, 330kW	12.2	6.0	n/a	19.6	28.4	3000
BBV 6	BBV H.	Sport/Util.	99kW	5.3	2.5	495	12.9	n/a	600
GH-2006	British H.C.	Comm.	4 Gas turbine, 11334kW	56.4	27.9	195000	25.8	30.9	3000
CCGH 045	British H.C.	Public Ser.	1 Gas turbine, 896kW	14.7	7.7	8500	20.6	30.9	n/a
CCGH Siyay	GKN W.A.	Public Ser.	4 Diesel engines, 2818kW	28.5	12.0	70000	23.2	30.9	25000
Mariah 425	Mariah H.	Sport/Util.	Yamaha Vmax 600cc	4.2	2.0	320	n/a	22.2	480
Hovetrek	Neoteric	Sport/Util.	Fuji EC50PM-02, 39kW	4.2	2.5	200	15.6	20.0	272
Shuttle	Scat H.	Comm.	2 Diesel engines	7.1	4.0	850	12.9	15.5	600
SAH2200	Slingsby	Comm.	Diesel engine, 238kW	10.6	4.2	n/a	16.5	20.6	2200
LCAC	Textron	Military	4 Gas turbines, 11930kW	26.8	14.3	149500	20.6	20.6	60000
Odyssey	Pacific H.	Comm.	Diesel engine, 221kW	10.5	4.5	3750	19.6	n/a	2400
Explorer	Pacific H.	Comm.	Toyota 4L V8, 194kW	7.3	3.5	1600	18.5	n/a	1200
Slider	Pacific H.	Sport/Util.	Twin cylinder, 34kW	3.5	1.9	265	19.4	n/a	200

The expert system will find the matching craft's length and width from the knowledge base after users input the total craft weight. For better estimation of these two parameters, more than 70 data sheets of existing ACVs manufactured in the past are researched and summarized. In Figure 2.9 and Figure 2.10, small dots represent the data set for each ACV collected. The author found the correlation among those dots and produced the curves with power approximation. The horizontal axis of each figure is log-scaled due to a wide range of craft's weights.

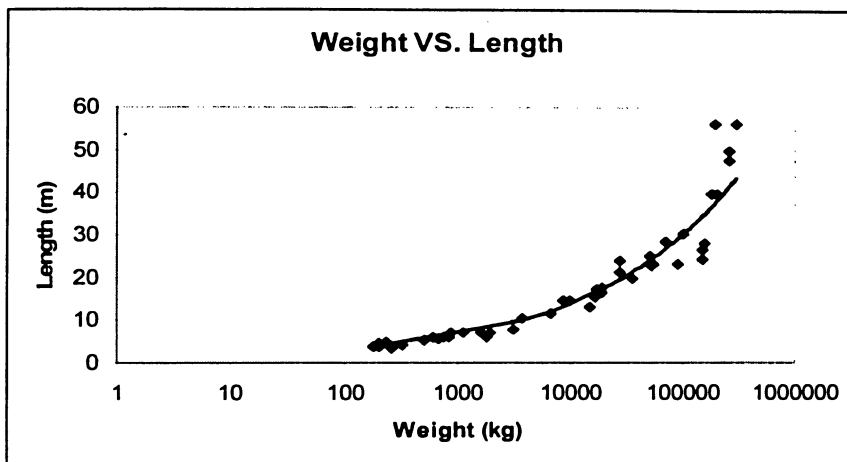


Figure 2.9: Approximated curve in the relation of craft's weight and length

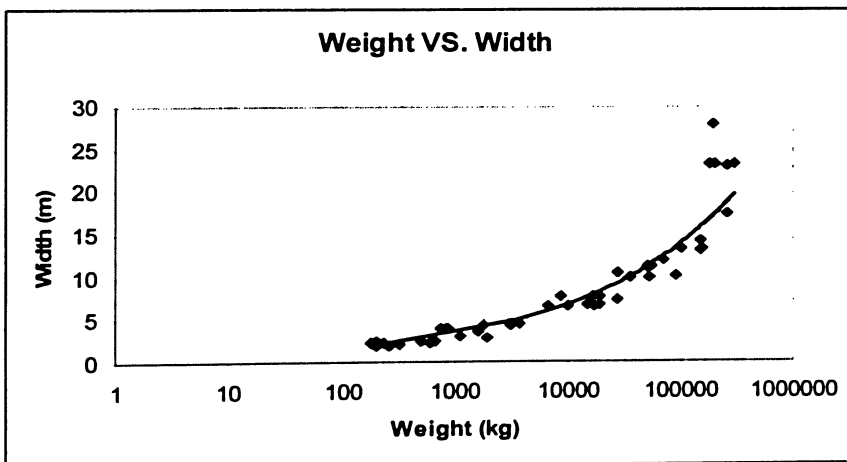


Figure 2.10: Approximated curve in the relation of craft's weight and width

The second step of design process is to decide the general weight distribution within the given total craft weight. Since weight distribution is very difficult to define in the consistent outline, there are many different guidelines available in each country. In this thesis, the weight distribution rule is referred in the terminology of the U.S. Navy Ship Work Breakdown Structure (SWBS) [1,4]. The weight of ACVs is generally separated into the two different parts. They are the Light ship part and Load part.

In Light ship part, there are mainly seven different elements consisted. They are the Structure group, Propulsion group, Electrical group, Command and Surveillance group, Auxiliary System group, Outfit and Furnishings group, and Armament group. In Load part, there are also several groups presented such as crew and provisions, stores and fresh water, disposable payload, and fuel. Thus the total craft weight is the sum of the weights from the seven groups in Light ship part and from the four groups in Load part. Table 2.2 shows the typical weight distribution of ACVs in SWBS.

Table 2.2: Weight distribution of ACVs in SWBS

<b>ACV Weight Distribution</b>	
<b>Light ship</b>	<b>Load</b>
Structure	Crew and Provisions
Propulsion	Stores and Fresh water
Electrical	Disposable payload
Command and Surveillance	Fuel
Auxiliary System	
Outfit and Furnishings	
Armament/Equipments	

The following equations for weight distribution are formulated based on the past trends and common design rules [4].

### 1) Structural weight

$$\frac{W_1}{W} = \frac{0.28}{W^{1/3}} + \frac{0.04W^{1/3}}{(0.0064Pc/\sqrt{s})^{1/3}} \quad \text{if } 0.0064 \times \frac{Pc}{\sqrt{s}} \text{ is near } 0.5 \quad (2.1)$$

$$\frac{W_1}{W} = 0.24 + \frac{0.007W^{1/3}}{(0.0064Pc/\sqrt{s})^{1/3}} \quad \text{if } 0.0064 \times \frac{Pc}{\sqrt{s}} \text{ is near } 1.0 \quad (2.2)$$

$$\frac{W_1}{W} = 0.21 + \frac{0.008W^{1/3}}{(0.0064Pc/\sqrt{s})^{1/3}} \quad \text{if } 0.0064 \times \frac{Pc}{\sqrt{s}} \text{ is near } 2.0 \quad (2.3)$$

where  $\frac{Pc}{\sqrt{s}}$  is cushion density in  $N/m^3$ ,

$Pc$  is cushion pressure in  $N/m^2$ ,

$s$  is cushion area in  $m^2$  ( $= \text{length} \times \text{width}$ ),

$W$  is total vehicle weight in tons.

### 2) Propulsion System weight

$$\frac{W_2}{W} = \frac{W_2}{P} (3.28V) \left( \frac{1}{550 \text{Transport\_Efficiency}} \right) \quad (2.4)$$

where  $P$  is total power (kW),

$V$  is maximum velocity (m/s),

$$\frac{W_2}{P} = 1.25 + \frac{74}{\sqrt{P/0.7457}}$$

### 3) Electrical System weight

$$\frac{W_3}{W} = 0.00034W^{1/2} + \frac{0.10}{W^{1/2}} \quad (2.5)$$

#### 4) Command and Surveillance weight

$$\frac{W_4}{W} = \frac{0.14}{W^{1/3}} - \frac{W_3}{W} \quad (2.6)$$

#### 5) Auxiliary System weight

$$\frac{W_5 - W_{L_s}}{W} = 0.0024W^{1/3} + \frac{0.06}{W^{1/3}} \quad (2.7)$$

$$\text{where } \frac{W_{L_s}}{W} = 0.044 + \frac{0.08}{W^{1/3}} \text{ (from total lift system)}$$

#### 6) Outfit and Furnishings weight

$$\frac{W_6}{W} = 0.003W^{1/3} + \frac{0.07}{W^{1/3}} \quad (2.8)$$

#### 7) Armament/Equipments

$$\frac{W_7}{W} = \frac{0.50}{W^{1/3}} \quad (2.9)$$

#### 8) Load weight

$$W_L = W - W_E = W - (W_1 + W_2 + W_3 + W_4 + W_5 + W_6 + W_7) \quad (2.10)$$

In the parametric study, the expert system will perform the computation of main parameters with the given relationships. The relationships are from the equations established in many literatures and statistical data, and they are stored in the knowledge base components. The purpose of this computation is to find the general characteristics of

ACVs within the given main dimensions and weight, so that the design can further be developed from the known characteristics. The subsystem components can also be built based on this parametric study.

The first parameter being analyzed is the cushion pressure. It is obtainable from the relationship of the vehicle's total weight and its cushion area. The cushion area can be computed from the cushion length and width. In this thesis, the length and width of craft are approximated to the cushion length and width, even though the overall dimensions are slightly larger than the cushion dimensions of vehicle. The following equation describes general relationship of the cushion pressure and main dimensions of ACV.

$$P_c = \frac{W_{Total}}{Length \times Width} \quad (2.11)$$

where  $P_c$  is the cushion pressure in Pa,

$W_{Total}$  is the total craft weight in N.

The next parameter is the cushion flow which passes through the skirt and escapes out to the atmosphere. It is important to determine the proper amount of air flow, since too much of air flow costs more than enough in lift power system. In computation of cushion flow, the true leakage area beneath the skirt and the effect of stability and vehicle's performance due to the flow should be carefully studied in order to obtain the proper amount of cushion flow. The complexity of skirt motion is also one of the factors that give difficulty in determining the proper cushion flow. However for the initial stage of designing ACVs, it could be referred from the past data available. It shows the relationship of the nominal air gap with the vehicle's gross weight [4].

$$\frac{h}{L} = \frac{0.014}{(1.1W)^{1/3}} \quad (2.12)$$

where  $h$  is the air gap in m,

$L$  is the vehicle's cushion length in m.

The power requirement is another important parameter for the calculation and design of lift and thrust systems of the vehicle. This parameter is related to many factors of vehicle's characteristics such as craft size, speed, stability, performance aspect, and so on. However, the relationship of total power and total weight could be obtainable from the past trend and statistical data. Since the trend for total power requirement is useful only for the initial design stage, it is necessary to find the accurate value when the design process is further developed for various missions. Figure 2.11 shows the relationship of total power and craft's total weight. The power approximation is again applied to obtain the correlation. The x-axis is also log-scaled for a wide range of weights.

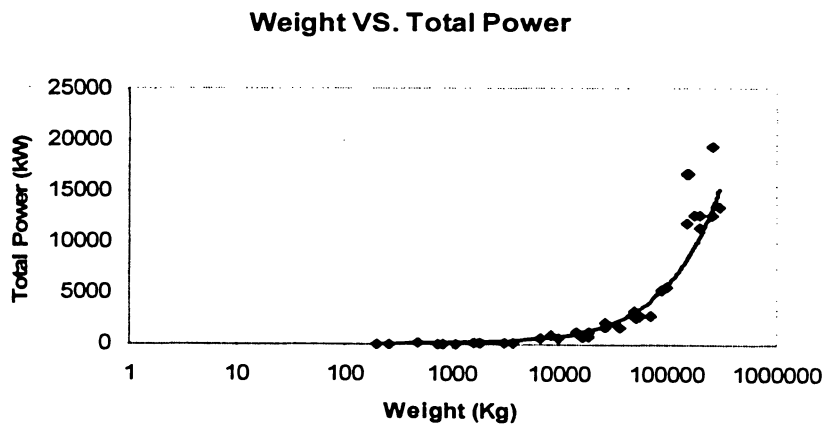


Figure 2.11: Approximated curve in the relation of craft's weight and total power

The next one is the transport efficiency that is the ratio of work done by the vehicle in moving the overall weight at a given speed and the total power requirement. The transport efficiency is given by the following equation.

$$\text{Transport Efficiency} = \frac{(1800W)(3.28V \text{ max})}{(550P/0.7457)} \quad (2.13)$$

where  $V \text{ max}$  is maximum speed in m/s,

$P$  is total power in kW.

In this section, the main dimensions were obtained, and the weight distribution and parametric study were performed. Now it will move on the second category “Main Subsystem Design” in the following section. All the values computed in this section will be passed down to the “Main Subsystem Design” category due to the characteristic of frame-base knowledge representation. Figure 2.12 describes the design process performed up to here with input parameters.

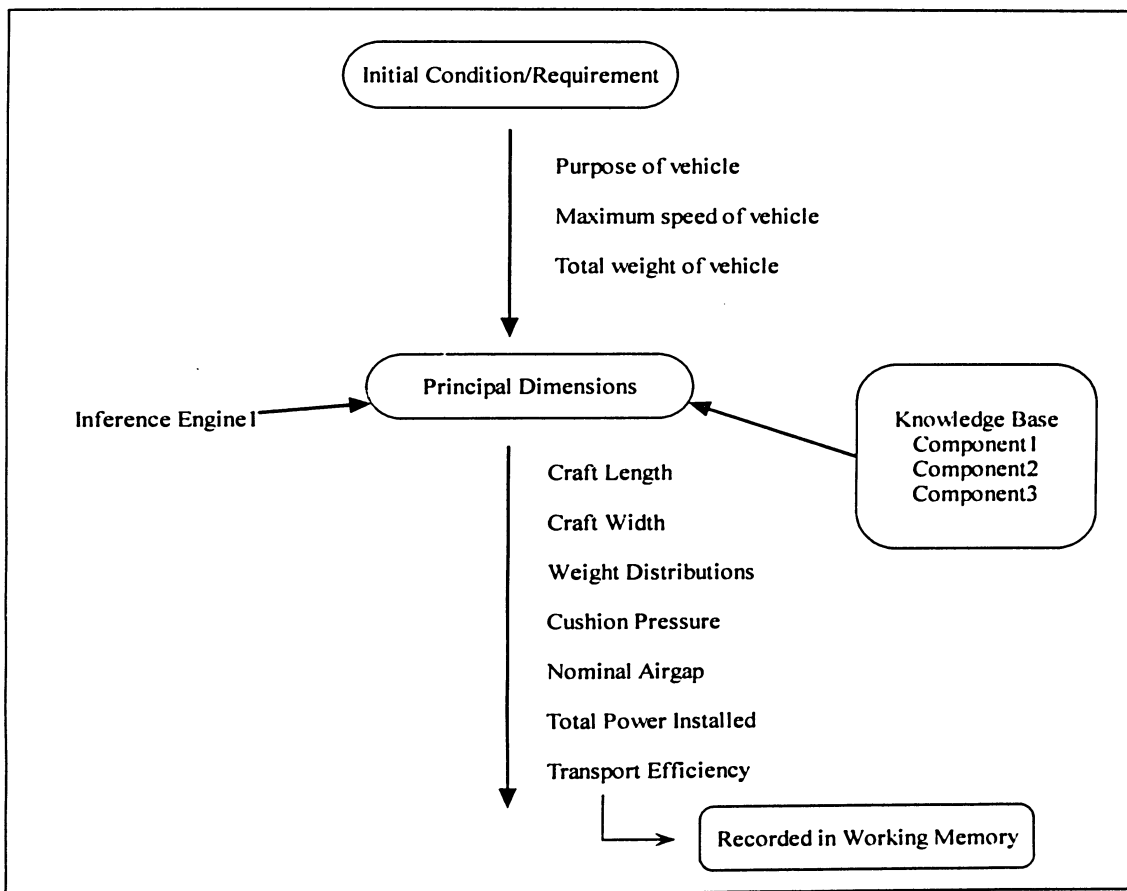


Figure 2.12: Design progress with determination of principal dimensions

## 2.6 Main Subsystem Design

Lift system in ACVs is very important and essential part of the overall design process, because the vehicles are supported by the air produced from the lift system. In other words, the dynamics, stability, and maneuverability of the vehicles are mainly characterized by the lift system and its properties. The lift system for the best characteristics of vehicle including stability and ride quality should provide the sufficient cushion pressure in order to support the vehicle over the various obstacles. It should also generate enough flow to reduce the drag and to create the better maneuverability. All these properties of the system are largely decided by the natures of selected fan. Hence in lift system design, the expert system will mainly focus on selection process of the proper fan which satisfies the given characteristics of ACVs.

Lift fan should be able to produce the sufficient pressure rise in order to compensate the dynamic losses through the various sections in lift system and to generate the required cushion pressure. Once the total pressure across the fan is known, then the total fan efficiency can be computed with the flow rate and power supplied to the fan. Finally the lift system efficiency is obtainable from the cushion pressure, total fan pressure, and total fan efficiency.

$$\eta_t = \frac{H_f Q}{P} \quad (2.14)$$

$$\eta_t = \frac{P_c}{H_f} \times \eta_t \quad (2.15)$$

where  $\eta_t$  is total fan efficiency,

$H_f$  is pressure rise across the fan,

$Q$  is flow rate,

$P$  is power supplied to the fan,

$\eta_l$  is lift system efficiency,

$P_c$  is cushion pressure.

The selection for fan should be made based on the above properties as well as the economic consideration. This means that the fan should produce the sufficient pressure and flow rate at minimum power consumption. Some parameters need to be estimated for the selection process of proper fan. They are the coefficients of pressure and flow.

Pressure Coefficient:

$$\psi = \frac{P}{\rho n^2 D^2} \quad (2.16)$$

Flow Coefficient:

$$\phi = \frac{Q}{nD^3} \quad (2.17)$$

where  $P$  is pressure rise in the fan,

$\rho$  is air density,

$n$  is fan rotational speed,

$D$  is fan maximum diameter.

Then the specific speed and specific diameter for fan can further be established from the pressure and flow coefficients.

Specific Speed:

$$N_s = \frac{\phi^{1/2}}{\psi^{3/4}} = \frac{nQ^{1/2}}{(P/\rho)^{3/4}} \quad (2.18)$$

Specific Diameter:

$$D_s = \frac{\psi^{1/4}}{\phi^{1/2}} = \frac{D(P/\rho)^{1/4}}{Q^{1/2}} \quad (2.19)$$

They are in non-dimensional form and describe the fan property with respect to unit pressure and unit flow. From the past experience and statistical data, the empirical relationship [4] between specific speed and specific diameter could be established in the following form.

$$Ds = 0.90 + \frac{2}{Ns} \quad (2.20)$$

Moreover, the total fan efficiency is also written in the function of specific speed.

$$\eta_t = 0.85 - 0.02Ns \quad (2.21)$$

Fan can be designed and built to the required specification by the specialist and suppliers, or commercially available kinds can also be utilized directly. There are three common fans manufactured such as the Centrifugal fan, Axial flow fan, and Mixed flow fan. A centrifugal fan provides the high pressure at small flow rates, while axial flow fan generates a large flow but relatively low pressure. The character of mixed flow fan is somewhat in middle of centrifugal fan and axial flow fan. Then the specific speed [4] guides for the selection of proper fan such that if it is less than three, centrifugal fan is appropriate. Otherwise axial flow fan is generally chosen. A mixed flow fan can be selected for the range close to three of specific speed. The noise level, weight, size of fan and engine are also important factors when the lift system is designed. The following figure describes the fan selection process.

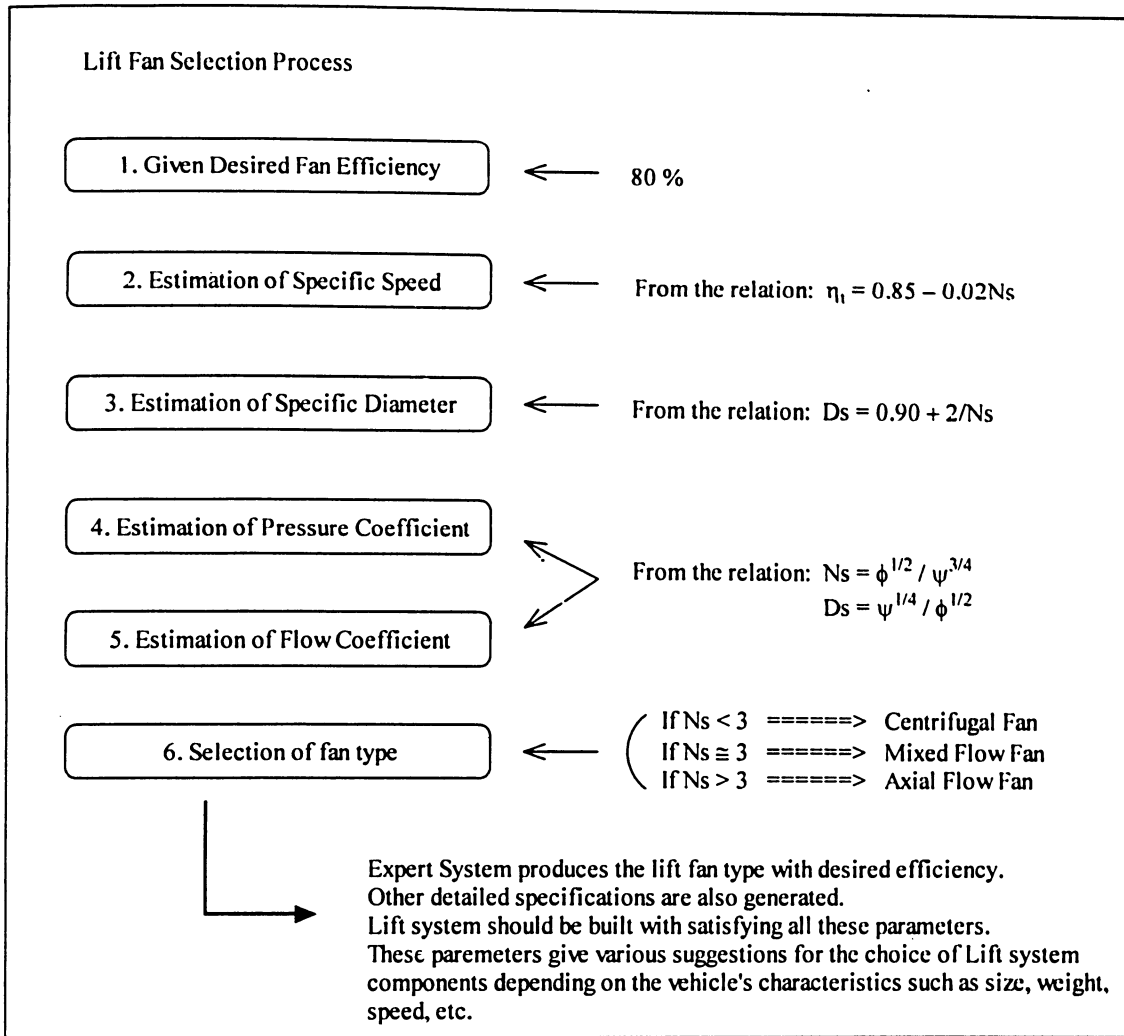


Figure 2.13: Lift fan selection process

The propulsion system has been developed in several forms since the early development years of ACVs. Many different methods have been applied for the propulsion system such as water propulsion, track and wheel systems, etc. However most of them except air propellers and gas turbine system have failed to implement due to a lack of efficiency. The propulsion system is designed with the consideration of efficiency, reliability, weight, and economic point of view. The combination of air propellers and gas turbine system satisfies the above considerations in somewhat more than other propulsion systems. Thus air propellers and gas turbine system have currently become the most

widely used in ACV's propulsion system. A good propulsion system should be able to demonstrate some characteristics with respect to its primary functions [1]. First of all, it should propel the vehicle at the desired speeds at proper thrust generation. Secondly it is required to provide the necessary acceleration and deceleration for the desired maneuverability and safety purposes. The propulsion system could also participate in the directional control by generating the necessary thrust vectoring.

In this thesis work, the expert system will focus on the design of propulsion system with combination of air propellers and gas turbine system. For air propellers, the efficiency is usually achieved more than 55 percent. The maximum efficiency, however, can go up to more than 65 percent with the proper vehicle's speed. For gas turbine system, it has several unique advantages. For example, there is no need to build the separate energy source, since the engine is already installed for the lift system. Thus the propulsion unit and lift system unit can share the same power source. The alternative choice for propulsion engine can be made with a diesel engine. Diesel engine is more appropriate for smaller ACVs because it generally produces less power than gas turbine system.

The skirt determines the vehicle's dynamic responses on rough sea condition or over other terrains. The cushion system provides the adequate cushion pressure in order to lift the vehicle over the obstacles and irregular surfaces. Hence the design of skirt and cushion system should be carried out for the desired characteristics of vehicle's responses. The main functions of skirt and cushion system is to provide the sufficient cushion pressure so that it can raise the vehicle above the certain height, depending on the obstacles. The system also contributes to the stiffness and damping of the air cushion so

that it can act like a suspension system and help the dynamic responses of vehicle. Finally the skirt and cushion system improve the dynamic stability in pitch, roll, and heave motions of vehicle. In order to design the skirt and cushion system, it is necessary to analyze the forces acting on the skirt with the fluid interaction caused by lift fan system. Since this process is quite complicated, the actual analysis for the skirt and cushion system design will be omitted in this work, but it will be applied in the second part of the thesis that is the optimization of skirt system with GA.

In this section, main subsystems have been designed with expert system. Among three subsystems such as lift system, propulsion system, and skirt and cushion system, design of lift system is mainly focused and other systems are simply selected with most commonly used components in the real world. Hence other subsystems will be improved in later development of expert system with more detailed specifications. Figure 2.14 shows the design of main subsystem.

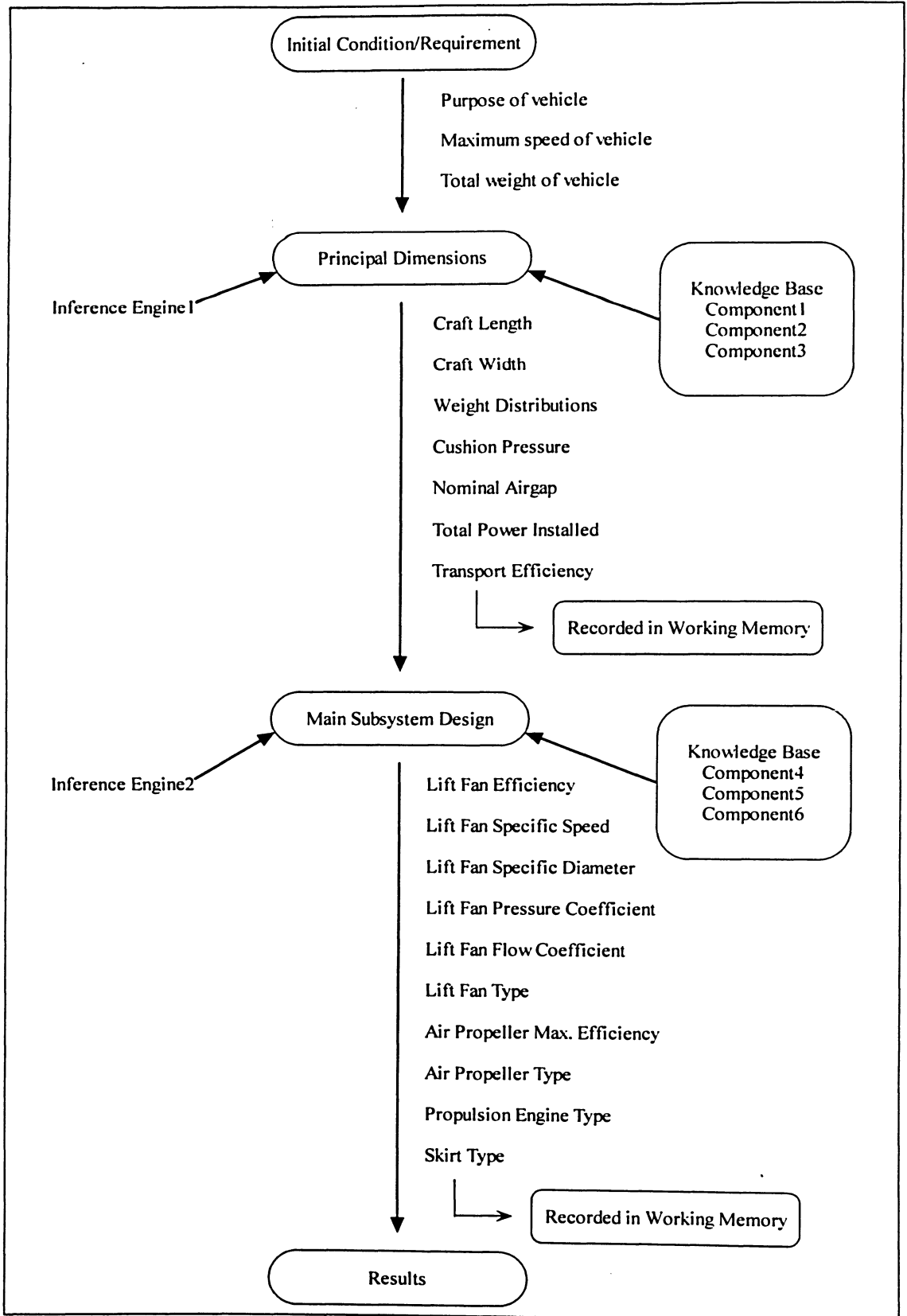


Figure 2.14: Design progress with main subsystem design

## 2.7 Tests of Expert System

The program codes for expert system on initial design of ACVs has been built and tested in this thesis. The results are compared with the existing vehicles, the CCG Waban-Aki and U.S. Navy's LCAC. The given design parameters such as vehicle total weight, maximum speed, and purpose of the vehicle are inputted in order to initiate the expert system. Then expert system produces the general information including the vehicle's initial parameters and weight distributions. It furthermore establishes the initial configuration of several subsystems of the vehicles based on the design components introduced in earlier section. The following tables are the results of tests from expert system on the two different ACVs, the CCG Waban-Aki and LCAC.

Table 2.3: Results of expert system on Waban-Aki

	<b>Waban-Aki</b>	
<b>Input Parameters</b>		
Craft Mass (Kg)	36,740	
Purpose	Utility	
Maximum Speed (m/s)	25.8	
	<b><i>Expert System</i></b>	<b><i>Original System</i></b>
<b>General Information</b>		
Speed Category	Medium	Medium
Craft Length (m)	21.6	21.0
Craft Width (m)	10.2	8.6
Cushion Pressure (Pa)	1,637	n/a
Nominal Airgap	0.0041	n/a
Total Power (kW)	2,442	1,760
Transport Efficiency	3.11	n/a
<b>Weight Distribution</b>		
Structural (Kg)	8,582	n/a
Propulsion System (Kg)	4,626	n/a
Electrical System (Kg)	682	n/a
Command and Surveillance (Kg)	865	n/a
Auxiliary (Kg)	3,457	n/a
Outfit and Furnishings (Kg)	1,140	n/a
Armament/Equipments (Kg)	5,526	n/a

Light ship Weight (Kg)	24,878	24,290
Load Weight (Kg)	11,862	12,450
<b>Lift System</b>		
Fan Efficiency	0.8	n/a
Specific Speed	2.5	n/a
Specific Diameter	1.7	n/a
Pressure Coefficient	0.0554	n/a
Flow Coefficient	0.0814	n/a
Fan Type	Centrifugal	Centrifugal
<b>Propulsion System</b>		
Max. Efficiency of Air Propeller	0.65	n/a
Type of Propeller	Shrouded	Shrouded
Propulsion Engine	Gas Turbine	Gas Turbine
<b>Skirt and Cushion System</b>		
Skirt Type	Bag - Finger	Bag - Finger

Table 2.4: Results of expert system on LCAC

	LCAC	
<b>Input Parameters</b>		
Craft Mass (Kg)	150,000	
Purpose	Military	
Maximum Speed (m/s)	20.6	
	<i>Expert System</i>	<i>Original System</i>
<b>General Information</b>		
Speed Category	Medium	Medium
Craft Length (m)	34.6	27.0
Craft Width (m)	15.9	14.0
Cushion Pressure (Pa)	2,684	n/a
Nominal Airgap	0.0026	n/a
Total Power (kW)	8,268	11,600
Transport Efficiency	2.99	n/a
<b>Weight Distribution</b>		
Structural (Kg)	43,250	n/a
Propulsion System (Kg)	12,029	n/a
Electrical System (Kg)	1,849	n/a
Command and Surveillance (Kg)	2,103	n/a
Auxiliary (Kg)	12,465	n/a
Outfit and Furnishings (Kg)	4,367	n/a
Armament/Equipments (Kg)	14,116	n/a
Light ship Weight (Kg)	90,179	95,569
Load Weight (Kg)	59,821	54,431
<b>Lift System</b>		

Fan Efficiency	0.8	n/a
Specific Speed	2.5	n/a
Specific Diameter	1.7	n/a
Pressure Coefficient	0.0554	n/a
Flow Coefficient	0.0814	n/a
Fan Type	Centrifugal	Centrifugal
<b>Propulsion System</b>		
Max. Efficiency of Air Propeller	0.65	n/a
Type of Propeller	Shrouded	Shrouded
Propulsion Engine	Gas Turbine	Gas Turbine
<b>Skirt and Cushion System</b>		
Skirt Type	Bag - Finger	Bag - Finger

As seen in tables, the errors between the original system and expert system for craft length and width in Waban-Aki are found as 2.9 % and 18.6 %, respectively. The errors of these parameters in LCAC are computed as 28.1 % and 13.6 %, respectively. Thus some parameters are found close to the original dimensions, while the other parameters are somewhat different from the original values. The improvement for these errors is recommended in the following section 2.8. Nevertheless overall estimations provide the helpful guideline for beginners in an initial design phase by showing the rough idea about the initial shape and configurations. These dimensions could be re-generated in more accurate values with more collected data sets. In the case of total power installed, the values predicted from expert system are different compared to the original system as much as 38.9 %. As explained in the previous section, the total power can be calculated for the specific missions or purposes in preliminary design phase. Hence the total power found from expert system needs to be accurately corrected when the design process is further developed. However expert system still predicted the total power that may give some estimation and idea for designers in an initial design stage.

Once the general information was created for Waban-Aki and LCAC, the weight distribution was made for these ACVs. As expected, the structural weight is the heaviest component in the total weight distribution. Moreover a component of load weight takes almost 35 % of total vehicle's weight. This percentage for load weight is reasonable and easily found in several ACVs manufactured in the past. The error made in load weight between the original system and expert system was 4.7 % and 9.9 % for Waban-Aki and LCAC, respectively. Hence the expert system produced reasonably close value to the original load weight for both ACVs.

For the design of lift system, the expert system computed the fan efficiency, specific speed, specific diameter, pressure coefficient, and flow coefficient based on the general trend and design rules. Then within those parameters, it selected the specific type of lift fan. The centrifugal fan was chosen by expert system in this test. This type of fan is also utilized for real manufactured Waban-Aki and LCAC vehicles. Hence the expert system produced the precise choice for the lift fan as what human experts would do in the real world. The propulsion system was also designed with the expert system and compared with the existing ACVs. However the choices for propulsor and engine were simply selected as an air propeller and gas turbine. The detailed specification could be designed based on the characteristics of ACVs such as mission, purposes, available system and components, financial affordability, environmental restrictions, and so forth. The efficiency of propulsion system was set according to the general trend and recommendation. For the design of skirt and cushion system, bag and finger skirt was again simply selected by expert system because it is currently the most updated and advanced form of skirt system.

## **2.8 Discussion and Recommendation**

Expert system designed the initial configuration of ACVs within the given constraints. Some of parameters showed somewhat different values from the original values, but they still provided the useful guideline and estimation for initial design phase. In order to make them more accurate, more data sets need to be collected and design rules should be updated with newly developed ACVs. Overall performance of expert system is reasonably satisfactory, and it helps designers in an initial design stage with showing the rough configurations of vehicle. In order to build more detailed and complete expert system for the initial design of ACVs, some recommendations are described as follows.

1. It showed the strong correlation for small and medium size vehicles in overall dimension estimations (in the estimation of craft length and width with respect to total craft weight), while weak relationship was revealed for large size vehicles. Hence ACV database for large size vehicles needs to be reinforced with more collected data sets.
2. In vehicle's weight distribution, the main weight components can be divided into more specified subcomponents so that it can make it easier for designers to build such systems with well distributed weight restrictions. It will also reduce the errors in weight estimations.
3. For parametric study, a few selected parameters carried out for the estimation in order to depict the characteristics of vehicles. The more parameters need to be studied in order to describe the complete nature of vehicles.

4. In lift system design, it performed the simple fan characteristics and type of lift fan. In later development, the database related to commercial lift fan manufacturers and their specifications can be collected and implemented to the selection process of lift fan with detailed description and availability.
5. In propulsion system design, the dimensions, type, design speed, static thrust, and material of air propellers can be further developed with expert system in future research work for complete propulsion system.
6. Skirt and cushion system design was simply selected as a bag and finger skirt in this thesis work. For recommendation for improved design, it is necessary to determine the detailed dimensions and specification of the bag and finger skirt. For example, finger length, number of fingers, number of orifices used for air flow paths, dimensions of bag section, and material are such elements. They could also be optimized for better performance of the vehicles. This is done with the GA technique in next chapter.
7. In the codes of expert system, the module of explanation may be built and implemented so that users can have better understanding about how the solutions are produced.

### 3. OPTIMIZATION OF SKIRT SYSTEM WITH GA

#### 3.1 Overview of Skirt Optimization with GA

The skirt system of ACVs is optimized with the GA for improved ride quality and stability as second part of the thesis work. The specific program codes have been written to implement the GA for skirt optimization. The procedure is described as follows. At the beginning of optimization process, design constraints or initial conditions are inputted in order to initiate the performance. The given design restrictions are the total vehicle mass and the dimensions of ACV hard structure;  $M_c$ ,  $L_c$ ,  $B_c$ ,  $D_b$ , and  $H_b$ . These parameters should be fixed during the optimization process. Figure 3.1 shows the parameters for the

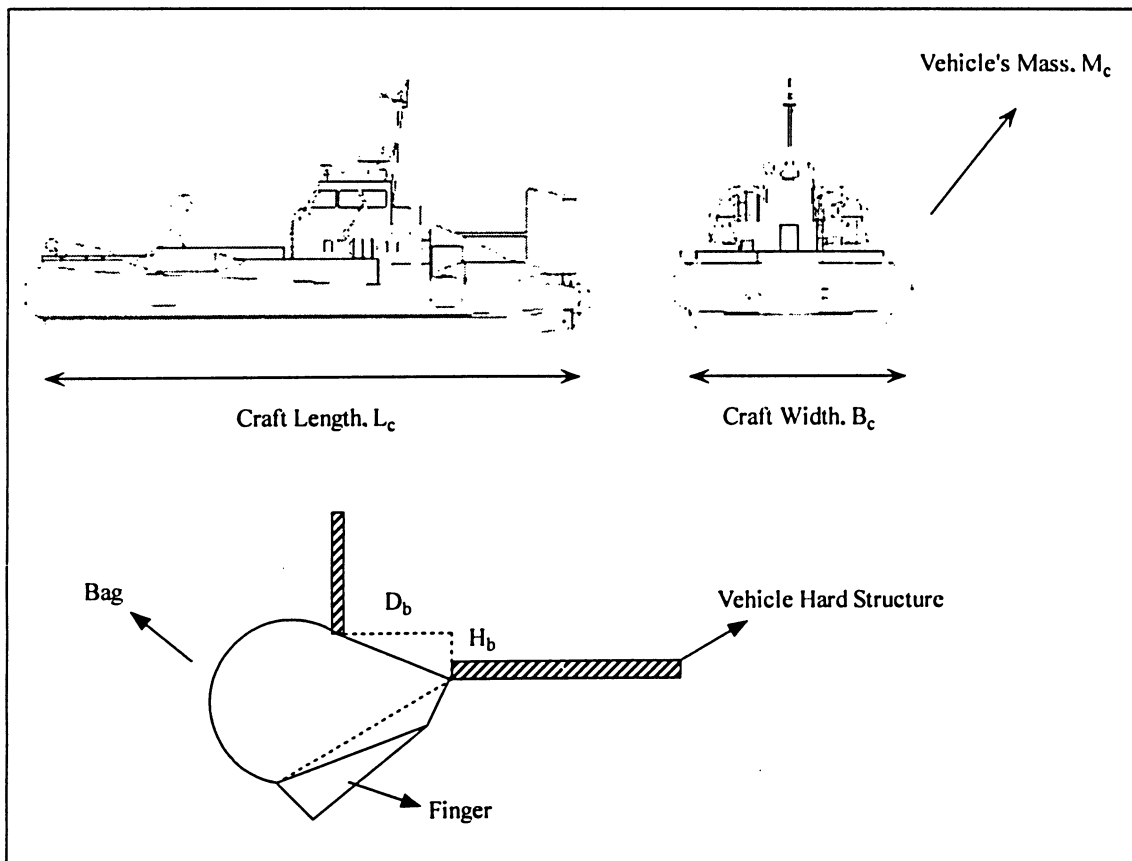


Figure 3.1: Design restrictions for ACVs

design restrictions. Then the GA produces more estimated parameters based on the given design restrictions in order to obtain the vehicle's characteristics such as system matrix, frequency response curves, and other important properties. The linearized equations of motion at equilibrium point are used for prediction of vehicle's behavior. After that, the GA is implemented to optimize the skirt system for improved ride quality and stability. The targeted parameters to be optimized for better performance of the vehicle are the dimensions of outer bag and inner bag, and the pressure ratio of bag and cushion;  $L_1$ ,  $L_2$ ,  $L_3$ ,  $L_4$ ,  $L_{ob}$ , and  $p_b/p_c$ . Figure 3.2 illustrates these parameters. Then the GA will produce the best values for these parameters with its main components. For the validation of test results, two existing ACVs are demonstrated for skirt optimization. Figure 3.3 describes the overall process of the GA on skirt optimization.

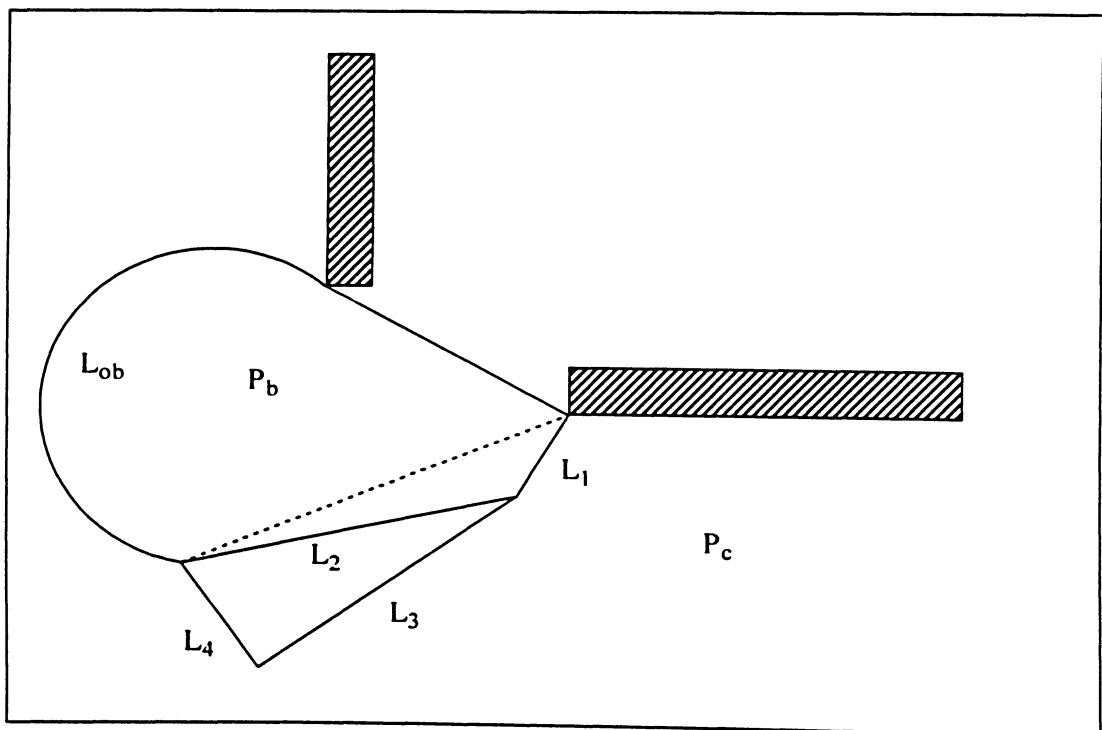


Figure 3.2: Design parameters to be optimized

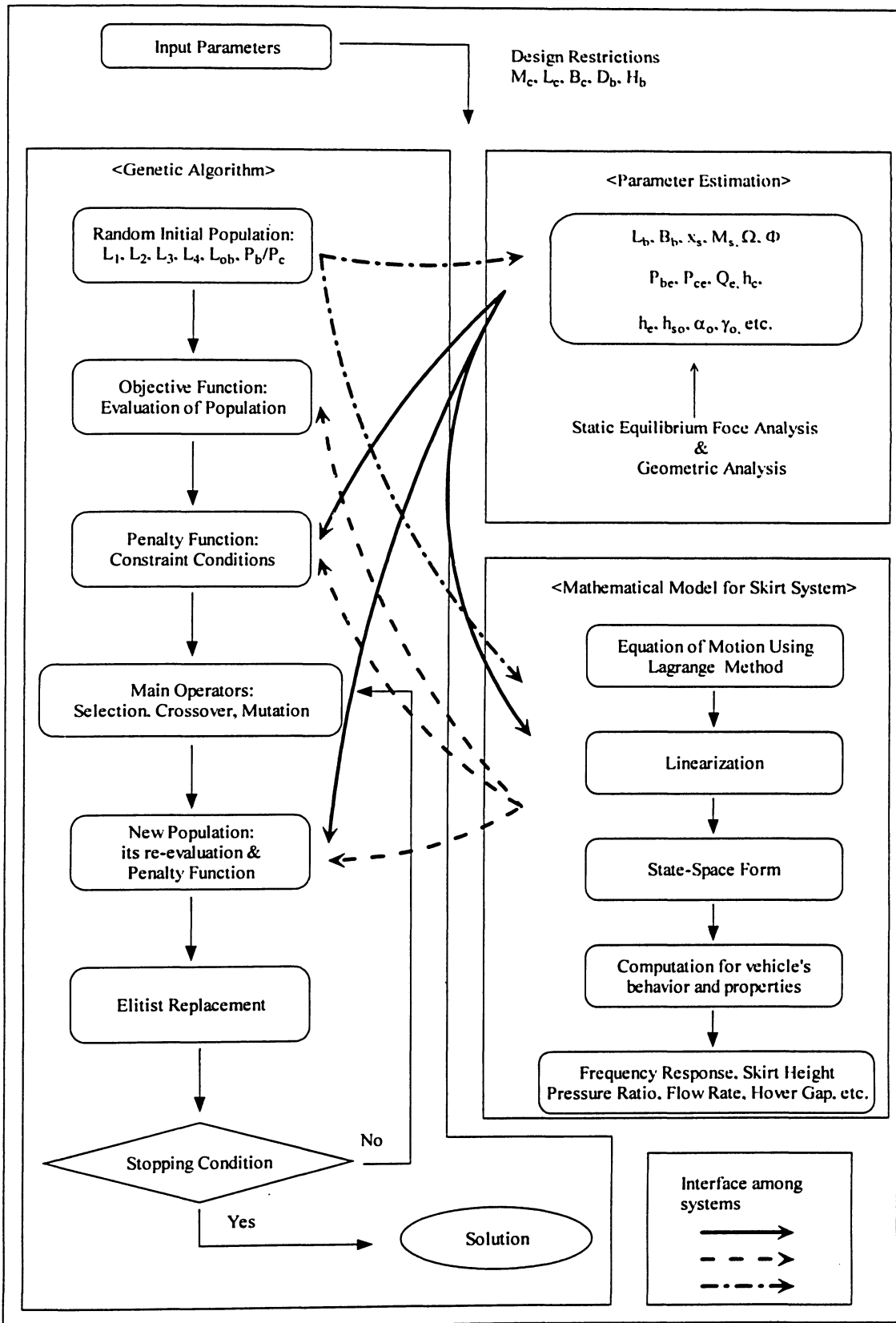


Figure 3.3: Overall process of the GA on skirt optimization

### 3.2 Code Development for GA and Skirt System with MATLAB

The codes were developed in MATLAB in order to implement the GA for the optimization of skirt system of ACVs. Since the optimization process for ACVs bag and finger skirt system is quite complex, the codes were developed under several categories. Then the main source code operates the entire system by interfacing with other source codes in different categories. Finally it will produce the optimized skirt system for improved ride quality and stability. The followings are the list of codes built and applied for the skirt optimization with the GA.

#### Genetic Algorithm Codes

GA.m	Main source code initiating the optimization process
input_data.m	Initial conditions for GA are inputted (Population size, Maximum number of generations, Coefficient of penalty, Coefficient of elitist, etc.)
initial_pop.m	Initial population is randomly generated
decode.m	Binary coded potential solutions are decoded into actual values
objfunction.m	Population is evaluated by objective function with linearized equations of motion for skirt system Penalty function and rank function are also included
rsselect.m	Remainder Stochastic Sampling method is applied
point_cross.m	Single point crossover is performed
two_point_cross.m	Two point crossover is performed
random_cross.m	Random crossover is performed

single_mut.m	Single bit mutation is performed
two_mut.m	Two bit mutation is performed
elitist.m	Best portion of population is reserved without any destruction
output_data.m	Best optimized solution is recorded in this file

### **Parameter Estimation Codes**

input_para.m	Input parameters are estimated in this file
static_cond.m	Parameters $H_{co}$ , $\alpha_o$ , $Q_{co}$ , $\gamma_o$ at equilibrium conditions are computed
equilibrium_equations.m	Equilibrium equations used for static force analysis on skirt system

### **Linearized Equations of Motion Codes**

deri_elem.m	Derivatives at equilibrium conditions are presented
state_space.m	State-space form of linearized equations is obtained
bode_plot.m	Bode plot and eigenvalues are computed

### **Other Source Codes**

drawing.m	Optimized and original skirt shapes are drawn
input_file1.m	Original properties of skirt system is recorded
input_file2.m	Optimized properties of skirt system is recorded
rnd.m	An integer between low and high boundaries is randomly generated
flip.m	Integer 1 or 0 is randomly generated

These GA codes have been developed in long period of time and many modifications and additions of advanced GA components have carried out during the research period. In order to validate the GA codes, several experiments and tests have been performed. Those experiments ranged from a simple function optimization to complicated optimization problems. For example, airline fleet assignment and landing sequence of aircrafts were demonstrated with the GA codes [17,30]. Furthermore, optimization of cantilever beam was also tested with the GA codes by the author. Hence these GA codes are very genuine with the author's great effort contributed to the development of codes from the beginning to the modification, enhancement, tests, and validation. The following sections will describe some of the components implemented in the skirt optimization. Figure 3.4 illustrates the flow chart for the interaction of the program codes.

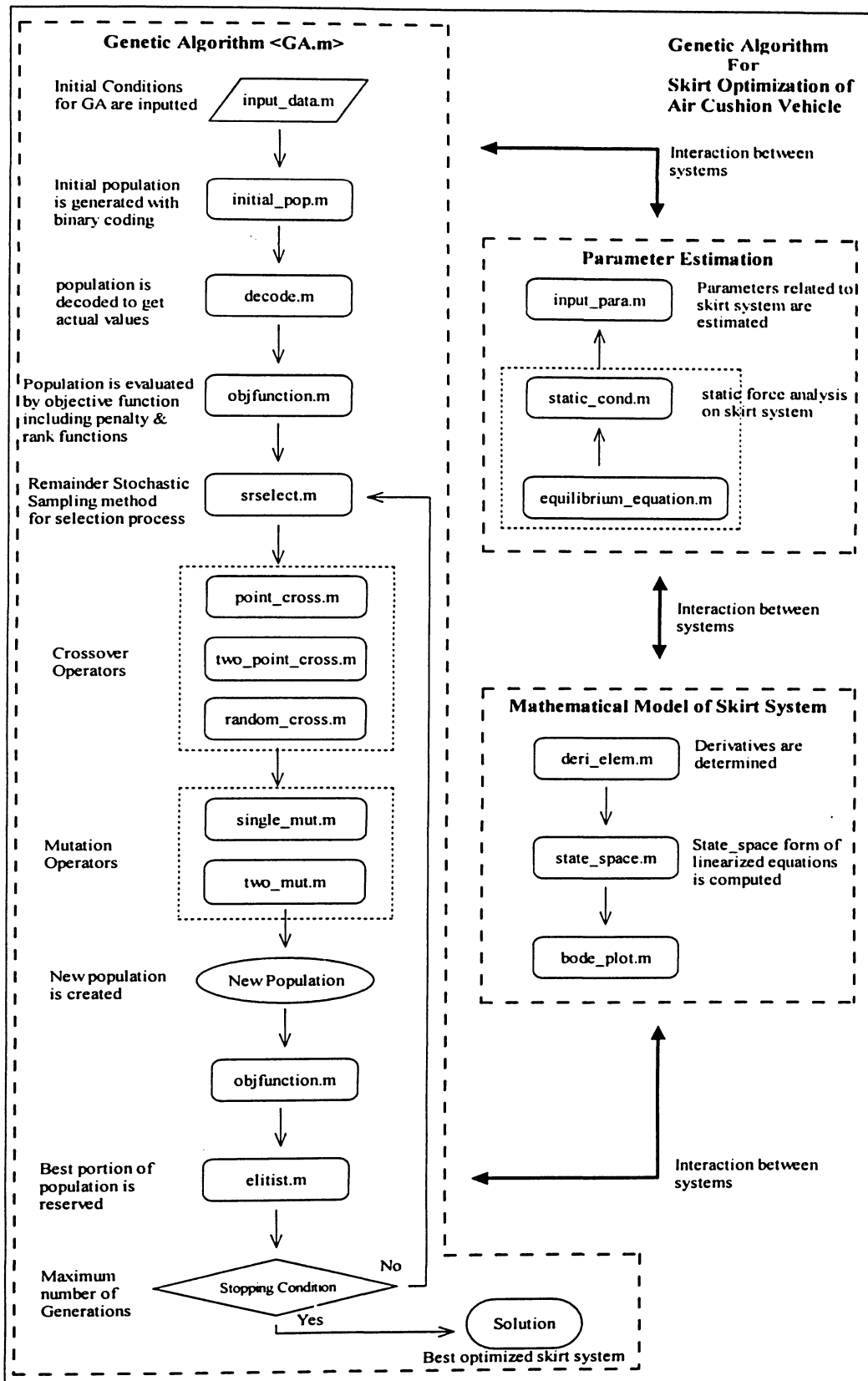


Figure 3.4: Flow chart of program codes for the GA and skirt system

### 3.3 Model of the Bag and Finger Skirt

The model of the Bag and Finger skirt system involves the consideration of dynamic behavior of the skirt structure, the fluid mechanical processes in the cushion and air supply system, and the vehicle dynamics combined with the interaction of all three. The skirt material effects can also play a role in skirt dynamics [31], and the geometry of the typical cushion can be complex, and the skirt geometry can undergoes large changes during the vehicle motion. Furthermore, to adequately describe the cushion air escape process, the model must account for intermittent skirt-surface contact around the craft periphery arising from craft motion and from wave action; this can have major effects on the dynamics. Hence, some assumptions [23,32] are applied to simplify the formulation and analysis.

The geometry of skirt is determined by static equilibrium of forces, considering the skirt as a two dimensional section of an inflated membrane. Since very little lateral curvature exists in the skirt except for the skirt corners, the model is restricted to the two-dimensional representation [3]. It is also assumed to undergo the pure heave motion at constant speed over long waves without pitch, roll, and yaw. In this case the surface disturbance or ground motion is equivalent to a flat horizontal surface moving in pure heave under the cushion, and the resultant craft motion in the vertical plane can also be assumed to be pure heave. The sliding friction between the skirt and ground is ignored. The model is also assumed to be symmetrical and confined to move in a plane parallel to a cross section of the model. Finally the outer bag is assumed to form the arc shape all the time for the simplification of model. Furthermore since the ratio of bag pressure to

material surface weight per unit area is usually large, the outer bag can be assumed to be a massless inelastic and subject to a spatially uniform bag pressure.

The model is mainly consisted of three distinct parts that are outer-bag, inner-bag, and fingers. The air flow generated from the lift fan first goes to the bag, and it escapes to the atmosphere through the fingers. The inner bag is supported by the two rigid links that are assumed to be massless. The two rigid links are capable of forming the different angles with respect to horizontal level, and one end of each link is connected together. The mass of skirt is concentrated at the centroid of the finger and its location can be determined by the geometric parameters of skirt. Figure 3.5 depicts the simplified mathematical model of two dimensional section of the bag and finger skirt.

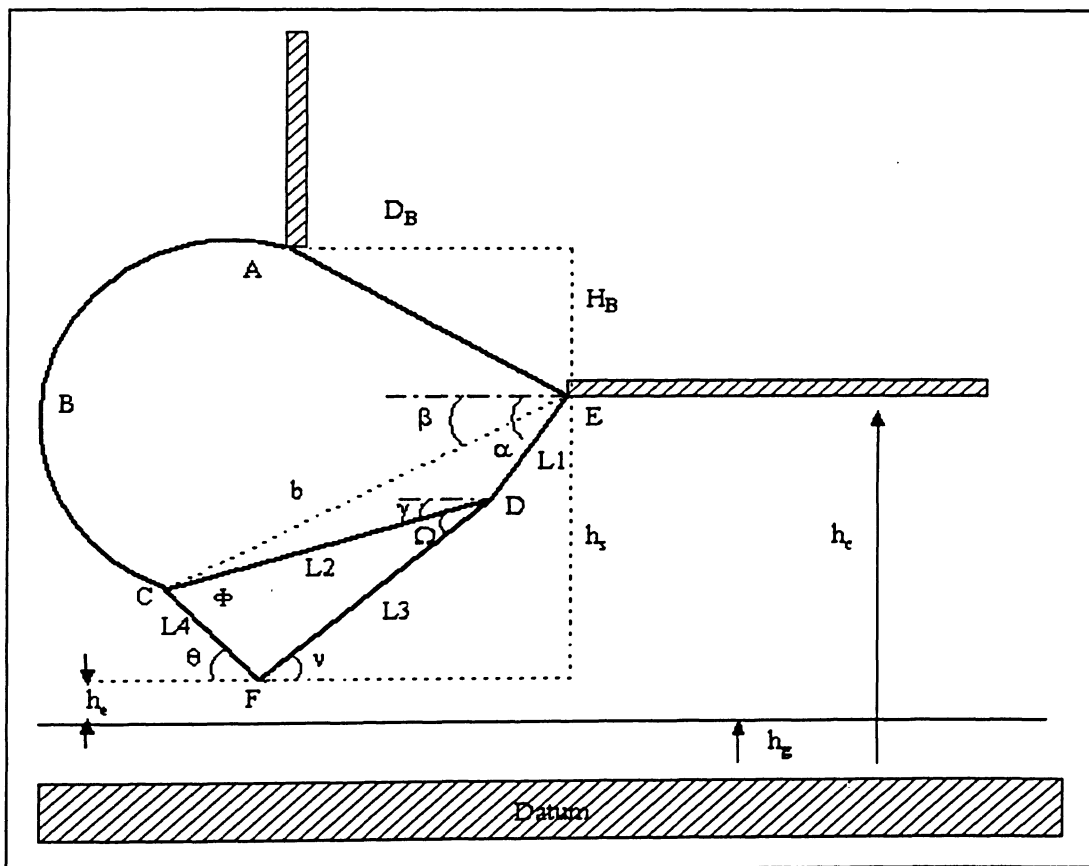


Figure 3.5: Two dimensional section of the bag and finger skirt

The performance of ACVs depends upon an adequate and continuous supply of low pressure air. Considering now the fluid mechanics, the air flow  $Q_b$  from the vehicle lift fan into the bag is modeled as a quasisteady response to the fluctuating  $p_b(t)$  by specifying a function of the form  $p_b = f_b(Q_b)$  representative of a steady fan characteristic. The volume flux  $Q_c$  from bag to cushion through the orifices in the inner bag and from cushion to atmosphere  $Q_a$  through the hovergap are assumed to be quasisteady and described by Bernoulli's law together with suitable discharge coefficients. With  $h_e$  defined as the distance between the bottom tips of the fingers and the surface, the discharge coefficient for  $Q_a$  depends on the finger geometry through both the hovergap  $h_e$  and the finger orientation angle  $\theta$ . The bag and cushion volumes  $V_b$  and  $V_c$  are modeled as lumped pneumatic capacitances, this being included because the compressibility of the cushion air has been shown to significantly affect dynamics under certain operating conditions, and can be a source of dynamic instability [33].

As shown in Figure 3.5 with  $h_c$  and  $h_g$  being the craft base and surface heights above a suitable inertial datum, the fluid dynamics is coupled to the skirt and craft dynamics through mass conservation laws for the variable  $V_b(\alpha, \gamma)$  and  $V_c(\alpha, \gamma, h_c, h_g)$ , and through the modulation of  $h_e$ . Thus the system has three degrees of freedom,  $h_c$ ,  $\alpha$ , and  $\gamma$  with input  $h_g(t)$  and output  $h_c(t)$ . The equations of motion for the ACV's dynamics including the skirt system are formulated using the Lagrange Method. With the generalized coordinates  $q_i$ , Lagrange's equations for the  $N$  degrees of freedom can be expressed as following.

$$\frac{d}{dt} \left( \frac{\partial T}{\partial \dot{q}_i} \right) - \frac{\partial T}{\partial q_i} + \frac{\partial P}{\partial q_i} = Q_i^{nc} \quad (3.1)$$

Here,  $Q_i^{NC}$  represents the non-conservative forces associated with the generalized coordinates  $q_i$ .

$$Q_i^{NC} = p_b V_i^{ob} + (p_b - p_c) V_i^{ih} + p_c V_i^f \quad (3.2)$$

There are three independent variables which are the craft heave displacement  $h_c$ , the angles  $\alpha$  and  $\gamma$  for the skirt geometry. Therefore the generalized coordinates become  $q_1 = h_c$ ,  $q_2 = \alpha$ , and  $q_3 = \gamma$ . The mass of the skirt is assumed to be lumped at the centroid of the finger. Then the kinetic and potential energies are derived as the following equations.

$$T = \frac{1}{2} M_s \left[ L_1^2 \dot{\alpha}^2 + L_M^2 \dot{\gamma}^2 + 2L_1 L_M \dot{\alpha} \dot{\gamma} \cos(\gamma_M - \alpha) - 2\dot{h}_c (L_1 \dot{\alpha} \cos \alpha + L_M \dot{\gamma} \cos \gamma_M) \right] + \frac{1}{2} M_c \dot{h}_c^2 + \frac{1}{2} I_s \dot{\gamma}^2 \quad (3.3)$$

$$P = M_c g h_c - M_s g (L_1 \sin \alpha + L_M \sin \gamma_M) \quad (3.4)$$

where  $I_s$  is the moment of inertia about the center of skirt mass,

$\gamma_M$  is the angle between the center of mass of the skirt and the horizontal,

$L_M$  is the distance between center of mass of the skirt and inner bag joint D,

$M_c$  is the total mass of the air cushion vehicle including the skirt mass, and

$M_s$  is the mass of the skirt.

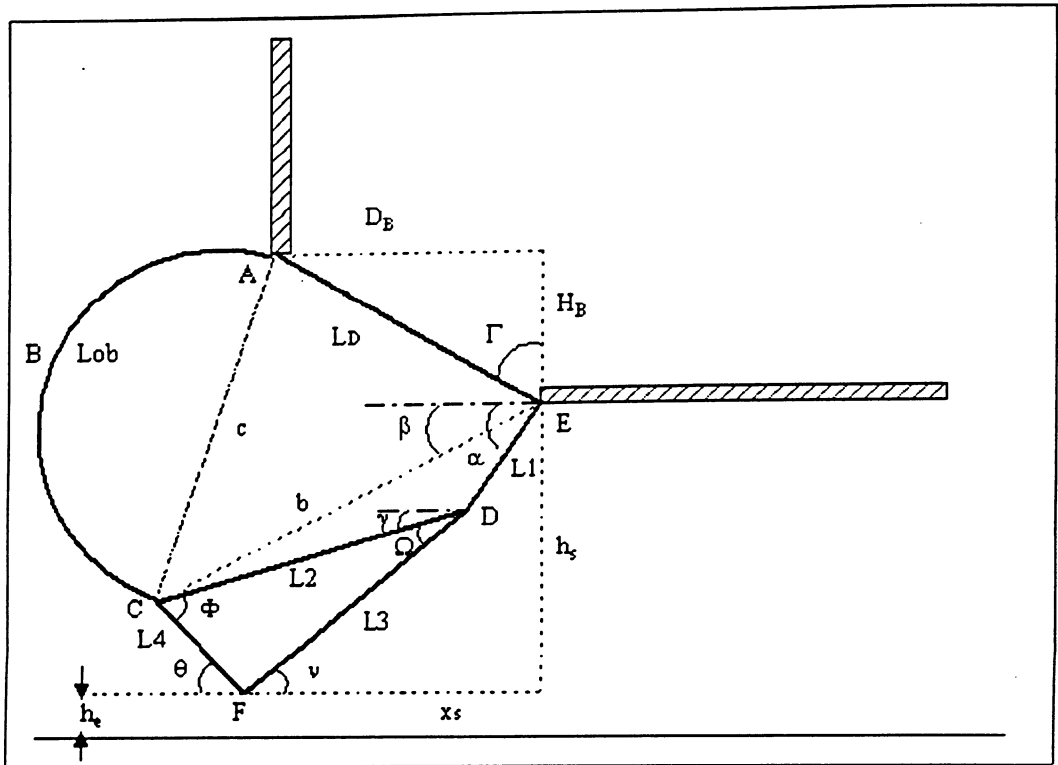


Figure 3.6: Parameters used for the skirt geometry

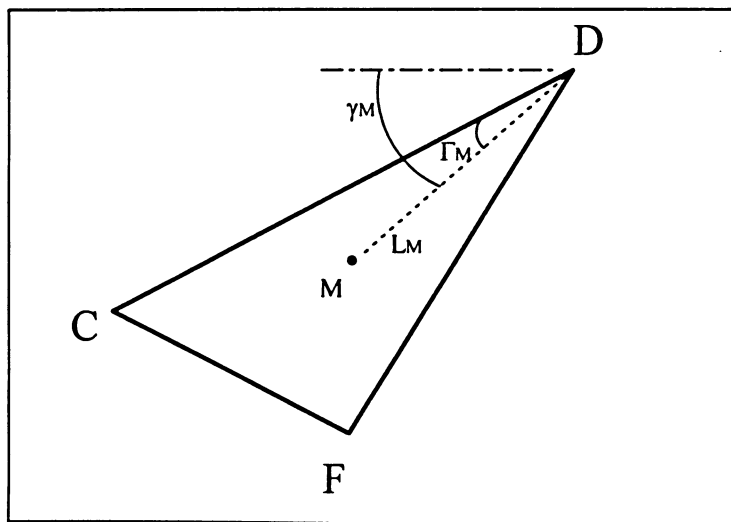


Figure 3.7: Parameters used for the finger geometry

With the Lagrange's equations, the nonlinear differential equations for the two dimensional skirt model are derived. The following equations are obtained for the motion of vehicle including the skirt system. The equations of motion as well as the bag and

cushion volume conservation equations are shown in Chung's paper [2]. The fluid mechanics equations are also presented in his paper.

The heave equation of motion for  $h_c$  is

$$\begin{aligned} M_c \ddot{h}_c + M_s [L_1 (\dot{\alpha}^2 \sin \alpha - \ddot{\alpha} \cos \alpha) + L_M (\dot{\gamma}^2 \sin \gamma_M - \ddot{\gamma} \cos \gamma_M)] + M_c g \\ = p_c \frac{\partial V_c}{\partial h_c} \end{aligned} \quad (3.5)$$

The skirt equation of motion for  $\alpha$  is

$$\begin{aligned} M_s L_1 [L_1 \ddot{\alpha} - L_M \sin(\gamma_M - \alpha) \dot{\gamma}^2 + L_M \cos(\gamma_M - \alpha) \ddot{\gamma} - \ddot{h}_c \cos \alpha - g \cos \alpha] \\ = p_h V_\alpha^{oh} + (p_h - p_c) V_\alpha^{ih} + p_c V_\alpha^f \end{aligned} \quad (3.6)$$

The skirt equation of motion for  $\gamma$  is

$$\begin{aligned} M_s L_M [L_M \ddot{\gamma} + L_1 \sin(\gamma_M - \alpha) \dot{\alpha}^2 + L_1 \cos(\gamma_M - \alpha) \ddot{\alpha} - \ddot{h}_c \cos \gamma_M - g \cos \gamma_M] + I_s \ddot{\gamma} \\ = p_h V_\gamma^{oh} + (p_h - p_c) V_\gamma^{ih} + p_c V_\gamma^f \end{aligned} \quad (3.7)$$

The bag volume conservation law is

$$\dot{p}_h = \frac{1}{C_h} \left[ Q_h - Q_c - \frac{\partial V_h}{\partial \alpha} \dot{\alpha} - \frac{\partial V_h}{\partial \gamma} \dot{\gamma} \right] \quad (3.8)$$

$$\text{where } \dot{V}_h = \frac{\partial V_h}{\partial \alpha} \dot{\alpha} + \frac{\partial V_h}{\partial \gamma} \dot{\gamma}$$

The cushion volume conservation law is

$$\dot{p}_c = \frac{1}{C_c} \left[ Q_c - Q_a - \frac{\partial V_c}{\partial \alpha} \dot{\alpha} - \frac{\partial V_c}{\partial \gamma} \dot{\gamma} - \frac{\partial V_c}{\partial h_c} (\dot{h}_c - \dot{h}_g - \frac{\partial h_c}{\partial \alpha} \dot{\alpha} - \frac{\partial h_c}{\partial \gamma} \dot{\gamma}) \right] \quad (3.9)$$

$$\text{where } \dot{V}_c = \frac{\partial V_c}{\partial \alpha} \dot{\alpha} + \frac{\partial V_c}{\partial \gamma} \dot{\gamma} + \frac{\partial V_c}{\partial h_c} \dot{h}_c \text{ and } \dot{h}_c = \dot{h}_c - \dot{h}_g - \frac{\partial h_c}{\partial \alpha} \dot{\alpha} - \frac{\partial h_c}{\partial \gamma} \dot{\gamma}$$

The flow from bag to cushion is

$$Q_c = A_b \operatorname{sgn}(p_b - p_c) \sqrt{\frac{2|p_b - p_c|}{\rho}} \quad (3.10)$$

The flow from cushion to atmosphere is

$$Q_a = L_p h_f(h_c, \theta) \operatorname{sgn}(P_c) \sqrt{\frac{2|p_c|}{\rho}} \quad (3.11)$$

$$\text{where } L_p = 2(B_h + L_h) + 8x_s$$

$B_h$  and  $L_h$  are the width and length of the vehicle base between inner bag attachment points, respectively. The functions  $V_\alpha^{oh}, V_\alpha^{ih}, V_\alpha^f, V_\gamma^{oh}, V_\gamma^{ih},$  and  $V_\gamma^f$  are the rates, with respect to the  $\alpha$  and  $\gamma$ , at which the surfaces ABC, CDE and CF sweep out volumes as the skirt moves.  $h_f$  is an effective leak height which allows air leakage from the atmosphere into the cushion, when the pressure in the cushion is smaller than the pressure in the atmosphere. This function can be determined analytically from the geometry of the segments, or it can be determined experimentally. The following equation is expressed in the non-dimensional form to apply it for the full size vehicles.

$$h_f = B_f f_a \left( \frac{h_c}{B_f}, \theta \right) \quad (3.12)$$

where  $B_f$  is the finger width, and  $\theta$  is defined in Figure 3.5. The function  $f_a$  is the product of the area between the bottom of the fingers and the surface with a discharge coefficient dependent on  $\theta$ . As  $h_c$  decreases from  $h_c > 0$ ,  $h_f$  initially depends linearly on  $h_c$ . Then, when surface contact occurs at  $h_c = 0$ , further decrease in  $h_c$  causes  $h_f$  to decrease nonlinearly as the tips of the fingers (at F in Figure 3.6) collapse, shutting off the flow [32].

The air in the bag and cushion is assumed to be compressible, and at any instant in time the pressures are assumed to be uniform throughout the volumes. Then, the bag and the cushion air mass conservation laws take the following forms.

$$C_b \dot{p}_b + \dot{V}_b = Q_b - Q_c \quad (3.13)$$

$$C_c \dot{p}_c + \dot{V}_c = Q_c - Q_a \quad (3.14)$$

In these equations,  $C_b$  and  $C_c$  are the pneumatic capacitances of  $V_b$  and  $V_c$ , given respectively by  $C_b = V_b / \gamma P_a$  and  $C_c = V_c / \gamma P_a$ . Where  $\gamma$  is the ratio of specific heats, which is 1.4 for air. The term  $\dot{V}_b$  in equation (3.13) is associated with flexible skirt deformation under the action of  $p_b$  and term  $\dot{V}_c$  in equation (3.14) is associated with both vehicle motion and flexible skirt deformation under the action of  $p_c$ .

### 3.4 The Linearized Equations of Motion

The nonlinear equations in the previous section are linearized about an equilibrium point with the standard linear analysis techniques. Let the instantaneous value of a quantity be  $x_i$ , and a function be  $F(x_1, x_2, \dots, x_N)$ , then these are expressed as the following equations.

$$x_i = (x_i)_0 + \delta x_i \quad (3.15)$$

$$F = F_0 + \sum_{i=1}^N \left( \left( \frac{\partial F}{\partial x_i} \right)_0 \delta x_i \right) \quad (3.16)$$

In the above equations, “0” means that the quantity is evaluated at the equilibrium condition, and  $\delta x_i$  is the increment of  $x_i$  over the equilibrium condition. For the two dimensional skirt model with capacitance effects, it is  $X^T = [\dot{\alpha}, \dot{\gamma}, \alpha, \gamma, p_h, p_c, \dot{h}_c, h_c]$  with the input  $h_g(t)$ . Then with a linearization process there are the eight first order differential equations that are two equations for the vehicle heave dynamics  $h_c$ , two equations each for the skirt displacements  $\alpha$  and  $\gamma$ , and one equation each for the pneumatic capacitances of the bag and cushion volumes. The heave velocity of the craft and angular velocity of the skirt geometry ( $\alpha, \gamma$ ) are denoted as  $R_h, R_\alpha$  and  $R_\gamma$ , respectively.

The heave motion equations for  $h_c$  are

$$\delta \dot{h}_c = \delta R_h \quad (3.17)$$

$$\begin{aligned} & [M_c] \delta \dot{R}_\alpha + [-M_s L_1 \cos \alpha_0] \delta \dot{R}_\alpha + [-M_s L_M \cos \gamma_{M0}] \delta \dot{R}_\gamma \\ & = \left[ p_{co} \left( \frac{\partial^2 V_c}{\partial h_c^2} \right)_0 \right] \delta h_c + \left[ p_{co} \left( \frac{\partial^2 V_c}{\partial \alpha \partial h_c} \right)_0 \right] \delta \alpha + \left[ p_{co} \left( \frac{\partial^2 V_c}{\partial \gamma \partial h_c} \right)_0 \right] \delta \gamma \end{aligned}$$

$$+ \left[ p_{c\alpha} \left( \frac{\partial^2 V_c}{\partial h_x \partial h_c} \right)_0 \right] \delta h_x + \left[ \left( \frac{\partial V_c}{\partial h_c} \right)_0 \right] \delta p_c \quad (3.18)$$

The skirt motion equations for  $\alpha$  are

$$\delta \dot{\alpha} = \delta R_\alpha \quad (3.19)$$

$$\begin{aligned} & [-M_S L_1 \cos \alpha_0] \delta \dot{R}_h + [M_S L_1^2] \delta \dot{R}_\alpha + [M_S L_1 L_M \cos(\gamma_{M0} - \alpha_0)] \delta \dot{R}_\gamma \\ &= \left[ -M_S L_1 g \sin \alpha_0 + p_{h\alpha} \left( \frac{\partial V_\alpha^{oh}}{\partial \alpha} \right)_0 + (p_{h\alpha} - p_{c\alpha}) \left( \frac{\partial V_\alpha^{ih}}{\partial \alpha} \right)_0 + p_{c\alpha} \left( \frac{\partial V_\alpha^f}{\partial \alpha} \right)_0 \right] \delta \alpha \\ &+ \left[ p_{h\alpha} \left( \frac{\partial V_\alpha^{oh}}{\partial \gamma} \right)_0 + (p_{h\alpha} - p_{c\alpha}) \left( \frac{\partial V_\alpha^{ih}}{\partial \gamma} \right)_0 + p_{c\alpha} \left( \frac{\partial V_\alpha^f}{\partial \gamma} \right)_0 \right] \delta \gamma \\ &+ [(V_\alpha^{oh})_0 + (V_\alpha^{ih})_0] \delta p_h + [(V_\alpha^f)_0 - (V_\alpha^{ih})_0] \delta p_c \end{aligned} \quad (3.20)$$

The skirt motion equations for  $\gamma$  are

$$\delta \dot{\gamma} = \delta R_\gamma \quad (3.21)$$

$$\begin{aligned} & [-M_S L_M \cos \gamma_{M0}] \delta \dot{R}_h + [M_S L_1 L_M \cos(\gamma_{M0} - \alpha_0)] \delta \dot{R}_\alpha + [M_S L_M^2 + I_S] \delta \dot{R}_\gamma \\ &= \left[ p_{h\alpha} \left( \frac{\partial V_\gamma^{oh}}{\partial \alpha} \right)_0 + (p_{h\alpha} - p_{c\alpha}) \left( \frac{\partial V_\gamma^{ih}}{\partial \alpha} \right)_0 \right] \delta \alpha \\ &+ \left[ -M_S L_M g \sin \gamma_{M0} + p_{h\alpha} \left( \frac{\partial V_\gamma^{oh}}{\partial \gamma} \right)_0 + (p_{h\alpha} - p_{c\alpha}) \left( \frac{\partial V_\gamma^{ih}}{\partial \gamma} \right)_0 \right] \delta \gamma \\ &+ [(V_\gamma^{oh})_0 + (V_\gamma^{ih})_0] \delta p_h + [(V_\gamma^f)_0 - (V_\gamma^{ih})_0] \delta p_c \end{aligned} \quad (3.22)$$

The bag volume conservation law equation is

$$\begin{aligned} \delta\dot{p}_h = & \left[ -\frac{1}{C_h} \left( \frac{\partial V_h}{\partial \alpha} \right)_0 \right] \delta R_\alpha + \left[ -\frac{1}{C_h} \left( \frac{\partial V_h}{\partial \gamma} \right)_0 \right] \delta R_\gamma \\ & + \left[ -\frac{1}{C_h} \left( \frac{1}{3A_{f1} Q_{ho}^2} + \frac{A_h^2}{\rho Q_{co}} \right) \right] \delta p_h + \left[ \frac{1}{C_h} \frac{A_h^2}{\rho Q_{co}} \right] \delta p_c \end{aligned} \quad (3.23)$$

where  $\delta p_h = -3A_{f1} Q_{ho}^2 \delta Q_h$  is the linearized fan characteristic equation.

The cushion volume conservation law equation is

$$\begin{aligned} \delta\dot{p}_c = & \left[ -\frac{1}{C_c} \{2(B_h + L_h) + 8x_{so}\} \left( \frac{\partial h_f}{\partial h_c} \right)_0 \sqrt{\frac{2p_{co}}{\rho}} \right] \delta h_c \\ & + \left[ -\frac{1}{C_c} \{2(B_h + L_h) \left( \frac{\partial h_f}{\partial \alpha} \right)_0 + 8x_{so} \left( \frac{\partial h_f}{\partial \alpha} \right)_0 - 8L_1 \sin \alpha_0 h_{fo}\} \sqrt{\frac{2p_{co}}{\rho}} \right] \delta \alpha \\ & + \left[ -\frac{1}{C_c} \{2(B_h + L_h) \left( \frac{\partial h_f}{\partial \gamma} \right)_0 + 8x_{so} \left( \frac{\partial h_f}{\partial \gamma} \right)_0 - 8L_3 \sin(\Omega + \gamma_0) h_{fo}\} \sqrt{\frac{2p_{co}}{\rho}} \right] \delta \gamma \\ & + \left[ -\frac{1}{C_c} \left( \frac{\partial V_c}{\partial h_c} \right)_0 \right] \delta R_h + \left[ -\frac{1}{C_c} \left\{ \left( \frac{\partial V_c}{\partial \alpha} \right)_0 - \left( \frac{\partial V_c}{\partial h_c} \right)_0 L_1 \cos \alpha_0 \right\} \right] \delta R_\alpha \\ & + \left[ -\frac{1}{C_c} \left\{ \left( \frac{\partial V_c}{\partial \gamma} \right)_0 - \left( \frac{\partial V_c}{\partial h_c} \right)_0 L_3 \cos(\Omega + \gamma_0) \right\} \right] \delta R_\gamma \\ & + \left[ \frac{1}{C_c} \frac{A_h^2}{\rho Q_{co}} \right] \delta p_h + \left[ -\frac{1}{C_c} \left\{ \frac{A_h^2}{\rho Q_{co}} + \frac{1}{2p_{co}} (2(B_h + L_h) + 8x_{so}) h_{fo} \sqrt{\frac{2p_{co}}{\rho}} \right\} \right] \delta p_c \\ & + \left[ \frac{1}{C_c} \left( \frac{\partial V_c}{\partial h_c} \right)_0 \right] \delta \dot{h}_c + \left[ -\frac{1}{C_c} \{2(B_h + L_h) + 8x_{so}\} \left( \frac{\partial h_f}{\partial h_c} \right)_0 \sqrt{\frac{2p_{co}}{\rho}} \right] \delta \dot{h}_c \end{aligned} \quad (3.24)$$

where  $x_{so} = L_1 \cos \alpha_0 + L_3 \cos(\Omega + \gamma_0)$

The linearized bag to cushion flow equation is

$$\delta Q_c = \left( \frac{\delta p_h - \delta p_c}{\rho Q_{cv}} \right) A_h^2 \quad (3.25)$$

The linearized cushion to atmosphere flow equation is

$$\begin{aligned} \delta Q_a = & \left[ \{2(B_h + L_h) + 8x_{so}\} \left( \frac{\partial h_f}{\partial h_c} \right)_0 \sqrt{\frac{2p_{cv}}{\rho}} \right] \delta h_c \\ & + \left[ \{2(B_h + L_h) \left( \frac{\partial h_f}{\partial \alpha} \right)_0 + 8x_{so} \left( \frac{\partial h_f}{\partial \alpha} \right)_0 - 8L_1 \sin \alpha_0 h_{fo}\} \sqrt{\frac{2p_{cv}}{\rho}} \right] \delta \alpha \\ & + \left[ \{2(B_h + L_h) \left( \frac{\partial h_f}{\partial \gamma} \right)_0 + 8x_{so} \left( \frac{\partial h_f}{\partial \gamma} \right)_0 - 8L_3 \sin(\Omega + \gamma_0) h_{fo}\} \sqrt{\frac{2p_{cv}}{\rho}} \right] \delta \gamma \\ & + \left[ \frac{1}{2p_{cv}} \{2(B_h + L_h) + 8x_{so}\} h_{fo} \sqrt{\frac{2p_{cv}}{\rho}} \right] \delta p_c \\ & + \left[ \{2(B_h + L_h) + 8x_{so}\} \left( \frac{\partial h_f}{\partial h_g} \right)_0 \sqrt{\frac{2p_{cv}}{\rho}} \right] \delta h_g \end{aligned} \quad (3.26)$$

All the equilibrium derivative terms in the above equations are presented in appendix B of the reference [2]. The set of these simultaneous differential equations could be expressed in a matrix form as follows.

$$H\dot{x} = Rx + Tu \quad (3.27)$$

where  $x = [\delta \dot{\alpha}, \delta \dot{\gamma}, \delta \alpha, \delta \gamma, \delta p_h, \delta p_c, \delta \dot{h}_c, \delta h_c]^T$ ,

$$u = [\delta \dot{h}_g, \delta h_g]^T.$$

Then the linearized equations for ACV heave dynamics can be represented in a compact state-space form.

$$\dot{x} = Ax + Bu \quad (3.28)$$

where  $A = H^{-1}R$ ,

$$B = H^{-1}T.$$

The outputs of a linear system can be related to the state variables and the input by the state equation.

$$Y = Cx \quad (3.29)$$

where the  $C$  matrix depends on the system input and output choices, and  $Y$  is the set of outputs. From the state-space matrices, the linear response of the craft can be obtained. Moreover the stability of the system can be known from the system matrix. Other important parameters representing the vehicle's characteristics can also be computed.

### 3.5 Parameter Estimation

In order to optimize the properties of the bag and finger skirt system for improved ride quality and better stability, the parameters involved in the equations of motion should be estimated to predict the motion of vehicle. The parameters are categorized into the several groups related to the craft structure system, the skirt system, cushion flow system, and the lift fan system. In this section the estimation for some of the parameters is addressed.

The parameters involved in the craft system are the craft's mass, length, width, base length and base width. The craft's mass, length, and width have to be initially given for the design requirement. The approximation of these parameters can be estimated from the following relationships.

$M_c$  = the given craft mass including the skirt,

$L_c$  = the given craft length,

$B_c$  = the given craft width,

$D_b, H_b$  = the given lengths defining the craft base geometry,

$$L_b = \text{the craft base length} = L_c - 2x_s \quad (3.30)$$

$$B_b = \text{the craft base width} = B_c - 2x_s \quad (3.31)$$

where  $x_s$  is the lateral deflection of the skirt, and its relationship is described in the previous section.

The parameters in the skirt system are the skirt mass and dimension. In these parameters, some of them are to be optimized for better ride quality and stability. The following relations describe these parameters.

$M_s$  = the skirt mass estimated from the area density and total skirt area.

$L_1, L_2, L_3, L_4$  = the lengths defining geometry of inner bag and finger, which are being optimized,

$L_{ob}$  = the length of outer bag, which is being optimized,

$$\Omega = \text{the angle related to the finger geometry} = \cos^{-1}\left(\frac{L_2^2 + L_3^2 - L_4^2}{2L_2L_3}\right) \quad (3.32)$$

$$\Phi = \text{the angle related to the finger geometry} = \sin^{-1}\left(\frac{L_3 \sin \Omega}{L_4}\right) \quad (3.33)$$

The cushion flow system has the following parameters which are estimated in the equilibrium condition.

$p_{ce}$  = the equilibrium cushion pressure estimated from  $M_c, L_c, B_c$

$$= \frac{M_c g}{L_c B_c} \quad (3.34)$$

$Q_e$  = the equilibrium flow rate estimated from the correlation by experience

$$= \left[ 4.5 \times 10^{-3} + 5.9 \times 10^{-4} \left( \frac{p_{ce}}{\rho_a g L_c} \right) \right] \sqrt{\frac{2(L_c B_c)^2 p_{ce}}{\rho_a}} \quad (3.35)$$

$\frac{p_{bc}}{p_{ce}}$  = the ratio of bag pressure and cushion pressure, which is being optimized,

$h_c$  = distance between bottom tips of fingers and ground that is estimated from the static equilibrium force analysis.

The parameters related to the lift fan system are the effective area of bag to cushion feed hole orifices, reference bag pressure, reference volume flow from fan to bag, and constant for fan characteristic law. These parameters are explained in detail in the reference [2].

There are some other parameters related to the geometry of skirt at the equilibrium condition. They are the angles defining the bag geometry,  $\alpha_0, \gamma_0$  at equilibrium conditions and the height of craft base,  $H_c$ . These parameters can be estimated from the equilibrium force analysis. The following figure describes the parameters estimated from the given design requirements.

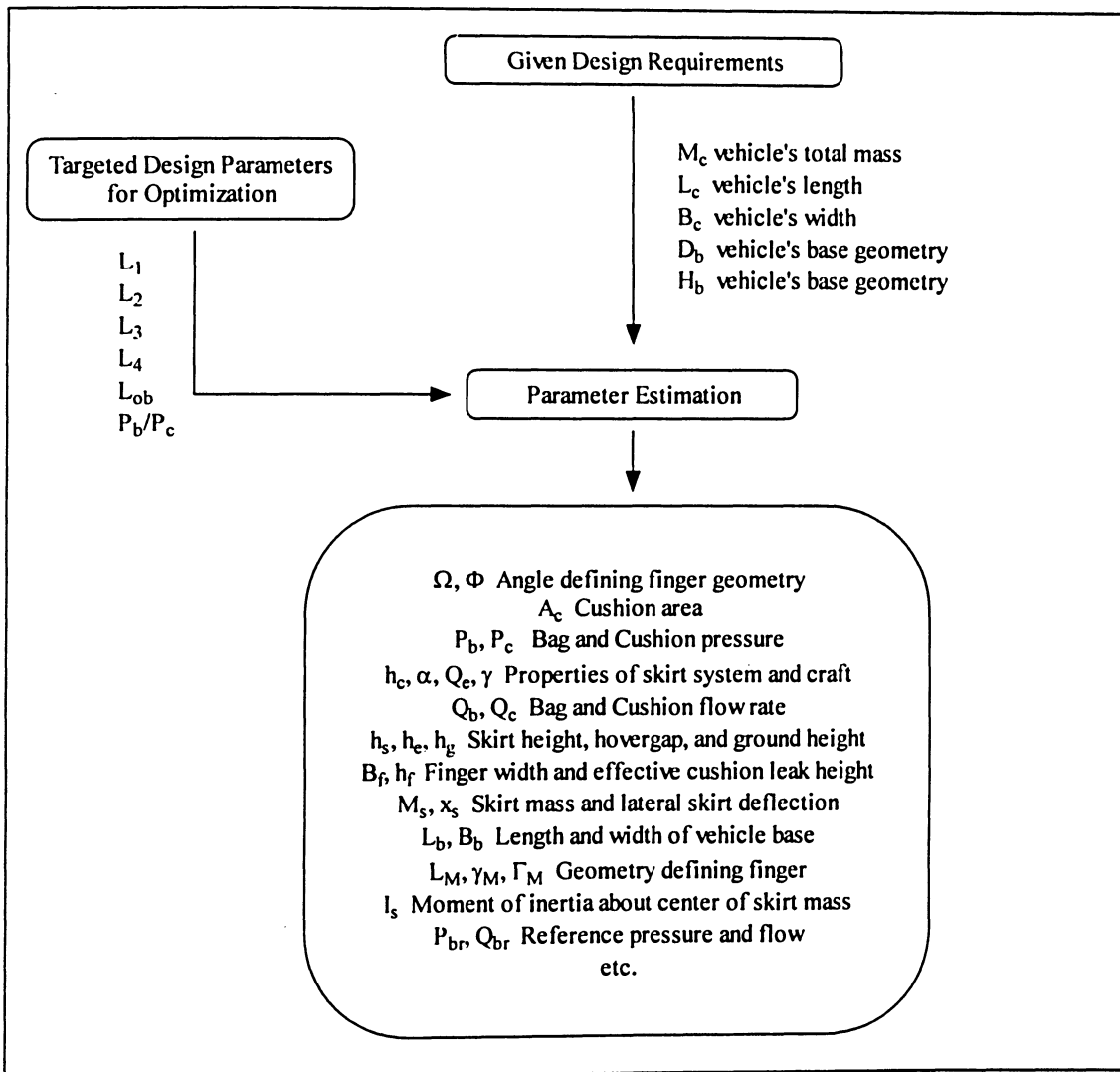


Figure 3.8: Parameter estimation

### 3.6 Implementation of GA

The initial population is randomly generated at the beginning of optimization process. The population is composed of several individuals which are the potential solutions. Representing each individual is called the *coding* and it should present all the design variables through the coding process. There are commonly two kinds of representing methods available such as binary representation and real number representation [34,35].

In a binary coding, each variable is coded as a bit string. The bit strings for the variables are concatenated together to give a single bit string (or chromosome) which represents an entire vector of variables. In a real number coding, the actual value of variable is directly used instead of converting it to a bit string. The main advantage of this coding method compared to the binary one is that it can use the value of variable directly without any conversion. This can save a great deal of time when it is computed in the algorithm. The major drawback, however, is that it can be applicable only when the values of variables are fixed, discontinuous or relatively easy to represent. Such an example can be shown in aircraft landing sequence optimization [30].

In this thesis work, the binary coding is applied because all the design variables are easily represented in the binary numbers and it is easier to interact with the algorithm itself. Then the population is composed with 30 of such individuals. Table 3.1 shows a sample individual coded in binary numbers. In this sample individual, each variable uses the four bits to represent its value. Thus one individual has the total 24 bits to represent the entire potential solution point, because there are total six different variables of skirt geometry and pressure ratio being optimized. Since this individual is in binary number,

the decoding method is required to convert the coded variables to the actual real number. The decoding method is based on the same mechanism of coding method.

Table 3.1: Sample individual with binary coding

$L_1$				$L_2$			
1	0	0	0	1	1	0	1
$L_3$				$L_4$			
1	0	1	0	0	1	1	0
$L_{ob}$				$p_b/p_c$			
0	1	0	1	0	1	0	1

Objective function is the given condition specified in the problem, which the individuals need to satisfy it in order to survive. The value obtained from the evaluation procedure by objective function for each individual is called the *fitness*. The decision is made whether the individual is good or bad for the given problem, according to how much this *fitness* value is. In this work for the optimization of the bag and finger skirt, the objective is to reduce the second peak magnitude and prevent the second peak frequency away from the range at which humans are most sensitive. Hence, the individual whose second peak magnitude is the least will get the best fitness value, while the one whose second peak magnitude is the most will obtain the worst fitness value. For the case of second peak frequency, the same principle will be applied as the second peak magnitude. Figure 3.9 illustrates the frequency response curve for original skirt system in the CCG Waban-Aki and LCAC. The optimized skirt system should produce lower magnitude and frequency of second peak than those from original skirt system.

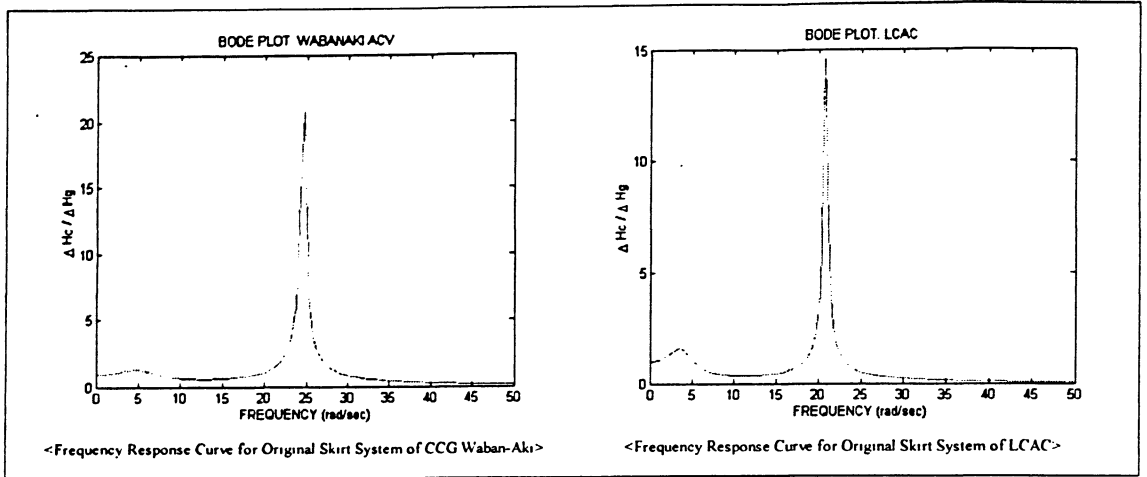


Figure 3.9: Frequency response curve for original skirt system

The better individuals are usually the ones who have the higher fitness value for the maximizing problems or vice versa. However, the concept about *better individual* might be changed depending on the conditions of problem. In other words, the fitness value is not the only factor judging whether the particular individual is better than others. For example, the individual who has the highest fitness value for the maximizing problem may not be in the feasible region, so that this point cannot be reachable in the reality and should be rejected during the selection process even though it has the highest fitness value [36]. This kind of problem generally happens in the constrained optimization problems. One of the solutions for the constrained optimization problem is to use the Penalty Approach. Several forms of penalty functions have been proposed in the GA literatures [37]. The common form of penalty function is given as following equation.

$$p(x) = C_p \cdot (\sum \max(g(x), 0) + \sum |h(x)|) \quad (3.36)$$

This penalty function consists of a penalty coefficient  $C_p$  multiplied by the sum of constraint violations. The penalty coefficient can be selected depending on the type of

optimization problem. For stiff problems, high value of penalty coefficient may be appropriate. This value can also be selected through the trial-and-error technique.

There are several constraints that should be considered for the realistic design in optimization of ACVs skirt system. Most of all, ACVs must be stable [38,39]. In order to reflect this constraint, penalty function will examine the eigenvalues of the skirt system from the linearized equations of motion. Then if it finds out the instability in the system, penalty function will assign the proper values for those individuals who have the instability. Since the objective function is to minimize the second peak magnitude and frequency, penalty function will add some values to those individuals, in order to make their fitness value worse. The next constraint is the skirt bounce of ACV. The skirt bounce is a dynamic instability of the skirt-cushion system caused by the interaction between the motion of the skirt and the cushion flow processes. This skirt bounce can be prevented or reduced by setting the proper pressure ratio of the bag and cushion. Thus if the pressure ratio is out of the proper range which is 1.0~1.6, then penalty function will assign the penalty values. The third constraint is the height of hover gap that is the distance from the bottom of the finger tips to the ground. Since the motion of ACVs is computed at the equilibrium conditions, the hover gap should always be the positive number. Hence if the skirt system produces the negative hover gap, then penalty function will again add the proper penalty values to the individuals. At last, there is an allowable range for the modification of dimensions in the bag and finger skirt geometry. If the dimensions are out of this range, then the shape of frequency response curve becomes unrealistic, and it is even impossible to compute the frequency response plots with those skirt dimensions. Thus penalty function will assign the proper penalty value to the

individuals depending on whether their parameters are in the allowable range. This allowable range can be determined by the experiments, experience or trial-and-error.

At the end of penalty function process in the GA all individuals will have the total fitness value which is the sum of the objective value and the penalty value. Among the individuals, the one who possesses the least total fitness value will become the best individual in the whole population and produce the best optimized properties of the bag and finger skirt system. Moreover the penalty value of the best individual should be zero, in order to produce the feasible design of the bag and finger skirt system. Figure 3.10 describes the constraint conditions applied in penalty function.

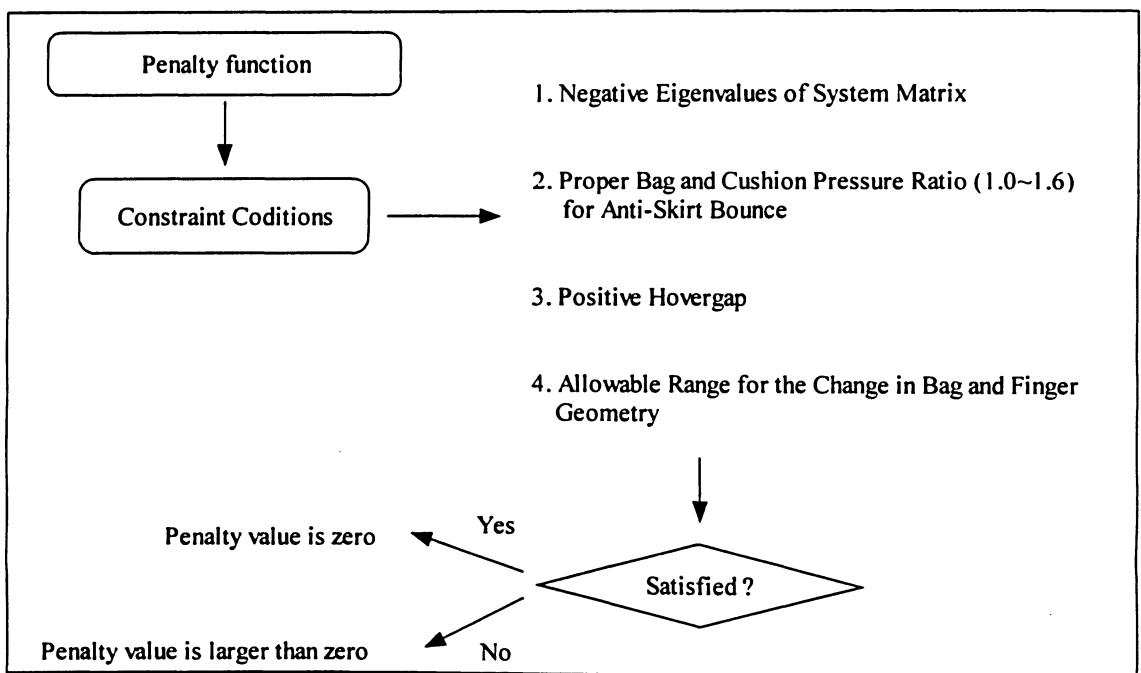


Figure 3.10: Constraint conditions in penalty function

The selection process is performed to choose the better individuals for further genetic processes. In order to select the better individuals, rank method is firstly used. According to rank method each individual gets its own rank in the whole population. This

method is more appropriate for the use in domains where the fitness range is extremely wide. In these domains it is feared that the first individuals with high fitness values will dominate the population and prevent other good individuals in other regions of the search space from being found [19].

Once all the individuals obtain their ranks, the selection is performed with the *remainder stochastic sampling method* [13]. The remainder stochastic sampling method usually works with the fitness values, but in this thesis it has been modified such that it works with rank values instead of fitness values of the individuals. In this method, average of rank values is computed, and then each individual's rank is divided by the average value. The value obtained from division is called expected number. This expected number is consisted of an integer part and the fraction part. Integer part indicates the number of copies of the individual. For instance, the individual, whose expected number is 4.3, will have four copies of the same chromosome during the selection process. Here, the term, *copy*, means the selection operator chooses the individual as many as the number of copies. Then the fraction parts of the expected numbers are used to provide the probability of each individual for the rest of selection process. This fraction part process will be continued until the total number of copies is reached to the original population size. As a result, the contents of population will be changed through the selection process such that it is now comprised of better individuals.

The individuals chosen from selection process go through the crossover process [14]. Crossover process produces the superior genes with the chosen individuals, so that the ones after crossover process likely have the high probability of possessing the lower total fitness value which is closer to the best optimized solution point. There have been

several forms of crossover operator came out for the past years [40, 41]. In this thesis, the three common types of crossover operator have been applied.

First type of crossover operator is ‘Single Point Crossover’. This one basically does a cut and paste operation on the genotypes of the parents to produce newborns. Figure 3.11 illustrates this operation. In order to carry out this operation, a single point in the chromosome should be selected. Then the genes before the point will be remained the

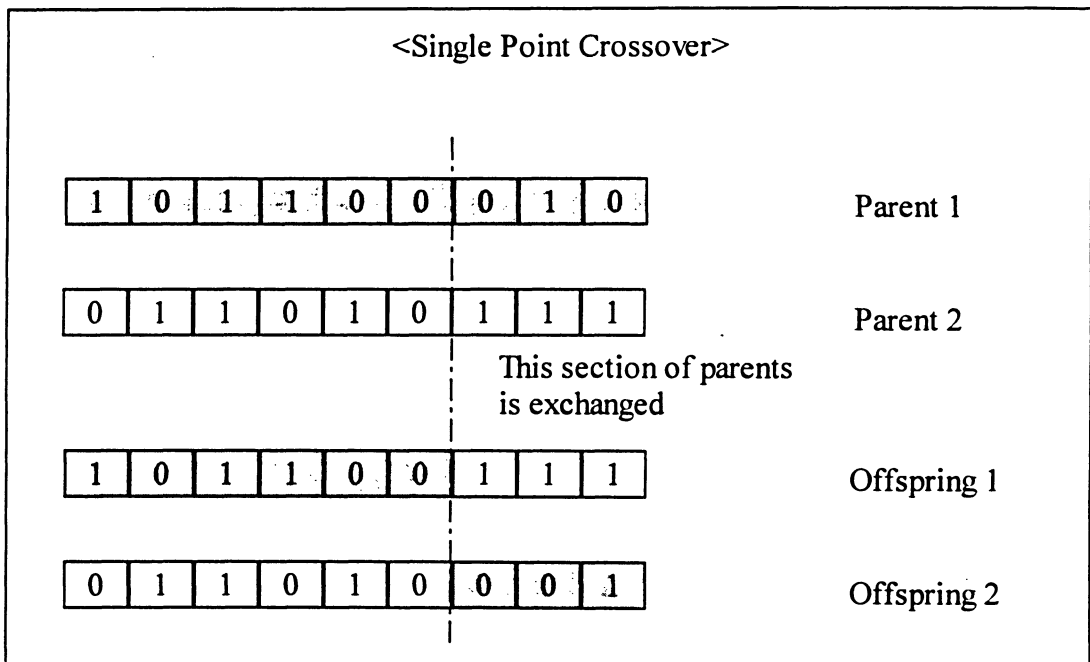
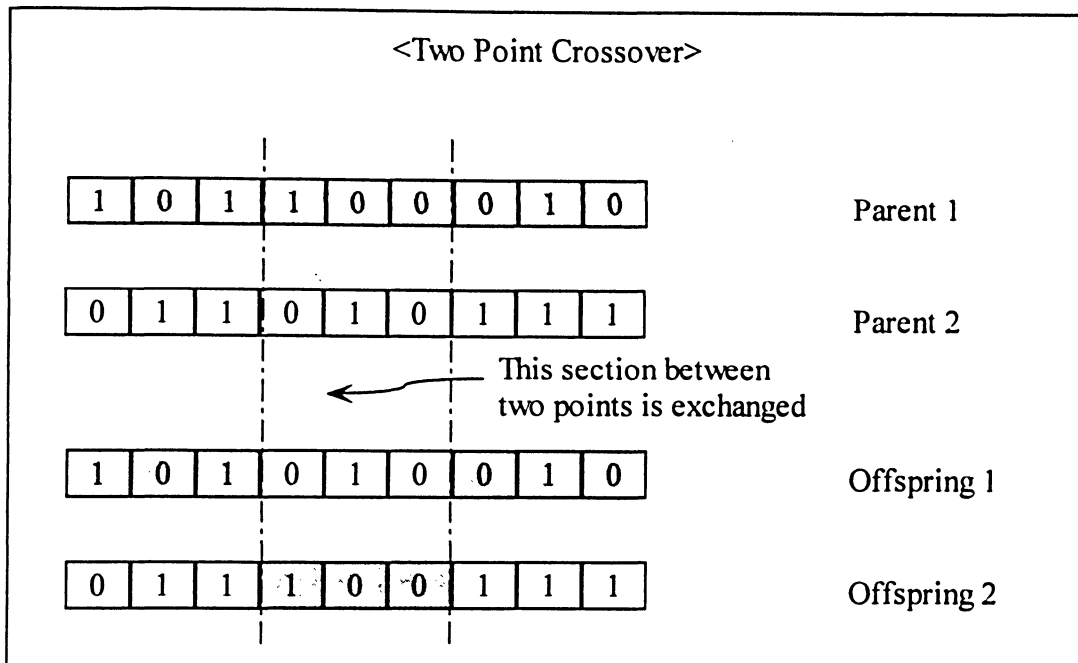


Figure 3.11: Single point crossover

same and the genes after the point will be changed with another chromosome. Through this process, the new chromosome will be formed which is referred as ‘*Offspring*’.

The second type of Crossover operator is ‘Two Point Crossover’. This operator is performed in a similar way of Single Point Crossover, but the only difference is that the two points in the genotypes of the parents will be used for exchanging the information. Figure 3.12 describes this crossover operator.



• Figure 3.12: Two point crossover

The third type of crossover operator is 'Random Crossover'. In this operator, each bit in a new individual is selected randomly from the corresponding position in either parent. For example in Figure 3.13, if the first bit in the offspring 1 is selected from the parent 2 then the value of bit in the first position is going to be '0', while if the second bit in the offspring 1 is chosen from the parent 1 then the value of bit in second position is '0'. This selection of parents for each bit of offspring 1 is performed at random. The offspring 2 is also built based on the same principle of offspring 1.

Since single point crossover has a simplest form, its performance time is the shortest among the three common types of operator. However, it has the major problem which is a great deal of difficulty searching the space. Unless both parents are close to each other, single point crossover may produce a bad newborn even if it starts with two good parents [13]. In the case of two point crossover, it performs better than single point crossover but the computational time will be increased. The random crossover operator is

not trapped in the problem single point crossover has and it introduces a lot of diversity. Therefore, in the thesis all three crossover methods are simultaneously applied due to the unique characteristic of each method described above.

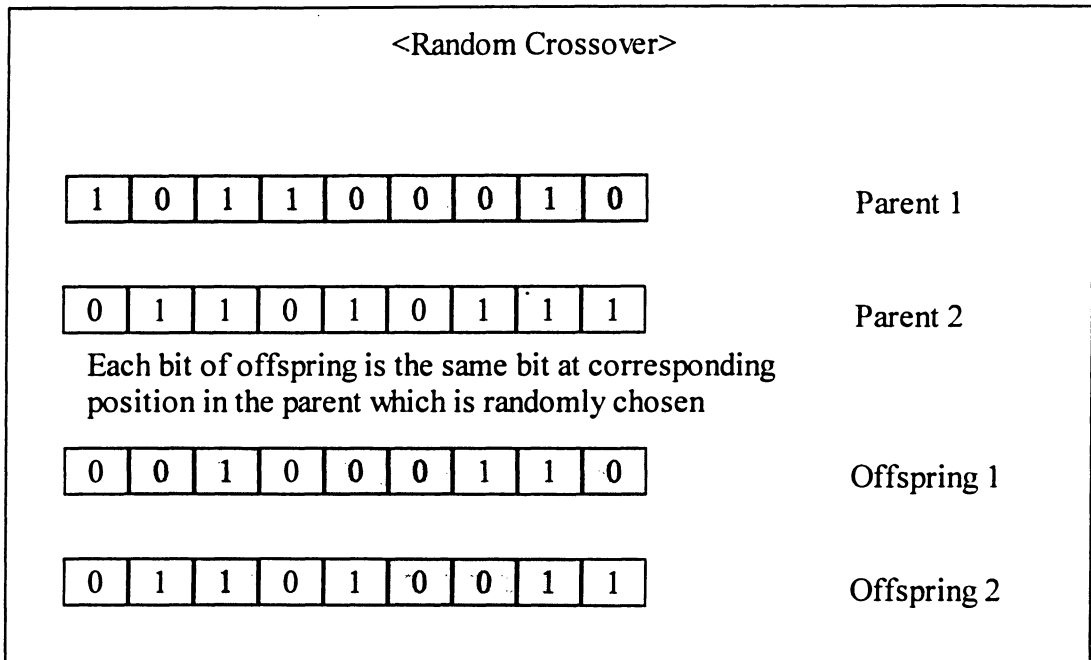


Figure 3.13: Random crossover

Mutation process comes after crossover process in the GA. Its main role is to provide the diversity in the population. It gives the chance to explore the entire search space by changing randomly the bit values in the chromosome. It is especially important when the solution point is trapped in the local optimums. That solution point can be escaped by changing the genes in the chromosome through the mutation process. There are two common forms of mutation operator used in this thesis work.

The first one is 'Single Bit Mutation'. It basically changes the bit value based on a probability of mutation, one at a time. For example, if the bit value is 'one' at the first position in the chromosome with probability of mutation 0.8 then it is likely changed

from 'one' to 'zero'. The bit values at the rest of positions in the same chromosome will be mutated based on the same principle applied to the bit value at the first position.

Figure 3.14 illustrates this mutation operator.

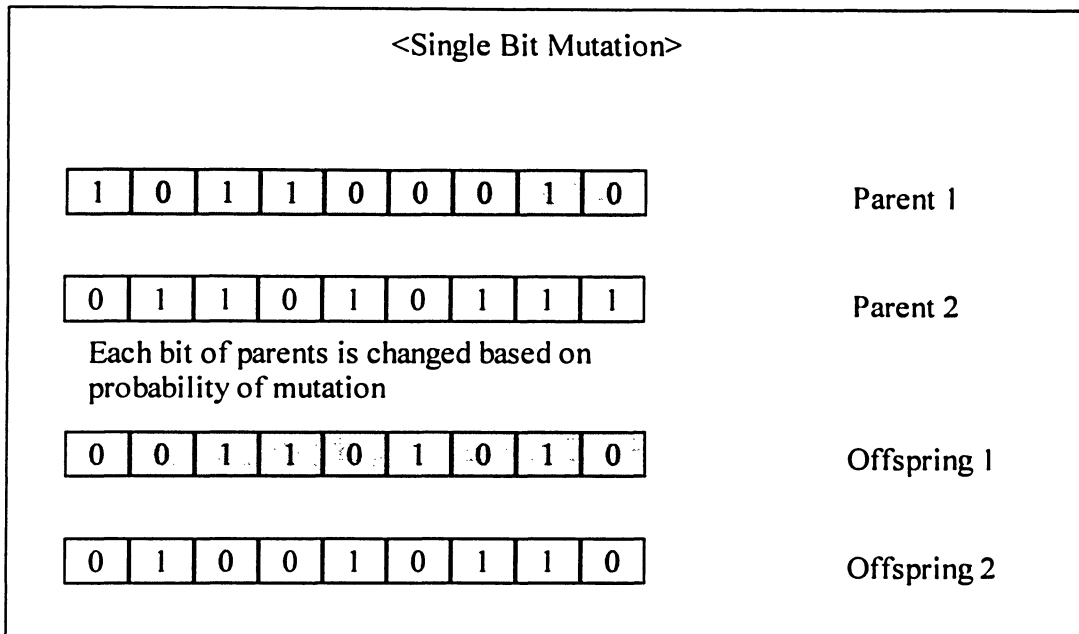


Figure 3.14: Single bit mutation

The other type of mutation operator is 'Two Bit Mutation'. This operator exchanges the bit values at two randomly selected positions in the same chromosome. For instance, if the first and fourth positions are randomly selected from the parent then the bit values at those chosen positions are exchanged and the rest of bit values will remain the same as that of parent. Figure 3.15 describes this mutation operator.

These two common types of mutation operator provide the extra chances to find the best solution for the given problem and help not to be trapped in the local optimums. This can be seen in the nature such as mutated birds for the specific environment in order to survive. Since each of mutation method has unique characteristics, all two mutation processes are again simultaneously performed in the GA.

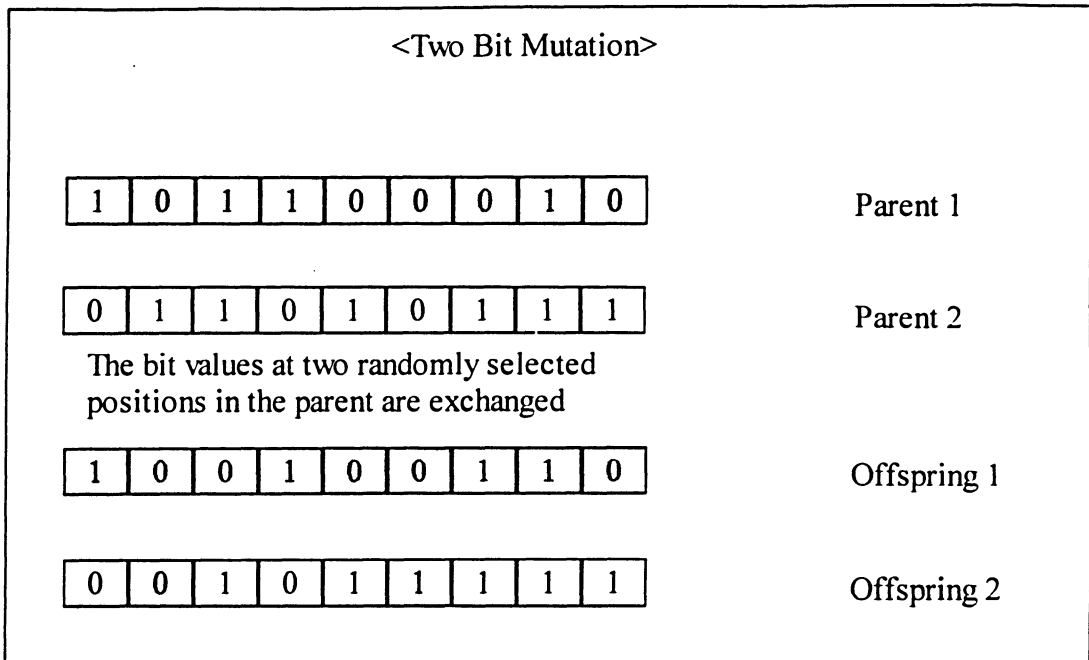


Figure 3.15: Two bit mutation

After the crossover and mutation processes, the current population will be composed of better individuals whose genes are now superior compared to the ones in the old population. These individuals have a good structure and information about the best optimized solution point, so that the portion of them will be kept during the next genetic process without any interference or modification. This is done by the elitist replacement. This strategy provides the fast convergence in the solution and also keeps the good structures of individuals for future reference in the next generation process.

At the end of genetic procedure, the algorithm checks the stopping condition, and if it meets the condition the optimization process will be ceased. The condition used in this thesis is to stop the GA if the current generation is reached the maximum number of generations which is pre-set by user. The maximum number of generations is generally recommended to use the multiple of the population size. For example, if population size is 30 then the maximum number of generations can be 60, 90, 120, and so on. Then the

point obtained at the last stage of generation is the best optimized solution and it produces the lowest second peak magnitude and second peak frequency by the combination of optimized design variables. The following table shows all the parameters used in the GA such as population size, length of an individual, maximum number of generations, etc.

Table 3.2: Parameters used in the GA on skirt optimization problem

Population size	30 individuals
Max. Generations	180 steps
Length of an individual	24 bits
Elitist reservation	10% of population size
Crossover methods	Single Point Crossover Two Point Crossover Random Crossover
Mutation methods	Single bit mutation Two bit mutation
Design variables of skirt system	$L_1, L_2, L_3, L_4, L_{ob}, p_h/p_c$
Design restriction of skirt system	$M_c, L_c, B_c, D_b, H_b$

### 3.7 Results of Experiments

The bag and finger skirt system of ACVs is optimized using the optimization technique, the GA, and its results are compared with the existing skirt system in terms of all the important properties and frequency responses in this section.

#### 3.7.1 Optimization on Waban-Aki Skirt

For the model of ACV skirt system, CCG Waban-Aki is chosen for the optimization. The total craft mass, craft length, craft width, and the lengths defining craft's base geometry are initially given as  $M_c = 36,740$  kg,  $L_c = 21$  m,  $B_c = 8.60$  m,  $D_b = 1.39$  m, and  $H_b = 0.975$  m, respectively. Within these initial design constraints, the skirt system is optimized with the GA technique.

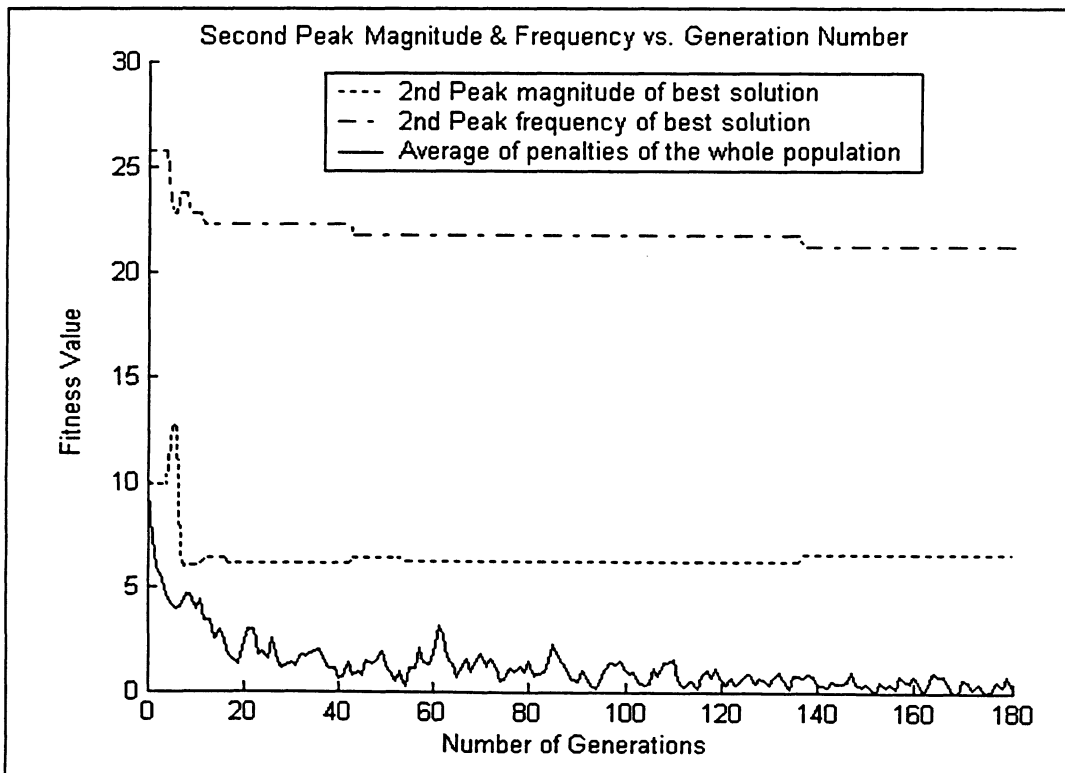


Figure 3.16: Overall performance of GA on Waban-Aki skirt optimization

In Figure 3.16 the overall performance of the GA on skirt optimization is depicted. The upper two lines in the figure represent the 2<sup>nd</sup> peak's frequency and magnitude of best solution obtained in each generation step. Since the tradeoff exists between the 2<sup>nd</sup> peak's frequency and magnitude, the GA was trying to find the optimal point where those two properties meet the best condition without losing any particular side. The convergence of 2<sup>nd</sup> peak's frequency and magnitude occurred after the number of generations reached around 140 steps. The third line which is located at the bottom of Figure 3.16 represents the average penalty value of whole population at each generation step. This line does not have a convergence for most of optimization problems, since the stochastic optimization method like GA has always the perturbation in the results. That is why this line is not smooth, but rather be disturbed slightly at every generation step.

Table 3.3: Properties of the original and optimized skirt systems in Waban-Aki

	Waban-Aki				
	$M_c(\text{kg})$	$L_c(\text{m})$	$B_c(\text{m})$	$D_b(\text{m})$	$H_b(\text{m})$
<b>Original skirt</b>	36,740	21	8.6	1.39	0.975
<b>Optimized skirt</b>	36,740	21	8.6	1.39	0.975
	$M_s(\text{kg})$	$L_1(\text{m})$	$L_2(\text{m})$	$L_3(\text{m})$	$L_4(\text{m})$
<b>Original skirt</b>	932.27	0.180	2.02	1.69	1.10
<b>Optimized skirt</b>	932.43	0.164	1.90	1.70	1.08
	$L_{ob}(\text{m})$	$\Omega(\text{rad})$	$p_{ce}(\text{Pa})$	$Q_e(\text{m}^3/\text{s})$	$p_{be}/p_{ce}$
<b>Original skirt</b>	2.60	0.576	2,000	95.088	1.2
<b>Optimized skirt</b>	2.64	0.600	2,000	97.161	1.1
	$h_e(\text{m})$	$\alpha_o(\text{rad})$	$\gamma_o(\text{rad})$	$H_c(\text{m})$	$h_{so}(\text{m})$
<b>Original skirt</b>	0.0036	0.498	0.187	1.2576	1.254
<b>Optimized skirt</b>	0.0039	0.422	0.174	1.2586	1.2547

The optimized skirt should be met the several stability requirements and the main objective – improved ride quality. Table 3.3 shows the dimensions and other properties of original skirt system and optimized skirt system. According to Mantle [4], he explained some factors which can improve the stability in heave motion. However those suggestions are not necessarily required to fulfill the stability criteria. Since the ACV systems are very complex and inter-related each other, it is not easy to pin-point the conditions for the stability requirements. Nevertheless those suggestions may help to understand the system in terms of how they are related each other in some ways.

In order to improve the stability in heave motion, it is recommended to increase the air gap height and flow rate. In Table 3.3, the result of optimization on Waban-Aki skirt shows that the air gap height of optimized skirt was increased from 3.6 mm to 3.9 mm and the flow rate of that was also increased from 95.088 m<sup>3</sup>/s to 97.161 m<sup>3</sup>/s. Hence the stability of optimized skirt system is improved according to Mantle's recommendation. However the pressure ratio was decreased from 1.2 to 1.1. This change degrades the stability of vehicle, but as mentioned earlier there are many factors interacted together for the stability, and the GA optimization method tries to find the solution which falls into the best optimized conditions even though some of factors couldn't be fully satisfied. For the loss of pressure ratio, the compensation for stability was made from the improvement of other skirt properties such as the dimensions of bag and finger. The mass of optimized skirt was not changed much compared to the original skirt. The outer bag length was increased from 2.6 m to 2.64 m. This change eventually contributes the vehicle's stability by providing more flexibility and ability to absorb more energy caused from the ground or during the vehicle's heave motion. Other dimensions

such as the lengths and angles related to the bag and finger were also changed to provide better stability and ride quality. Furthermore eigenvalues of the system matrix were checked and satisfied for the stability criteria. The modification on design parameters was also performed in allowable range. Other constraint conditions were also met.

The comparison of original and optimized skirts of Waban-Aki was also made in a view of frequency response. The second peak's magnitude and its frequency of original model were found as 20.8 units and 24.7 rad/s, while those of optimized model were obtained as 6.6 units and 21.2 rad/s. Thus the second peak's magnitude and its frequency were reduced significantly through the optimization process. The percentages of reduction in these properties are 68.3 % and 14.2 %, respectively. This result indicates that the magnitude of disturbance during the vehicle's heave motion is reduced more than a half of that in original skirt system. Furthermore the frequency of second peak was far from the range which humans feel the most sensitivity during the heave motion. Thus the changes in both second peaks magnitude and its frequency provide better ride quality than the ones in original skirt system. Therefore, it is proven from the above results that a small change of geometry can improve ride quality a lot. Figure 3.17 and 3.18 depicts the frequency curve and phase shift curve for the original and optimized skirts of Waban-Aki. The actual physical shapes of original and optimized skirts are also plotted in Figure 3.19.

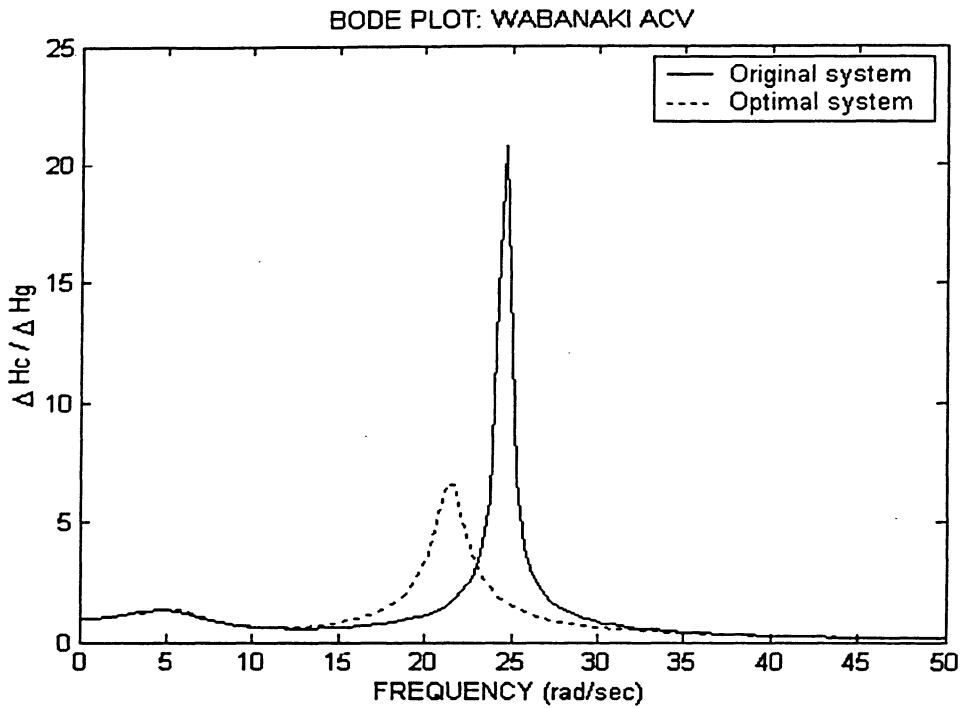


Figure 3.17: Frequency response curve for the original and optimized skirts of Waban-Aki

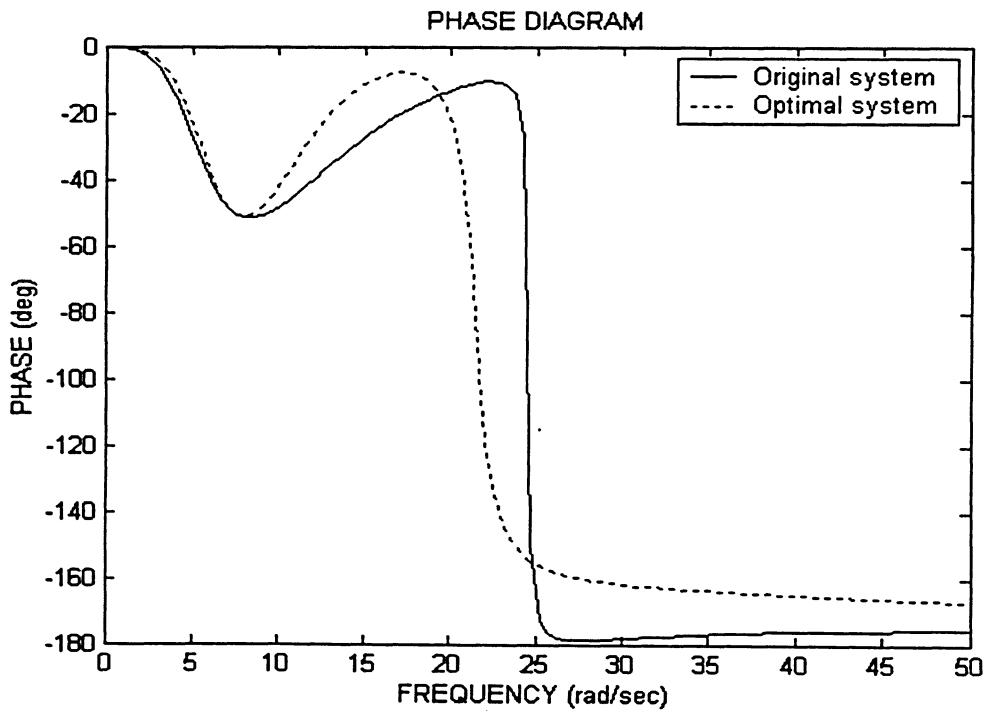


Figure 3.18: Phase shift curves for the original and optimized skirts of Waban-Aki

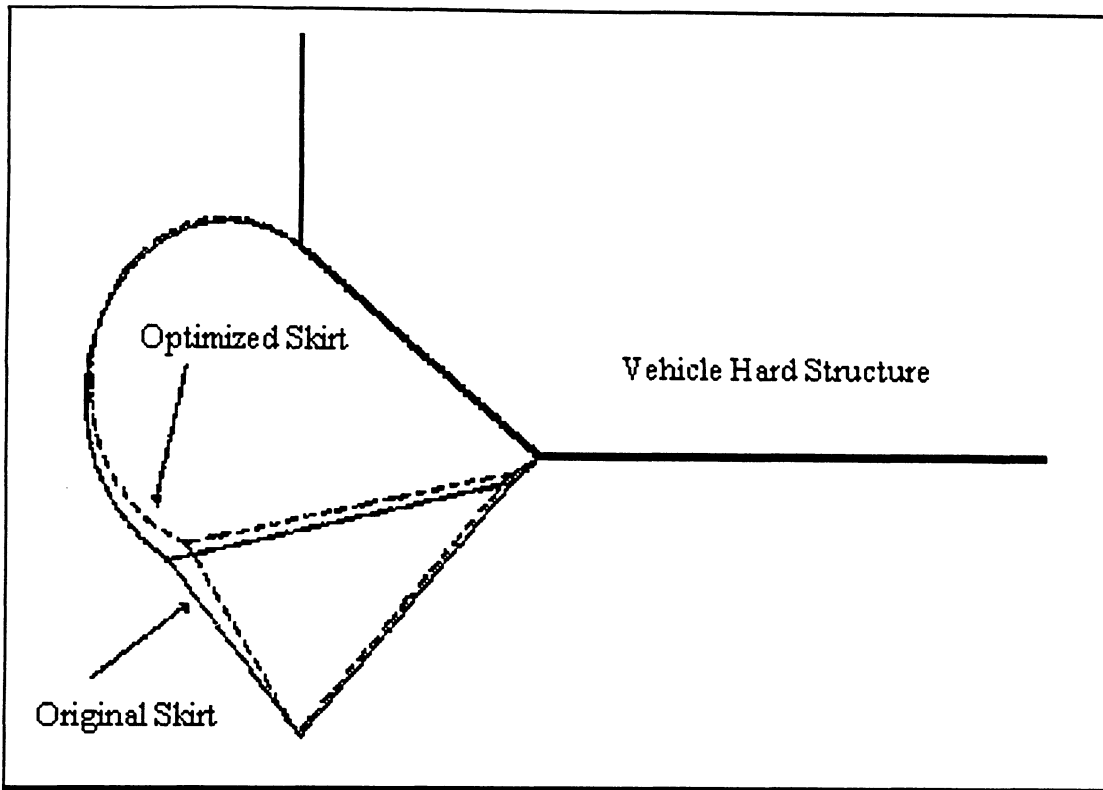


Figure 3.19: Physical shapes of the original and optimized skirts of Waban-Aki

### 3.7.2 Optimization on LCAC Skirt

LCAC is also chosen as another example of a bag and finger skirt optimization with the GA. The initial conditions given for the vehicle dimensions are the followings:

$$M_c = 150,000 \text{ kg}, L_c = 27 \text{ m}, B_c = 14 \text{ m}, D_h = 1.81 \text{ m}, \text{ and } H_h = 1.27 \text{ m}.$$

Figure 3.20 shows the overall performance of the GA on LCAC skirt optimization. All the important properties of the graph were explained in the previous section under the case of Waban-Aki skirt optimization. As shown in the figure, the GA found the point of optimal solution after 42 generation steps. This is quite fast convergence compared to the previous case of Waban-Aki skirt system. The reason is that the original skirt has the properties closed to the optimal solution already, so that it didn't take time for a long to

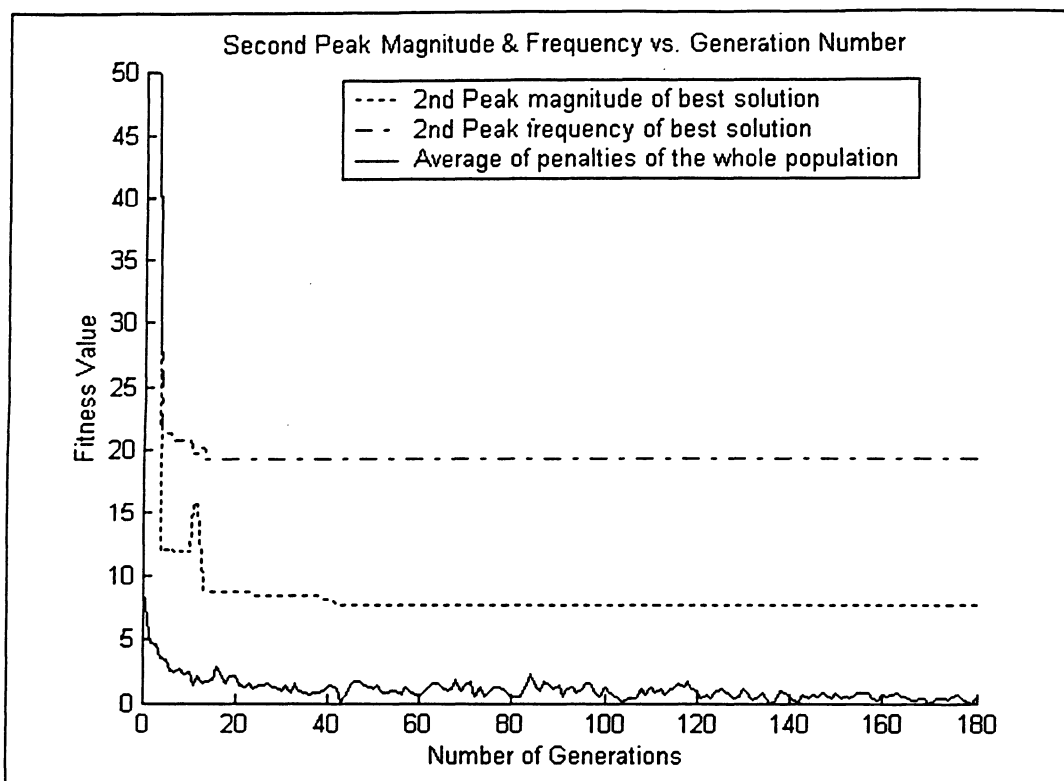


Figure 3.20: Overall performance of GA on LCAC skirt optimization

reach that point. It is also known from the fact that the magnitude of optimization level made on the skirt of LCAC is less than the case on the skirt of Waban-Aki. Nevertheless the GA produced the quite significant reduction in the 2<sup>nd</sup> peak's frequency and magnitude of LCAC skirt system.

All the properties of optimized and original skirts of LCAC are shown in the following Table 3.4. The results showed the reduced air gap height from 38.8 mm to 23.0 mm. This change contributes the instability of vehicle. However, the system of optimized skirt produced the compensation for this instability by generating longer outer bag length and changes in other dimensions. That is why the optimized skirt has better stability and ride comfort compared to the original skirt system, even if it has the reduced air gap height. The flow rate and pressure ratio of bag and cushion for optimized skirt were

found almost same as the original skirt system. Finally eigenvalues of the system proved that the overall stability of skirt system was satisfied by producing all negative values. Other stability and design constraints were also fulfilled.

Table 3.4: Properties of the original and optimized skirt systems in LCAC

	LCAC				
	$M_c(\text{kg})$	$L_c(\text{m})$	$B_c(\text{m})$	$D_b(\text{m})$	$H_b(\text{m})$
<b>Original skirt</b>	150,000	27	14	1.807	1.267
<b>Optimized skirt</b>	150,000	27	14	1.807	1.267
	$M_s(\text{kg})$	$L_1(\text{m})$	$L_2(\text{m})$	$L_3(\text{m})$	$L_4(\text{m})$
<b>Original skirt</b>	1,913	0.270	3.03	2.535	1.65
<b>Optimized skirt</b>	1,902	0.280	3.12	2.350	1.75
	$L_{ob}(\text{m})$	$\Omega(\text{rad})$	$p_{ce}(\text{Pa})$	$Q_c(\text{m}^3/\text{s})$	$p_{be}/p_{ce}$
<b>Original skirt</b>	3.90	0.576	3,893	380.0	1.20
<b>Optimized skirt</b>	4.20	0.589	3,893	379.9	1.18
	$h_c(\text{m})$	$\alpha_o(\text{rad})$	$\gamma_o(\text{rad})$	$H_c(\text{m})$	$h_{so}(\text{m})$
<b>Original skirt</b>	0.0388	0.4178	0.1015	1.7371	1.6983
<b>Optimized skirt</b>	0.0230	0.5315	0.2016	1.8350	1.8120

The second peak's magnitude and its frequency of original model are found as 14.64 units and 20.7 rad/s, while those of optimized model are obtained as 7.69 units and 19.2 rad/s. The percentages of reduction in 2<sup>nd</sup> peak's magnitude and frequency between the original and optimized skirt systems are computed as 47 % and 7 %, respectively. The reduction in both of characteristics contributes improved ride quality and stability. The frequency and phase shift curves are plotted in Figure 3.21 and 3.22. Figure 3.23 illustrates the actual physical shapes of original and optimized skirts.

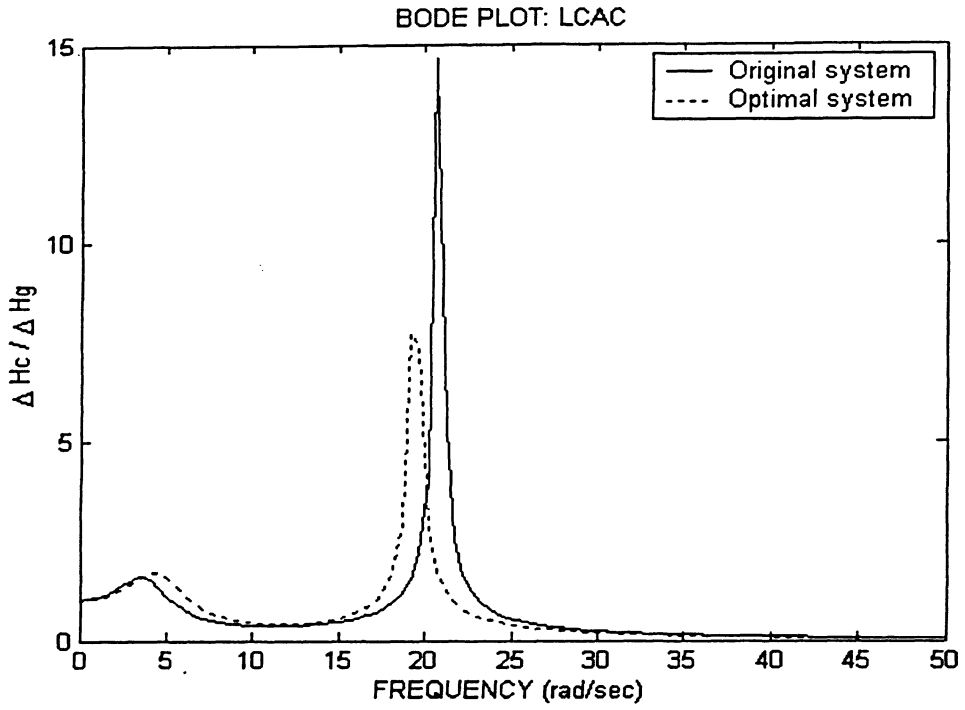


Figure 3.21: Frequency response curves for the original and optimized skirts of LCAC

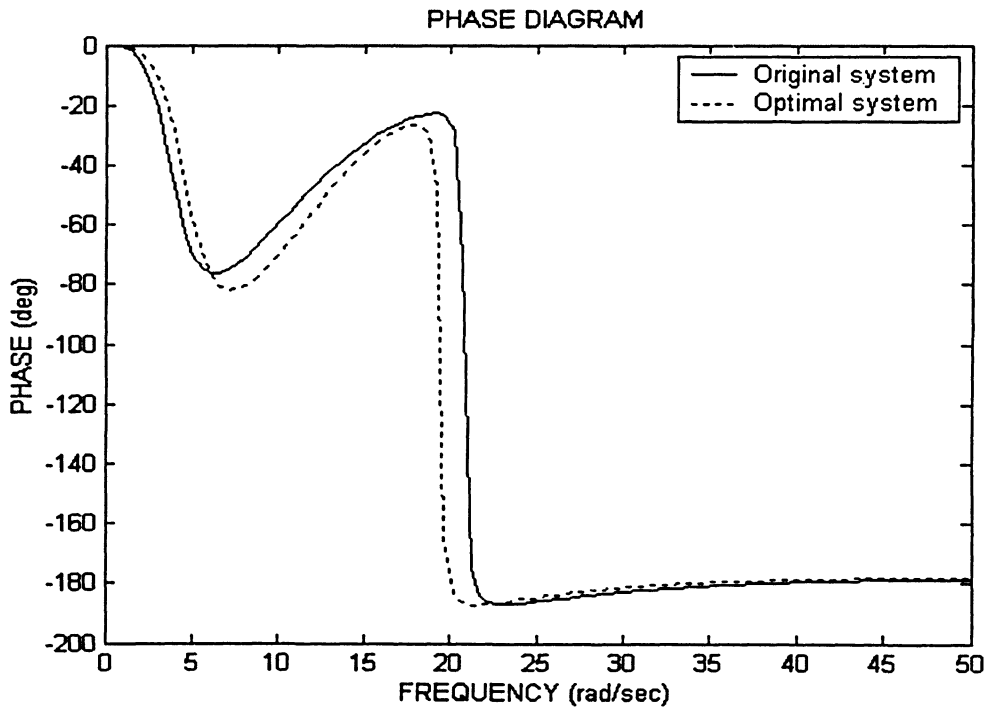


Figure 3.22: Phase shift curves for the original and optimized skirts of LCAC

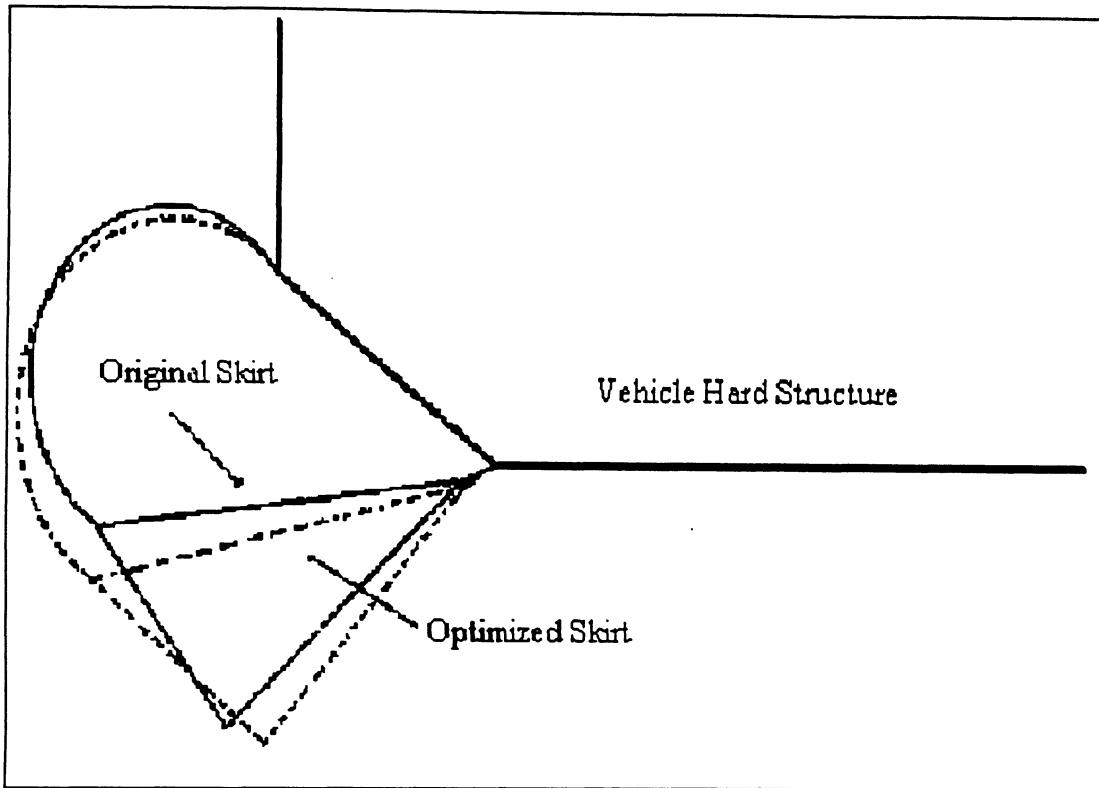


Figure 3.23: Physical shapes of the original and optimized skirts of LCAC

### 3.7.3 Effect of various skirt masses on optimization

In this section, the effect of different skirt masses on skirt optimization with the GA is addressed. The original skirt material is an elastomer coated fabric composite and its area density is  $2.8 \text{ kg/m}^2$ . The second skirt material for comparison purpose is an arbitrary chosen material which area density is  $1.4 \text{ kg/m}^2$ . Unlike previous experiments for skirt optimization, the GA has now two different skirt material choices. Hence, design variables include the continuous parameters as well as discontinuous ones, while in previous experiments only continuous parameters were considered. Then the lengths of individual and computation time are increased compared to previous experiments. The objective function of the GA is also changed to evaluate and assign the proper fitness

value. For the general information about the effect of different skirt masses on ACV performance, it was found that the magnitude of second peak in the frequency response curve will be decreased while its frequency will be increased for the reduced skirt mass [2]. Since it is not possible to reduce both of magnitude and frequency of second peak at the same time, objective function is modified so that it will produce the lowest second peak magnitude without any concern or interest about its frequency range. The reason is that much reduced magnitude of second peak does not disturb ride comfort even though it is in the sensitive frequency range.

Same parameters in previous experiments are again applied for this optimization practice. The only difference is the objective function and the freedom for the GA to choose different skirt material properties. The results of this new experiment are plotted in Figures 3.24, 3.25, 3.26, and 3.27 with original system and fixed skirt mass system.

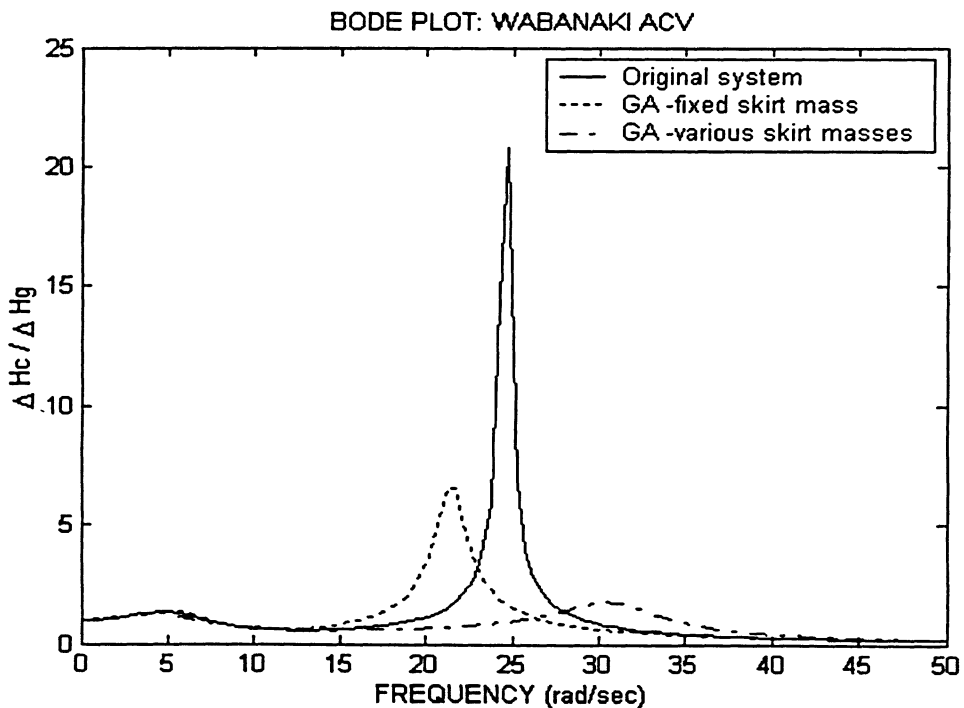


Figure 3.24: Frequency response curves for different skirt mass condition on Waban-Aki

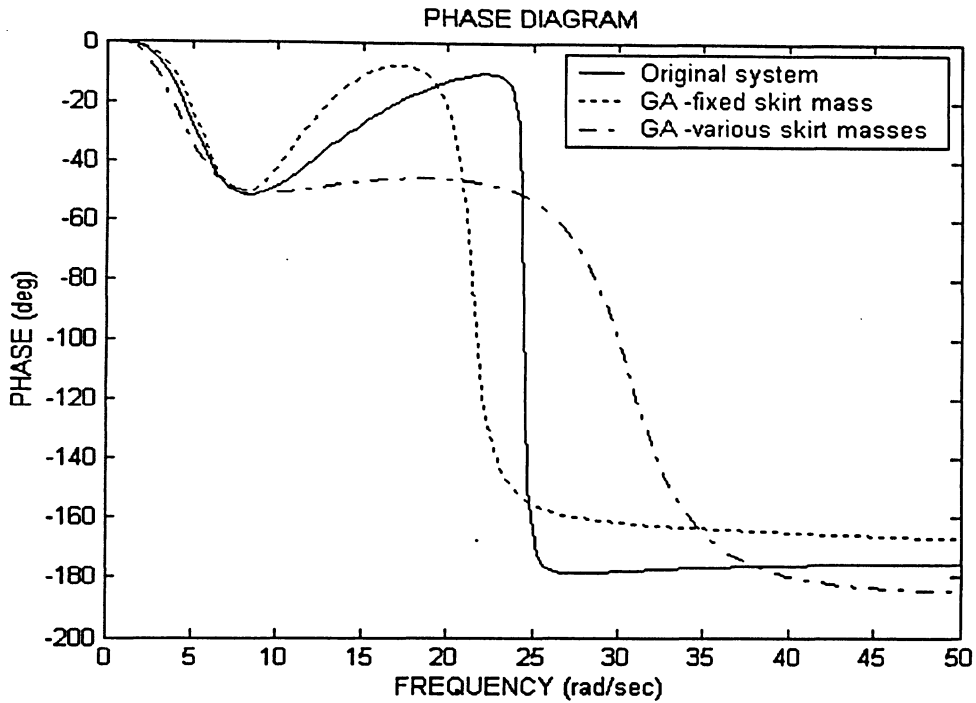


Figure 3.25: Phase shift curves for different skirt mass condition on Waban-Aki

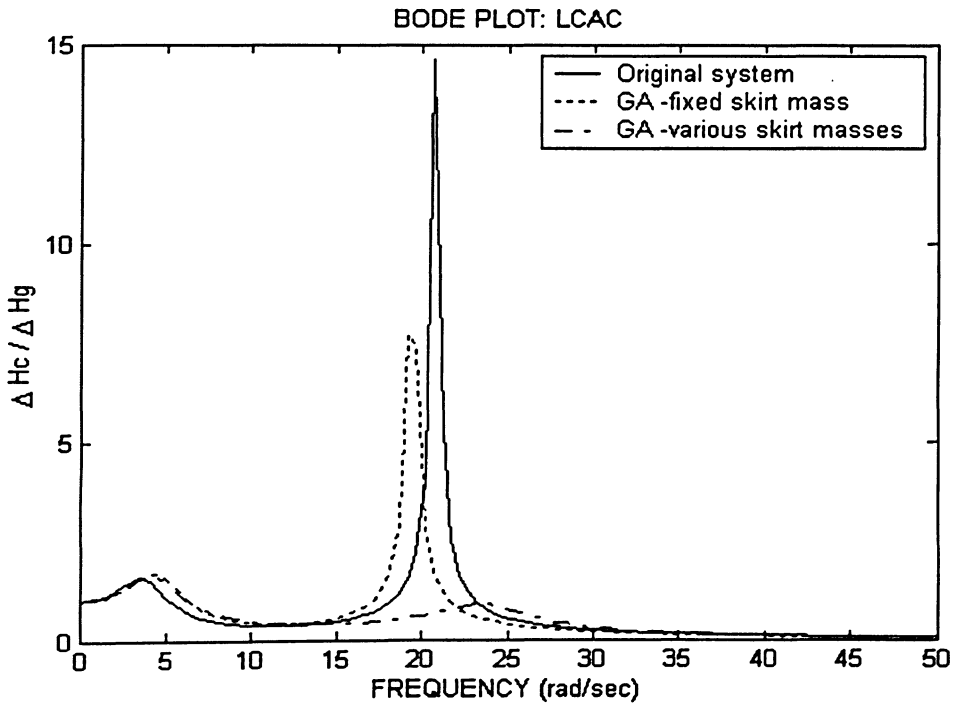


Figure 3.26: Frequency response curves for different skirt mass condition on LCAC

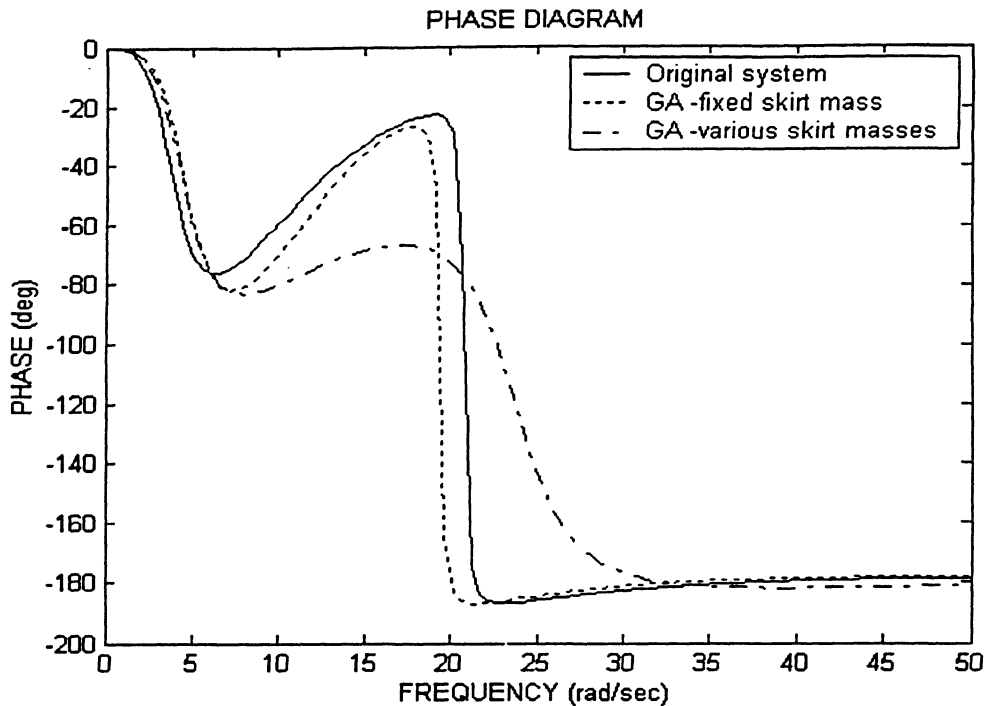


Figure 3.27: Phase shift curves for different skirt mass condition on LCAC

The results showed that the GA selected the new skirt material property which is a half area density of original skirt material in order to produce the second peak's magnitude as low as possible. Thus the skirt mass for Waban-Aki and LCAC becomes 501 kg and 958 kg, respectively. In the frequency response curves, the second peak's magnitude of Waban-Aki and LCAC was reduced in a great magnitude, compared to the original skirt system and the optimized skirt system with fixed skirt mass. The pressure ratio and air gap of new optimized skirt system for Waban-Aki were found as 1.26 and 3.50 mm, respectively. Those for LCAC were also computed as 1.18 and 22.0 mm, respectively. Hence the pressure ratio for each ACV was set in the boundary of anti-skirt bounce to satisfy the stability. The air gap for each ACV was also obtained similar to that of first optimized skirt system with fixed skirt mass. Finally eigenvalues of system matrix and other design constraints were also satisfied for both cases of Waban-Aki and LCAC.

The following table summarizes the magnitude of second peak and percentage of reduction compared to the original skirt system.

Table 3.5: Second peak magnitude and percentage of reduction for each system

	<b>Waban-Aki</b>	
	2 <sup>nd</sup> Peak Magnitude (unit)	Percentage of Reduction (%)
Original system without optimization	20.80	0
Optimized system with fixed skirt mass	6.60	68.3
Optimized system with various skirt masses	1.76	91.5
	<b>LCAC</b>	
	2 <sup>nd</sup> Peak Magnitude (unit)	Percentage of Reduction (%)
Original system without optimization	14.64	0
Optimized system with fixed skirt mass	7.69	47
Optimized system with various skirt masses	0.90	93.9

In conclusion, it was found that the reduced skirt mass can decrease the magnitude of second peak in the frequency response curve even though it increases the frequency of second peak. However the increased frequency can be ignored by producing a small magnitude of second peak's magnitude. Hence the GA further optimized the skirt system with the reduced skirt area density and found the lowest magnitude of second peak with satisfying all the stability criteria. Since the magnitude of second peak is much reduced, the ride comfort and quality are further improved compared to the previous optimized system with fixed skirt area density. This is very significant result and implies that the ride comfort can be improved much further using the reduced skirt material density in real application. This characteristic should be noticed by the manufacturers of ACVs, and the research for advanced material of skirt should be carried on.

## 4. CONCLUSIONS

As an amphibious vehicle, the ACV is a unique marine craft that provides the ability to travel over rough surfaces as well as at high speeds. In this thesis, design of ACVs was carried out with the Artificial Intelligence; Expert System and Genetic Algorithm. The program codes of these two techniques were specifically built and implemented for the design of ACVs.

In the first part of the thesis, initial design of ACVs was performed with the expert system. The main dimensions, weight distributions, and parametric properties were successfully generated with the expert system. A simple configuration of subsystems such as lift system, propulsion system, and skirt and cushion system were also created. Since the design of ACVs is very complicated, it was carried out based on the simplified model and some of design steps were omitted in an initial design phase. These simplifications and omissions could be replaced with more accurate design process in later development. In order to build a satisfactory and accurate expert system, more than 70 existing ACV data sets were collected and analyzed. Furthermore the statistical data, past trends, and much literature were also referred and used.

For the validation of expert systems, tests were performed on the two existing ACVs, the CCG Waban-Aki and LCAC. The overall performance was quite satisfactory compared to the original system even though some design parameters were obtained with some errors. These errors should be corrected when the design phase is further developed. As an initial design stage, these errors should be acceptable and provide the helpful guideline and estimation for the designers. In order to produce better estimation of design

parameters and configurations, more data sets and literature need to be collected and analyzed. Moreover the ACV database should also be updated with the newly developed technologies. In conclusion the implementation of expert system on initial design of ACVs was successfully carried out. The results of tests were quite satisfactory and stable in an initial design phase. The valuable design tool, expert system, is surely helpful for non-expert designers and beginners.

In the second part of the thesis, the bag and finger skirt of ACVs was optimized with the robust search technique; the GA. The GA is the search technique that can be applicable to most engineering problems and those of other fields. The past several years have shown its robustness and flexibility on optimization problems. Furthermore it can search the solution point with great speed even though there are complicated constraint conditions. Such a powerful tool was applied for the optimization of the bag and finger skirt system. The example ACVs were again selected as the CCG Waban-Aki and LCAC. The linearized equations of motion for the vehicle were used to predict the behaviors of the vehicles as well as the skirts.

The design variables of skirt system were the dimensions of outer bag, inner bag, and finger, and pressure ratio of the bag and cushion. Then the original parameters and the optimized parameters were compared. The optimization of skirt results the increment in the outer bag length. It indicates that the skirt has more flexibility and is able to absorb more energy from the ground or during the motion of vehicles. The increased air gap height and flow rate also contribute the vehicle's better stability in heave motion. The frequency response curves for the original and optimized models were compared in terms of the second peak magnitude and frequency. The results showed that the optimized skirt

has the greatly reduced second peak magnitude and frequency, so that it provides the better quality of ride compared to the original skirt configuration. The skirt bounce problem in optimized skirt was also solved by getting the pressure ratio of bag and cushion as 1.10 and 1.18 for the CCG Waban-Aki and LCAC, respectively, which is in the allowable range for anti-skirt bounce.

The optimization of the skirt system with various material choices was also carried out by the GA. The results of experiments indicated that the GA can further optimize the skirt system with the reduced skirt area density. The GA produced the very small magnitude of second peak so that the ride comfort became much improved. All the stability criteria were also satisfied. Hence the reduced skirt mass improved ride quality while meeting the stability conditions at the same time. In conclusion the bag and finger skirt of both ACVs produced better ride quality as well as stability through the optimization process with the GA.

In future work, in the expert system part, more data sets for ACVs will be collected and summarized for better prediction of design parameters. At the same time, initial design phase will cover a wide range of design processes so that it can include the complicated model and constraints as well. The inputs for users will also be modified in a way that users can express their design options more freely. In the GA part skirt model will be modified to reflect more characteristics of real world behavior including the equations of motion, configuration of the bag and finger skirt, its parameter estimation, and so on. The codes for the GA are also going to be refined for more effective and efficient performance so that it can produce the solution faster. The constraint condition for the skirt optimization will be expanded further to contain more realistic conditions.

## REFERENCES

1. Amyot, J. R., "Hovercraft Technology, Economics and Applications", Elsevier Studies in Mechanical Engineering, Vol. 11, Elsevier, 1989.
2. Chung, J., "Theoretical Investigation of Heave Dynamics of an Air Cushion Vehicle: Bag and Finger Skirt", Ph.D. dissertation, Institute for Aerospace Studies, University of Toronto, 1997.
3. Ma, T. and Sullivan, P. A., "Dynamics of Responsive Skirts", Hovercraft Technology, Economics and Application, J. R. Amyot, ed., Elsevier Studies in Mechanical Engineering, Vol.11, Elsevier, Amsterdam, Chap.13, 1989.
4. Mantle, P. J., "Air Cushion Craft Development", David W. Taylor Naval Ship Research and Development Center, Bethesda, Maryland, DTNSRDC-80/012, 1980.
5. Tzafestas, Spyros, "Expert Systems in Engineering Applications", Springer-Verlag, 1993.
6. Reich, Y., Bertram, V., and Friesch, J., "The development of a Decision Support System for Propeller Design", In Proceedings of the 9<sup>th</sup> International Conference on Computer Applications in Shipbuilding, 1997.
7. Nah, Seung-Hyeog, "The Development of an Expert System for Aircraft Initial Design (DESAID)", Ph.D. dissertation, Cranfield Institute of Technology, 1991.
8. Neufeld, D. and Chung, J., "Development of an Expert System for Unmanned Aerial Vehicle Design", CASI 50<sup>th</sup> Annual General Meeting and Conference, Montreal, 2003.

9. Bulitko, V. V. and Wilkins, D. C., "Automated Instructor Assistant for Ship Damage Control", Proceedings of the 11<sup>th</sup> IAAI '99 Conference, Orlando, Florida, 1999.
10. Lucas, P., "Knowledge Acquisition for Decision-theoretic Expert Systems", AISB Quarterly, 94, 23-33, 1996.
11. Jung, T. and Chung, J., "Initial Design of Air Cushion Vehicles by Expert System", submitted to 17<sup>th</sup> International Sessions in 41<sup>st</sup> Aircraft Symposium, Japan Society of Aeronautics and Space Science, 2003.
12. Barzilay, R., DeCristofaro, J., Korelsky, T., Lavoie, B., McCullough, D., and Rambow, O., "A new approach to Expert System Explanations", In proceedings of INLG-1998, p.78-87.
13. Goldberg D. E., "Genetic Algorithms in Search, Optimization, and Machine Learning", Addison-Wesley, 1989.
14. Perez, R. E., "Aircraft Conceptual Design Using Genetic Algorithms", 8<sup>th</sup> AIAA/USAF/NASA/ISSMO Symposium on Multidisciplinary Analysis and Optimization, AIAA paper No., AIAA-2000-4938, 2000.
15. Perez, R. E., Behdinin, K., and Chung, J., "Airfoil Shape Optimization Using Genetic Algorithms", CASI 47<sup>th</sup> Annual Conference, Ottawa, Canada, May 2000.
16. Gen M. and Cheng R., "Genetic Algorithms & Engineering Optimization", John Wiley & Sons, Inc. 2000.
17. Jung, T. and Chung, J., "Airline Fleet Assignment using Genetic Algorithm" Genetic and Evolutionary Computer Conference (GECCO-2002) for late breaking papers, New York, 2002.

18. Chung, J. and Jung, T., "Optimization of an Air Cushion Vehicle Bag and Finger Skirt Using Genetic Algorithms", accepted to Journal of Aerospace Science and Technology, Elsevier 2003.
19. Rasheed K. M., "GADO: A Genetic Algorithm for continuous Design Optimization", Ph.D. dissertation, Computer Science, The State University of New Jersey, 1998.
20. Krishna Rao K.V., Muralidhar S., and Dhingra S. L., "Public Transport Routing and Scheduling using Genetic Algorithms", Proceedings of the 8th International Conference on Computer-Aided Scheduling of Public Transport (CASPT), 2000.
21. Ryan G. W., "A Genetic Search Technique for Identification of Aircraft Departures", NASA Contractor Report 4688, Dryden Flight Research Center, 1995.
22. Herrera F., Lozano M., and Verdegay J. L., "Tackling Real-Coded Genetic Algorithms: Operators and Tools for Behavioural Analysis", Artificial Intelligence Review, vol.12, 265-319, 1998.
23. Chung, J. and Sullivan, P.A., "Linear Heave Dynamics of an Air Cushion Vehicle Bag and Finger Skirt", Transaction of Japan Society for Aeronautical and Space Sciences, Vol.43, No.140, pp.39-45, 2000.
24. Lundstrom, R., Holmlund, P., and Lindberg, L., "Absorption of energy during vertical whole-body vibration exposure", Journal of Biomechanics, Vol.31, Issue4, pp.317-326, 1998.
25. Horvitz, E. J. and Breese, J. S., "Decision Theory in Expert Systems and Artificial Intelligence", International Journal of Approximate Reasoning, 2:247-302, 1988.

26. Zupan, B. and Cheng, M. K., "Response Time Optimization of Rule-Based Expert Systems", Proceedings of SPIE –Knowledge Based Artificial Intelligence System in Aerospace and Industry, Vol.2244, pp.240-248, 1994.
27. Shaw, M. and Gaines, B., "Comparing Conceptual Structures: Consensus, Conflict, Correspondence and Contrast", In Knowledge Acquisition, Vol.1, pp.341-363, 1989.
28. Cheetham, B. and Pomeroy, B., "Knowledge Acquisition for a Fluid Bed Reactor Expert System", Proceedings of SPIE –Knowledge Based Artificial Intelligence System in Aerospace and Industry, Vol.2244, pp.196-205, 1994.
29. Reiter, E., Robertson, R., and Osman, L., "Knowledge Acquisition for Natural Language Generation", In proceedings of INLG-2000, p.217-224.
30. Cheng, V.H.L., Crawford, L.S., and Menon, P.K., "Air Traffic Control Using Genetic Search Techniques", IEEE International Conference on Control Applications, August 22-27, Hawaii, 1999.
31. Chung, J., "Skirt-Material Damping Effects on Heave Dynamics of an Air-Cushion-Vehicle Bag-and-Finger Skirt", Canadian Aeronautics and Space Journal, Vol.48, No.3, pp.201-212, 2002.
32. Chung, J., Sullivan, P. A., and Ma, T., "Nonlinear Heave Dynamics of an Air Cushion Vehicle Bag and Finger Skirt", Journal of Ship Research, Vol.43, No.2, pp.79-94, 1999.
33. Sullivan, P. A., Hinchey, M. J., and Green, G. M., "A Review and Assessment of Methods for Prediction of the Dynamics Stability of Air Cushions," Journal of Sound and Vibration, Vol.84, No.3, (1982) pp337-358.

34. Kateman and Lucasius, Understanding and Using Genetic Algorithms, Chemometrics and Intelligent Laboratory Systems, vol25, p.99-145, 1994.
35. Wright A. H., "Genetic Algorithms for Real Parameter Optimization", Foundations of Genetic Algorithms 1, Morgan Kaufman, 205-218, 1991.
36. Coit D. W. and Smith A. E., "Penalty Guided Genetic Search for Reliability Design Optimization", Computers and Industrial Engineering, Special Issue on Genetic Algorithms, vol.30, number 4, 1996.
37. Rasheed K., "An Adaptive Penalty Approach for Constrained Genetic-Algorithm Optimization", The third annual conference on Genetic Programming (GP-98): Symposium on Genetic Algorithms (SGA-98), 1998.
38. Hinchey, M. J. and Sullivan, P. A., "On Hovercraft Over-Water Heave Stability", Journal of Sound and Vibration, Vol.163, Issue 2, pp.261-273, 1993.
39. Hinchey, M. J. and Sullivan, P. A., "Hovercraft Heave Stability", Canadian Aeronautics and Space Journal, Vol.30, No.2, pp.130-151, 1984.
40. Bradley C. Wallet, David J. Marchette, and Jeffery L. Solka, "A Matrix representation for genetic algorithms", Proceedings of Automatic Object Recognition IV of SPIE Aerosense, 1996.
41. P. Larranaga, C. M. H. Kuijpers, R. H. I. Inza, and S. Dizdarevic, "Genetic Algorithms for the Traveling Salesman Problem: A Review of Representations and Operators", Artificial Intelligence Review., vol.13, pp.129-170, 1999.
42. Chung, J., "Chaos and Nonlinear Heave Dynamics of an Air Cushion Vehicle Bag and Finger Skirt", ICNPAA 2002 International Conference on Nonlinear Problems in Aviation and Aerospace, Melbourne, Florida, 2002.

43. Sullivan, P. A., Charest, P. A., and MA, T., "Heave Stiffness of an Air Cushion Vehicle Bag and Finger Skirt", *Journal of Ship Research*, Vol.38, No.4, pp. 302-307. 1994.

# APPENDIX A. Codes for Linearized Equations of Motion of a Bag and Finger Skirt System

## deri\_elem.m

%%Derivatives and Matrix Elements (Two degrees of freedom Skirt Model, Linearized at equilibrium conditions)

function

```
[PAADD,PAGDD,PAHCDD,PGADD,PGGDD,PGHCDD,PHCADD,PHCGDD,PHCHCDD,PAA,PAG,PAPB,PAPC,PGA,PGG,PGP
B,PGPC,PPBAD, ...
PPBGD,PPBPB,PPBPC,PPCAD,PPCGD,PPCA,PPCG,PPCPB,PPCPC,PPCHCD,PPCHC,PHCA,PHCG,PHCPC,PHCHC,PPCHGD,
PPCHG, ...
    PHCHG] = deri_elem
```

```
[Bb,Db,Hb,LD,Lm,Mc,L1,L2,L3,L4,Lob,omega,Ms,LM,Lb,alphao,gammao,Gamma,sigmao,phi,muo,gammaMo,AfD,Aeff,Is,g,rho,C
b,Cc, ...
```

```
    heo,Bf,Pbo,Pco,Qbo,Qco,hfo,Xso] = input_para;
```

```
SL4=L4-(-heo)/(sin(phi-gammao));
```

```
%For Skrit Geometry 'alpha'
```

```
bo=(L1^2+L2^2+2*L1*L2*cos(alphao-gammao))^0.5;
```

```
betao=atan((L1*sin(alphao)+L2*sin(gammao))/(L1*cos(alphao)+L2*cos(gammao)));
```

```
co=(LD^2+bo^2+2*LD*bo*sin(betao-Gamma))^0.5;
```

```
da_db=(-1/(2*L1)+(L1^2-L2^2)/(2*L1*bo^2))/sin(alphao-betao);
```

```
dbeta_da=(L1^2+L1*L2*cos(alphao-gammao))/bo^2;
```

```
db_da=-L1*L2*sin(alphao-gammao)/bo;
```

```
db_dg=-db_da;
```

```
dbeta_dg=(L2^2+L1*L2*cos(alphao-gammao))/bo^2;
```

```
dc_db=1/co*(bo+LD*sin(betao-Gamma));
```

```
dc_dbeta=LD*bo/co*cos(betao-Gamma);
```

```
dc_da=dc_db*db_da+dc_dbeta*dbeta_da;
```

```
dc_dg=dc_db*db_dg+dc_dbeta*dbeta_dg;
```

```
daa_dab=((L2^2-L1^2)/(L1*bo^3)*db_da*sin(alphao-betao)-((L1^2-L2^2)/(2*L1*bo^2)-1/(2*L1))*cos(alphao-betao)*(1-
dbeta_da))/sin(alphao-betao)^2;
```

```
daa_dgb=((L2^2-L1^2)/(L1*bo^3)*db_dg*sin(alphao-betao)-((L1^2-L2^2)/(2*L1*bo^2)-1/(2*L1))*cos(alphao-betao)*(-
dbeta_dg))/sin(alphao-betao)^2;
```

```
dcs_da=(1/Lob*dc_da)*(sigmao*sin(sigmao)+cos(sigmao))/(sin(sigmao)-sigmao*cos(sigmao));
```

```
dcs_dg=(1/Lob*dc_dg)*(sigmao*sin(sigmao)+cos(sigmao))/(sin(sigmao)-sigmao*cos(sigmao));
```

```
dvoba_da=-Lm*(-L1*L2*sin(alphao-gammao)+LD*L1^2*(cos(betao-Gamma)*dbeta_da*bo-sin(betao-Gamma)*db_da)/bo^2 ...
```

```
    +LD*L1*L2*(-sin(alphao-gammao)*bo-cos(alphao-gammao)*db_da)/bo^2*sin(betao-Gamma) ...
```

```
    +cos(alphao-gammao)/bo*cos(betao-Gamma)*dbeta_da)+Lob*LD*L1^2*dcs_da*1/bo*cos(betao-
```

```
Gamma)/co ...
```

```
    +Lob*LD*L1^2*cos(sigmao)/sigmao*(-db_da/bo^2*cos(betao-Gamma)/co ...
```

```
    +1/bo*(-sin(betao-Gamma)*dbeta_da*co-cos(betao-Gamma)*dc_da/co^2) ...
```

```

+Lob*LD*L1*L2*dc_s_da*cos(betao-Gamma)/co*cos(alphao-gammao)/bo ...
+Lob*LD*L1*L2*cos(sigmao)/sigmao*((-sin(betao-Gamma)*dbeta_da*co-cos(betao-
Gamma)*dc_da)/co^2*cos(alphao-gammao)/bo ...
+cos(betao-Gamma)/co*(-sin(alphao-gammao)*bo-cos(alphao-
gammao)*db_da)/bo^2)) ...
+Lm*(-LD*L1*L2*(-sin(betao-Gamma)*dbeta_da*sin(alphao-gammao)/bo ...
+cos(betao-Gamma)*(cos(alphao-gammao)*bo-sin(alphao-gammao)*db_da)/bo^2) ...
+Lob*L1*L2*dc_s_da*sin(alphao-gammao)/co ...
+Lob*L1*L2*cos(sigmao)/sigmao*(cos(alphao-gammao)*co-sin(alphao-gammao)*dc_da)/co^2 ...
+Lob*LD*L1*L2*dc_s_da*sin(betao-Gamma)/co*sin(alphao-gammao)/bo ...
+Lob*LD*L1*L2*cos(sigmao)/sigmao*((cos(betao-Gamma)*dbeta_da*co-sin(betao-
Gamma)*dc_da)/co^2*sin(alphao-gammao)/bo ...
+sin(betao-Gamma)/co*(cos(alphao-gammao)*bo-sin(alphao-gammao)*db_da)/bo^2));

dviba_da=Lm*(-L1*L2*sin(alphao-gammao)-L1^2*L2*((cos(alphao-betao)*(1-dbeta_da)*bo-sin(alphao-
betao)*db_da)/bo^2*sin(alphao-gammao) ...
+sin(alphao-betao)/bo*cos(alphao-gammao)) ...
-L1^2*L2*((-sin(alphao-betao)*(1-dbeta_da)*sin(alphao-gammao)*da_db) ...
+cos(alphao-betao)*cos(alphao-gammao)*da_db+cos(alphao-betao)*sin(alphao-gammao)*daa_dab));

dvfa_da=-2*Lm*L1*L4*sin(alphao-gammao+phi);

dvoba_dg=-Lm*(L1*L2*sin(alphao-gammao)+LD*L1^2*(cos(betao-Gamma)*dbeta_dg*bo-sin(betao-Gamma)*db_dg)/bo^2 ...
+LD*L1*L2*((sin(alphao-gammao)*bo-cos(alphao-gammao)*db_dg)/bo^2*sin(betao-Gamma) ...
+cos(alphao-gammao)/bo*cos(betao-Gamma)*dbeta_dg)+Lob*LD*L1^2*dc_s_dg*1/bo*cos(betao-
Gamma)/co ...
+Lob*LD*L1^2*cos(sigmao)/sigmao*(-db_dg/bo^2*cos(betao-Gamma)/co ...
+1/bo*(-sin(betao-Gamma)*dbeta_dg*co-cos(betao-Gamma)*dc_dg)/co^2) ...
+Lob*LD*L1*L2*dc_s_dg*cos(betao-Gamma)/co*cos(alphao-gammao)/bo ...
+Lob*LD*L1*L2*cos(sigmao)/sigmao*((-sin(betao-Gamma)*dbeta_dg*co-cos(betao-
Gamma)*dc_dg)/co^2*cos(alphao-gammao)/bo ...
+cos(betao-Gamma)/co*(sin(alphao-gammao)*bo-cos(alphao-
gammao)*db_dg)/bo^2)) ...
+Lm*(-LD*L1*L2*(-sin(betao-Gamma)*dbeta_dg*sin(alphao-gammao)/bo ...
+cos(betao-Gamma)*(-cos(alphao-gammao)*bo-sin(alphao-gammao)*db_dg)/bo^2) ...
+Lob*L1*L2*dc_s_dg*sin(alphao-gammao)/co ...
+Lob*L1*L2*cos(sigmao)/sigmao*(-cos(alphao-gammao)*co-sin(alphao-gammao)*dc_dg)/co^2 ...
+Lob*LD*L1*L2*dc_s_dg*sin(betao-Gamma)/co*sin(alphao-gammao)/bo ...
+Lob*LD*L1*L2*cos(sigmao)/sigmao*((cos(betao-Gamma)*dbeta_dg*co-sin(betao-
Gamma)*dc_dg)/co^2*sin(alphao-gammao)/bo ...
+sin(betao-Gamma)/co*(-cos(alphao-gammao)*bo-sin(alphao-gammao)*db_dg)/bo^2));

dviba_dg=Lm*(L1*L2*sin(alphao-gammao)-L1^2*L2*((cos(alphao-betao)*(-dbeta_dg)*bo-sin(alphao-
betao)*db_dg)/bo^2*sin(alphao-gammao) ...
-sin(alphao-betao)/bo*cos(alphao-gammao)) ...
-L1^2*L2*((sin(alphao-betao)*(dbeta_dg)*sin(alphao-gammao)*da_db) ...
-cos(alphao-betao)*cos(alphao-gammao)*da_db+cos(alphao-betao)*sin(alphao-gammao)*daa_dgh));

dvfa_dg=2*Lm*L1*L4*sin(alphao-gammao+phi);

voba=-Lm*(bo^2+LD*bo*sin(betao-Gamma)+Lob*LD*bo*cos(sigmao)/sigmao*cos(betao-
Gamma)/co)*1/bo^2*(L1^2+L1*L2*cos(alphao-gammao)) ...
+Lm*(LD*cos(betao-Gamma)-Lob/co*cos(sigmao)/sigmao*(bo+LD*sin(betao-Gamma)))*(-L1*L2*sin(alphao-gammao)/bo);

viba=Lm*(bo^2*dbeta_da+L1*(sin(alphao-betao)+bo*cos(alphao-betao)*da_db)*db_da);

if heo>=0
vfa=2*Lm*L1*L4*cos(alphao-gammao+phi);
else
vfa=2*Lm*L1*SL4*cos(alphao-gammao+phi);
end

%For Skrit Geometry 'gamma'

dvobg_da=-Lm*(-L1*L2*sin(alphao-gammao)+LD*L2^2*(cos(betao-Gamma)*dbeta_da*bo-sin(betao-Gamma)*db_da)/bo^2 ...
+LD*L1*L2*((-sin(alphao-gammao)*bo-cos(alphao-gammao)*db_da)/bo^2*sin(betao-Gamma) ...
+cos(alphao-gammao)/bo*cos(betao-Gamma)*dbeta_da)+Lob*LD*L2^2*dc_s_da*1/bo*cos(betao-

```

```

Gamma)/co ...
+Lob*LD*L2^2*cos(sigmas)/sigmas*(-db_da/bo^2*cos(betao-Gamma)/co ...
+1/bo*(-sin(betao-Gamma)*dbeta_da*co-cos(betao-Gamma)*dc_da)/co^2) ...
+Lob*LD*L1*L2*dc_da*cos(betao-Gamma)/co*cos(alphao-gammao)/bo ...
+Lob*LD*L1*L2*cos(sigmas)/sigmas*(-sin(betao-Gamma)*dbeta_da*co-cos(betao-
Gamma)*dc_da)/co^2*cos(alphao-gammao)/bo ...
+cos(betao-Gamma)/co*(-sin(alphao-gammao)*bo-cos(alphao-
gammao)*db_da/bo^2)) ...
+Lm*(LD*L1*L2*(-sin(betao-Gamma)*dbeta_da*sin(alphao-gammao)/bo ...
+cos(betao-Gamma)*(cos(alphao-gammao)*bo-sin(alphao-gammao)*db_da/bo^2) ...
-Lob*L1*L2*dc_da*sin(alphao-gammao)/co ...
-Lob*L1*L2*cos(sigmas)/sigmas*(cos(alphao-gammao)*co-sin(alphao-gammao)*dc_da)/co^2 ...
-Lob*LD*L1*L2*dc_da*sin(betao-Gamma)/co*sin(alphao-gammao)/bo ...
-Lob*LD*L1*L2*cos(sigmas)/sigmas*((cos(betao-Gamma)*dbeta_da*co-sin(betao-
Gamma)*dc_da)/co^2*sin(alphao-gammao)/bo ...
+sin(betao-Gamma)/co*(cos(alphao-gammao)*bo-sin(alphao-gammao)*db_da/bo^2));

dvibg_da=Lm*(-L1*L2*sin(alphao-gammao)+L1^2*L2*((cos(alphao-betao)*(1-dbeta_da)*bo-sin(alphao-
betao)*db_da/bo^2*sin(alphao-gammao) ...
+sin(alphao-betao)/bo*cos(alphao-gammao)) ...
+L1^2*L2*(-sin(alphao-betao)*(1-dbeta_da)*sin(alphao-gammao)*da_db) ...
+cos(alphao-betao)*cos(alphao-gammao)*da_db+cos(alphao-betao)*sin(alphao-gammao)*daa_dab));

dvobg_dg=-Lm*(L1*L2*sin(alphao-gammao)+LD*L2^2*(cos(betao-Gamma)*dbeta_dg*bo-sin(betao-Gamma)*db_dg)/bo^2 ...
+LD*L1*L2*((sin(alphao-gammao)*bo-cos(alphao-gammao)*db_dg)/bo^2*sin(betao-Gamma) ...
+cos(alphao-gammao)/bo*cos(betao-Gamma)*dbeta_dg)+Lob*LD*L2^2*dc_dg*1/bo*cos(betao-
Gamma)/co ...
+Lob*LD*L2^2*cos(sigmas)/sigmas*(-db_dg/bo^2*cos(betao-Gamma)/co ...
+1/bo*(-sin(betao-Gamma)*dbeta_dg*co-cos(betao-Gamma)*dc_dg)/co^2) ...
+Lob*LD*L1*L2*dc_dg*cos(betao-Gamma)/co*cos(alphao-gammao)/bo ...
+Lob*LD*L1*L2*cos(sigmas)/sigmas*(-sin(betao-Gamma)*dbeta_dg*co-cos(betao-
Gamma)*dc_dg)/co^2*cos(alphao-gammao)/bo ...
+cos(betao-Gamma)/co*(sin(alphao-gammao)*bo-cos(alphao-
gammao)*db_dg/bo^2)) ...
+Lm*(LD*L1*L2*(-sin(betao-Gamma)*dbeta_dg*sin(alphao-gammao)/bo ...
+cos(betao-Gamma)*(-cos(alphao-gammao)*bo-sin(alphao-gammao)*db_dg/bo^2) ...
-Lob*L1*L2*dc_dg*sin(alphao-gammao)/co ...
-Lob*L1*L2*cos(sigmas)/sigmas*(-cos(alphao-gammao)*co-sin(alphao-gammao)*dc_dg)/co^2 ...
-Lob*LD*L1*L2*dc_dg*sin(betao-Gamma)/co*sin(alphao-gammao)/bo ...
-Lob*LD*L1*L2*cos(sigmas)/sigmas*((cos(betao-Gamma)*dbeta_dg*co-sin(betao-
Gamma)*dc_dg)/co^2*sin(alphao-gammao)/bo ...
+sin(betao-Gamma)/co*(-cos(alphao-gammao)*bo-sin(alphao-gammao)*db_dg/bo^2));

dvibg_dg=Lm*(L1*L2*sin(alphao-gammao)+L1^2*L2*((cos(alphao-betao)*(-dbeta_dg)*bo-sin(alphao-
betao)*db_dg)/bo^2*sin(alphao-gammao) ...
-sin(alphao-betao)/bo*cos(alphao-gammao)) ...
+L1^2*L2*((sin(alphao-betao)*(dbeta_dg)*sin(alphao-gammao)*da_db) ...
-cos(alphao-betao)*cos(alphao-gammao)*da_db+cos(alphao-betao)*sin(alphao-gammao)*daa_dgb));

vobg=-Lm*(bo^2+LD*bo*sin(betao-Gamma)+Lob*LD*bo*cos(sigmas)/sigmas*cos(betao-
Gamma)/co)*1/bo^2*(L2^2+L1*L2*cos(alphao-gammao)) ...
+Lm*(LD*cos(betao-Gamma)-Lob/co*cos(sigmas)/sigmas*(bo+LD*sin(betao-Gamma)))*(L1*L2*sin(alphao-gammao)/bo);

vibg=Lm*(bo^2*dbeta_dg+L1*(sin(alphao-betao)+bo*cos(alphao-betao)*da_db)*db_dg);

if heo>=0
vfg=2*Lm*L4*(L2*cos(phi)-L4/2);
else
vfg=2*Lm*SL4*(L2*cos(phi)-SL4/2);
end

%For Cushion Volume Conservation Law

dvit_dbt=Lm*bo*(Db*cos(betao)-Hb*sin(betao));

dvit_db=Lm*(Db*sin(betao)+Hb*cos(betao));

```

```

dvit_da=dvit_dbt*dbeta_da+dvit_db*db_da;

dvit_dg=dvit_dbt*dbeta_dg+dvit_db*db_dg;

dvc_da=Lm*(Bb*L1*cos(alphao)+L1^2*cos(2*alphao)-2*L1*L3*sin(muo)*sin(alphao)-2*heo*L1*sin(alphao));

if heo>=0
    dvc_dhe=Lm*(Bb+2*L1*cos(alphao)+2*L3*cos(muo));
else
    dvc_dhe=Lm*(Bb+2*L1*cos(alphao)+2*L3*cos(omega+gammao))+2*heo*(1/tan(muo)-2/sin(2*muo));
end
if heo>=0
    dvc_dg=Lm*(Bb*L3*cos(muo)+L3^2*cos(2*muo)+2*L1*L3*cos(alphao)*cos(muo)-2*heo*L3*sin(muo));
else
    dvc_dg=Lm*(Bb*L3*cos(muo)+L3^2*cos(2*muo)+2*L1*L3*cos(alphao)*cos(muo)-2*heo*L3*sin(muo))-
    heo^2*(csc(muo))^2+4*heo^2*cos(2*muo)/(sin(2*muo))^2;
end

dhf_da=-0.6*L1*cos(alphao);

dhf_dg=(-0.6*L3*cos(muo)*1000/Bf+0.105)*Bf/1000;

dhf_dhc=0.6;

%ForThe Heave motion

dvcvc_dhca=-2*Lm*L1*sin(alphao);

dvcvc_dhcg=-2*Lm*L3*sin(omega+gammao);

if heo>=0
    dvc_dhc=Lm*(Bb+2*L1*cos(alphao)+2*L3*cos(omega+gammao));
else
    dvc_dhc=Lm*(Bb+2*L1*cos(alphao)+2*L3*cos(omega+gammao))+2*(-heo)*cot(phi-gammao));
end

dvcvc_dhchc=0;

dhf_dhg=-0.6;

dvcvc_dhchg=0;

%Matrix Elements

PAADD=Ms*L1^2;
PAGDD=Ms*L1*LM*cos(gammaMo-alphao);
PAHCDD=-Ms*L1*cos(alphao);
PGADD=Ms*L1*LM*cos(gammaMo-alphao);
PGGDD=Ms*LM^2+Is;
PGHCDD=-Ms*LM*cos(gammaMo);
PHCADD=-Ms*L1*cos(alphao);
PHCGDD=-Ms*LM*cos(gammaMo);
PHCHCDD=Mc;

PAA=-Ms*L1*g*sin(alphao)+Pbo*dvoba_da+(Pbo-Pco)*dviba_da+Pco*dvfa_da;
PAG=Pbo*dvoba_dg+(Pbo-Pco)*dviba_dg+Pco*dvfa_dg;
PAPB=voba+viba;
PAPC=vfa-viba;
PGA=Pbo*dvobg_da+(Pbo-Pco)*dvibg_da;
PGG=-Ms*LM*g*sin(gammaMo)+Pbo*dvobg_dg+(Pbo-Pco)*dvibg_dg;
PGPB=vobg+vibg;
PGPC=vfg-vibg;
PPBAD=1/Cb*(voba+viba+dvit_da);
PPBGD=1/Cb*(vobg+vibg+dvit_dg);
PPBPB=1/Cb*(1/(-3*Af0*Qbo^2)-Aeff^2/(rho*Qco));
PPBPC=1/Cb*Aeff^2/(rho*Qco);
PPCAD=1/Cc*(dvc_da-dvc_dhe*L1*cos(alphao));

```

```

PPCGD=1/Cc*(dvc_dg-dvc_dhc*L3*cos(omega+gammao));
PPCA=-1/Cc*(2*(Lb+Bb)*dhf_da+8*Xso*dhf_da-8*L1*sin(alphao)*hfo)*(2*Pco/rho)^0.5;
PPCG=-1/Cc*(2*(Lb+Bb)*dhf_dg+8*Xso*dhf_dg-8*L3*sin(muo)*hfo)*(2*Pco/rho)^0.5;
PPCPB=1/Cc*Aeff^2/(rho*Qco);
PPCPC=-1/Cc*(Aeff^2/(rho*Qco)+1/(2*Pco)*(2*(Lb+Bb)+8*Xso)*hfo*(2*Pco/rho)^0.5);
PPCHCD=1/Cc*dvc_dhc;
PPCHC=-1/Cc*(2*(Lb+Bb)+8*Xso)*dhf_dhc*(2*Pco/rho)^0.5;
PHCA=Pco*dvcvc_dhca;
PHCG=Pco*dvcvc_dhcg;
PHCPC=dvc_dhc;
PHCHC=Pco*dvcvc_dhchc;

PPCHGD=1/Cc*dvc_dhc;
PPCHG=-1/Cc*(2*(Lb+Bb)+8*Xso)*dhf_dhg*(2*Pco/rho)^0.5;
PHCHG=Pco*dvcvc_dhchg;

```

### state space.m

%State-Space Form of Linearized Equations for two degrees of freedom skirt model with the capacitance effects

```
function [A,B] = state_space
```

```
[PAADD,PAGDD,PAHCDD,PGADD,PGGDD,PGHCDD,PHCADD,PHCGDD,PHCHCDD,PAA,PAG,PAPB,PAPC,PGA,PGG,PGPB,PGPC,PPBAD, ...
```

```
PPBGD,PPBPB,PPBPC,PPCAD,PPCGD,PPCA,PPCG,PPCPB,PPCPC,PPCHCD,PPCHC,PHCA,PHCG,PHCPC,PHCHC,PPCHGD,PPCHG, ...
```

```
PHCHG] = deri_elem;
```

%  $H \cdot X^2 = R \cdot X + T \cdot U$ , where X is the transpose matrix of [dhc,dalpha,dgamma,dhc2,dalpha2,dgamma2,dPb,dPc]

```
%
U is the transpose matrix of [dhg2,dhg]
H=[ 1 0 0 0 0 0 0 0 0
0 1 0 0 0 0 0 0 0
0 0 1 0 0 0 0 0 0
0 0 0 PHCHCDD PHCADD PHCGDD 0 0
0 0 0 PAHCDD PAADD PAGDD 0 0
0 0 0 PGHCDD PGADD PGGDD 0 0
0 0 0 0 0 0 1 0
0 0 0 0 0 0 0 1 ];
```

```
R=[ 0 0 0 1 0 0 0 0
0 0 0 0 1 0 0 0
0 0 0 0 0 1 0 0
PHCHC PHCA PHCG 0 0 0 0 PHCPC
0 PAA PAG 0 0 0 PAPB PAPC
0 PGA PGG 0 0 0 PGPB PGPC
0 0 0 0 -PPBAD -PPBGD PPBPB PPBPC
PPCHC PPCA PPCG -PPCHCD -PPCAD -PPCGD PPCPB PPCPC ];
```

```
T=[ 0 0
0 0
0 0
0 PHCHG
0 0
0 0
0 0
PPCHGD PPCHG ];
```

%  $X^2 = A \cdot X + B \cdot U$ , where A and B are state-space matrices

```
A=inv(H)*R;
```

```
B=inv(H)*T;
```

## bode\_plot.m

%%Bode Plot & Eigenvalues

function [mag,w,phase,eigenvals,he]=bode\_plot

global heo

[A,B] = state\_space;

%%Bode Plot%%

B1 = B \* [1;0];

B2 = B \* [0;1];

B = A\*B1 + B2;

C = [1 0 0 0 0 0 0];

D = C\*B1;

n = 100;

w = linspace(0.50,n);

for j = 1:n

[mag(j),phase(j),w(j)]=bode(A,B,C,D,1,w(j));

end

for j=1:n

if phase(j)>0

phase(j)=phase(j)-360;

end

end

%%Eigenvalues%%

eigenvals=eig(A);

%%Heo%%

he=heo;

## APPENDIX B. Codes for Parameter Estimation

### input\_para.m

```

%%Input data file (At equilibrium)

function
[Bb,Db,Hb,LD,Lm,Mc,L1,L2,L3,L4,Lob,omega,Ms,LM,Lb,alphao,gammao,Gamma,sigmao,phi,mu,gammaMo,AfD,Aeff,Is,g,rho,C
b,Cc ...
    ,heo,Bf,Pbo,Pco,Qbo,Qco,hfo,Xso] = input_para

global population ID heo

L1=population(ID).x(1);
L2=population(ID).x(2);
L3=population(ID).x(3);
L4=population(ID).x(4);
Lob=population(ID).x(5);

Pb_Pc=population(ID).x(6);
Db=1.39;
Hb=0.975;
Mc=36740;
Lc=21;
Bc=8.6;

omega=acos((L2^2+L3^2-L4^2)/(2*L2*L3));
phi=asin(L3/L4*sin(omega));

Ac=Lc*Bc;

rho=1.223;
g=9.81;
TA=15;

Pco=Mc*g/Ac;
Pbo=Pco*Pb_Pc;

Pcbar=Pco/(rho*g*Lc);           %Ma's formula
Qcbar=0.0045+0.000587*Pcbar;    %Ma's formula
Aeff=Ac*Qcbar/(Pbo/Pco-1)^0.5; %Ma's formula

[hco,alphao,Qc,gammao]=static_cond(L1,L2);

Qbo=Qc;
Qco=Aeff*(2*(Pbo-Pco)/rho)^0.5;

hso=L1*sin(alphao)+L3*sin(omega+gammao);
hgo=0;
heo=hco-hgo-hso;

Bf=1/3.4*hso*1000;           %mm, Ma's formula
hfo=(0.0323+0.6*heo*1000/Bf+0.105*(gammao-omega)-0.042)*Bf/1000;

Ms=(2*(Lc+Bc)*Lob+0.5*L4*L3*1.2*2*(Lc+Bc)/(Bf/1000))*2.8; %kg, for elastomer-coated fabric composite material, area
density is 2.8kg/m^2

Xso=L1*cos(alphao)+L3*cos(omega+gammao);
Lb=Lc-2*Xso;
Bb=Bc-2*Xso;

Lm=Lc;
LM=(2/3*L3^2+1/3*L4^2)^0.5;
LD=(Db^2+Hb^2)^0.5;

```

```

Gamma=asin(Db/LD);
ls=1/18*Ms*(L3^2+L4^2);
cgammaMo=omega-atan(L4/2/L3);
gammaMo=gammao+cgammaMo;
muo=omega+gammao;

SA=1;
SB=-0.16;
SC=0.0083;
bo=(L1^2+L2^2+2*L1*L2*cos(alphao-gammao))^0.5;
betao=atan((L1*sin(alphao)+L2*sin(gammao))/(L1*cos(alphao)+L2*cos(gammao)));
theta=atan(Hb/Db);
cee=(bo^2-2*LD*bo*cos(betao+theta)+LD^2)^0.5;
szeta=cee/Lob;
sigx=(-SB-(SB^2-4*SC*(SA-szeta))^0.5)/(2*SC)^0.5;
dsigx=(szeta*sigx-sin(sigx))/(cos(sigx)-szeta);
sigmao=sigx+dsigx;
zeta=1.4;
Pbr=Pbo; % Pbr & Qbr are reference pressure and flow, which are usually taken from equilibrium condition

Qbr=Qbo;
A0=((zeta-1)*Pbr)/Qbr^3;

bvb1=Lm*Lob^2*((2*sigmao-sin(2*sigmao))/(4*sigmao^2));
bvb2=Lm*bo*L1*sin(alphao-betao);
bvb3=Lm*(Db*bo*sin(betao)+Hb*bo*cos(betao));
vb=bvb1+bvb2+bvb3;
Cb=vb/(rho*(1.4*286.8*(TA+273.3)));

bvc=Bb*(hco-hgo)+(1/2)*L3^2*sin(2*muo)+(1/2)*L1^2*...
sin(2*alphao)+L1*L3*sin(muo)*cos(alphao)+...
L2*L3*sin(omega)+hco*(2*L1*cos(alphao)+2*L3*cos(muo))...
-2*hgo*(L1*cos(alphao)+L3*cos(muo))-L1^2*sin(2*alphao)...
-2*L1*L3*sin(alphao)*cos(muo)-2*L1*L3*sin(muo)*cos(alphao)...
-L3^2*sin(2*muo);
vc=Lm*bvc;
Cc=vc/(rho*(1.4*286.8*(TA+273.3)));

```

### static\_cond.m

%%This function computes the parameters Hco, Alphao, Qeo, Gammao at equilibrium conditions

```
function [hc,alpha,Qe,gamma]=static_cond(L1,L2)
```

```

%*****WABANAKI*****
%Initial Guess
Xf(1)=1.52;
Xf(2)=0.1;
Xf(3)=95.78;
Xf(4)=0.98*(L1+L2);

alpha=Xf(2)+acos(Xf(4)/(2*L1)+(L1^2-L2^2)/(2*L1*Xf(4)));
gamma=Xf(2)-acos(Xf(4)/(2*L2)+(L2^2-L1^2)/(2*L2*Xf(4)));

Xf(2)=alpha;
Xf(4)=gamma;
diff=1;

while (diff>0.0001)
    Xi=Xf;
    options=optimset('display','off');
    Xf=fsolve('equilibrium_equations',Xi,options);
    diff=abs(Xf(1)-Xi(1));
end

```

```

hc=Xf(1);
alpha=Xf(2);
Qe=Xf(3);
gamma=Xf(4);

```

### equilibrium\_equations.m

```
%Equilibrium equations for the Hco, Alphao, Qe, Gammao
```

```
function F=equilibrium_equations(X)
```

```
global population ID
```

```

L1=population(ID).x(1);
L2=population(ID).x(2);
L3=population(ID).x(3);
L4=population(ID).x(4);

```

```

Lob=population(ID).x(5);
Pb_Pc=population(ID).x(6);
Db=1.39;
Hb=0.975;
Mc=36740;
Lc=21;
Bc=8.6;

```

```

hco=X(1);
alphao=X(2);
Qe=X(3);
gammao=X(4);

```

```

omega=acos((L2^2+L3^2-L4^2)/(2*L2*L3));
phi=asin(L3/L4*sin(omega));
rho=1.223;
g=9.81;

```

```

Ac=Lc*Bc;
Pco=Mc*g/Ac;
Pbo=Pco*Pb_Pc;

```

```

hso=L1*sin(alphao)+L3*sin(omega+gammao);
Bf=1/3.4*hso*1000;
Ms=(2*(Lc+Bc)*Lob+0.5*L4*L3*1.2*2*(Lc+Bc)/(Bf/1000))*2.8;

```

```

Xso=L1*cos(alphao)+L3*cos(omega+gammao);
Lb=Lc-2*Xso;
Bb=Bc-2*Xso;

```

```

Lm=Lc;
LM=(2/3*L3^2+1/3*L4^2)^0.5;
LD=(Db^2+Hb^2)^0.5;

```

```

muo=omega+gammao;
bo=(L1^2+L2^2+2*L1*L2*cos(alphao-gammao))^0.5;
betao=atan((L1*sin(alphao)+L2*sin(gammao))/(L1*cos(alphao)+L2*cos(gammao)));

```

```
%***** RELATIONSHIP BETWEEN BEE,BETA AND ALPHA,GAMMA
```

```

db_da=-(L1*L2*sin(alphao-gammao))/bo;
db_dg=(L1*L2*sin(alphao-gammao))/bo;
dbeta_da=(L1^2+L1*L2*cos(alphao-gammao))/(bo^2);
dbeta_dg=(L2^2+L1*L2*cos(alphao-gammao))/(bo^2);

```

```
%***** FINGER GEOMETRY *****
```

```

he=hco-L1*sin(alphao)-L3*sin(omega+gammao);
hw=-he;
SL4=L4-hw/(sin(phi-gammao));

%***** BAG GEOMETRY *****

cgammaMo=omega-atan(L4/(2*L3));
gammaMo=gammao+cgammaMo;

%***** INNER BAG VOLUME DERIVATIVES *****

dal_db=((L1^2-L2^2)/(2*L1*bo^2)-(1/(2*L1)))/(sin(alphao-betao));
dvi_da=Lm*(bo^2*dbeta_da+L1*(sin(alphao-betao)+bo*cos(alphao-betao))*dal_db)*db_da;
dvi_dg=Lm*(bo^2*dbeta_dg+L1*(sin(alphao-betao)+bo*cos(alphao-betao))*dal_db)*db_dg;

%***** OUTER BAG ANGLE (SIGMA) *****

SA=1;
SB=-0.16;
SC=0.0083;
Gamma=asin(Db/LD);
theta=atan(Hb/Db);
cee=(bo^2-2*LD*bo*cos(betao+theta)+LD^2)^0.5;
szeta=cee/Lob;
sigx=((-SB-(SB^2-4*SC*(SA-szeta))^0.5)/(2*SC))^0.5;
dsigx=(szeta*sigx-sin(sigx))/(cos(sigx)-szeta);
sigmao=sigx+dsigx;

co=(LD^2+bo^2+2*LD*bo*sin(betao-Gamma))^0.5;

%***** DERIVATIVES OF C RESPECT TO ALPHA AND GAMMA

db_da=-L1*L2*sin(alphao-gammao)/bo;
db_dg=-db_da;
dbeta_da=(L1^2+L1*L2*cos(alphao-gammao))/bo^2;
dbeta_dg=(L2^2+L1*L2*cos(alphao-gammao))/bo^2;
dc_db=1/co*(bo+LD*sin(betao-Gamma));
dc_dbeta=LD*bo/co*cos(betao-Gamma);
dc_da=dc_db*db_da+dc_dbeta*dbeta_da;
dc_dg=dc_db*db_dg+dc_dbeta*dbeta_dg;

%***** OUTER BAG VOLUME DERIVATIVES *****

voba=-Lm*(bo^2+LD*bo*sin(betao-Gamma)+Lob*LD*bo*cos(sigmao)/sigmao*cos(betao-
Gamma)/co)*1/bo^2*(L1^2+L1*L2*cos(alphao-gammao)) ...
+Lm*(LD*cos(betao-Gamma)-Lob/co*cos(sigmao)/sigmao*(bo+LD*sin(betao-Gamma)))*(-L1*L2*sin(alphao-gammao)/bo);

vobg=-Lm*(bo^2+LD*bo*sin(betao-Gamma)+Lob*LD*bo*cos(sigmao)/sigmao*cos(betao-
Gamma)/co)*1/bo^2*(L2^2+L1*L2*cos(alphao-gammao)) ...
+Lm*(LD*cos(betao-Gamma)-Lob/co*cos(sigmao)/sigmao*(bo+LD*sin(betao-Gamma)))*(L1*L2*sin(alphao-gammao)/bo);

%***** AUXILIARY EQUATIONS *****

PB=Pbo;

%----- WABANAKI

PC=Pco;
he=hco-L1*sin(alphao)-L3*sin(omega+gammao);
hs=L1*sin(alphao)+L3*sin(omega+gammao);

%***** CUSHION FLOW FUNCTION *****
%----- WABANAKI

hecb=he*1000/Bf;
if hecb<-0.11827
CFFB=0;

```

```

elseif heb<0
  CFFB=0.0323+0.64*heb+3.90*heb^2+6.76*heb^3;
else
  CFFB=0.0323+0.6*heb;
end

FLFFB=CFFB+0.105*(gammao+omega)-0.042;
FLHE=FLFFB*B/1000;

%***** GENERALIZED FORCE DERIVATIVES *****

if he>=0
  DVCDHC=Lm*(Bb+2*L1*cos(alphao)+2*L3*cos(muo));
  DVFDA=2*Lm*L1*L4*cos(alphao+phi-gammao);
  DVFDG=2*Lm*L4*(L2*cos(phi)-(L4/2));
else
  DVCDHC=Lm*(Bb+2*L1*cos(alphao)+2*L3*cos(muo)+2*hw*cot(phi-gammao));
  DVFDA=2*Lm*L1*SL4*cos(alphao+phi-gammao);
  DVFDG=2*Lm*SL4*(L2*cos(phi)-(SL4/2));
end

%***** EQUILIBRIUM EQUATIONS *****

%*** HC EQUATION ***
F(1)=PC*DVCDHC-Mc*g;

%*** ALPHA EQUATION ***
F(2)=PB*voba+(PB-PC)*dvi_da+PC*DVFDA+Ms*g*L1*cos(alphao);

%*** CUSHION AIR ESCAPE LAW ***
if PC>0
  F(3)=Qe-(2*(Lb+Bb)+8*Xso)*FLHE*(2*PC/rho)^0.5;
else
  PCA=abs(PC);
  F(3)=Qe+(2*(Lb+Bb)+8*Xso)*FLHE*(2*PCA/rho)^0.5;
end

%*** GAMMA EQUATION ***
F(4)=PB*vobg+(PB-PC)*dvi_dg+PC*DVFDG+Ms*g*LM*cos(gammaMo);

```

## APPENDIX C. Codes for Genetic Algorithm

### GA.m

%%Genetic Algorithm for the optimization of skirt geometry and property of ACV

global population oldpopulation

%Reading from input\_data

[popsize,Npara,para\_length,maxgen,Coef\_penalty,n\_elit] = input\_data;

%Initialize

n=0;

initial\_pop(popsize,para\_length);

decode(popsize,Npara,para\_length);

objfunction(popsize,Npara,Coef\_penalty); %includes the ranking of each individual

%Loop until the last generation

hold on

for n=1:maxgen

oldpopulation=population;

Pc=0.9-0.3\*n/maxgen;

%'Pc' is the probability of crossover

Pm=0.1-0.07\*n/maxgen;

%'Pm' is the probability of mutation

%Genetic procedure

choices=rsselect(popsize);

i=1;

while(i<=popsize)

%Selection%

pick1=md(1,popsize-i+1);

mate1=choices(pick1);

if pick1~=popsize-i+1

choices(pick1)=choices(popsize-i+1);

end

pick2=md(1,popsize-i);

mate2=choices(pick2);

if pick2~=popsize-i

choices(pick2)=choices(popsize-i);

end

%Crossover(Three different crossover methods)%

k=md(1,3);

if k==1

[newborn1(i).chrom,newborn1(i+1).chrom] ...

=point\_cross(population(mate1).chrom,population(mate2).chrom,para\_length,Pc);

end

if k==2

[newborn1(i).chrom,newborn1(i+1).chrom] ...

=two\_point\_cross(population(mate1).chrom,population(mate2).chrom,para\_length,Pc);

end

if k==3

[newborn1(i).chrom,newborn1(i+1).chrom] ...

=random\_cross(population(mate1).chrom,population(mate2).chrom,para\_length,Pc);

end

%Mutation(Two different mutation methods)%

k=md(1,2);

if k==1

newborn2(i).chrom=single\_mut(newborn1(i).chrom,para\_length,Pm);

newborn2(i+1).chrom=single\_mut(newborn1(i+1).chrom,para\_length,Pm);

end

if k==2

newborn2(i).chrom=two\_mut(newborn1(i).chrom,para\_length,Pm);

newborn2(i+1).chrom=two\_mut(newborn1(i+1).chrom,para\_length,Pm);

end

```

    i=i+2;
end

%Make a population data after genetic procedure
for i=1:popsiz
    population(i).chrom=newborn2(i).chrom;
end

decode(popsiz,Npara,para_length);
objfunction(popsiz,Npara,Coef_penalty);

%New population contents after elitist reservation%
elitist(popsiz,Npara,n_elit);

temp1=max([oldpopulation.rank]);
for i=1:popsiz
    if temp1==oldpopulation(i).rank
        best_old=i;
        break;
    end
end
temp2=max([population.rank]);
for i=1:popsiz
    if temp2==population(i).rank
        best_new=i;
        break;
    end
end

%Graph
plot([n-1 n],[oldpopulation(best_old).sy population(best_new).sy],'b');
plot([n-1 n],[oldpopulation(best_old).sx population(best_new).sx],'m');
plot([n-1 n],[mean([oldpopulation.penalty]) mean([population.penalty])],'r');

end

legend('2nd Peak height of best solution','2nd Peak frequency of best solution','Average of penalties of the whole population');
title('Peak Height & Frequency vs. Generation Number');
xlabel('Number of Generations')
hold off

%Output the best one
output_data(popsiz);

```

### **input\_data.m**

```

%%Input file

function [popsiz,Npara,para_length,maxgen,Coef_penalty,n_elit] = input_data

popsiz=30;           %Population size, should be even number%
Npara=6;            %Number of parameters%
para_length=[4,4,4,4,4,4]; %length of each parameter's chromosome%
maxgen=180;         %Maximum number of generation%
Coef_penalty=1.5;  %Coefficient of penalty%
n_elit=popsiz*0.1; %Number of preseved individuals for elitism%

```

### **initial\_pop.m**

```

%%Initial population generator

function initial_pop(popsiz,para_length)

```

```
global population
```

```
lchrom=sum([para_length]);  
for i=1:popsi  
    for j=1:lchrom  
        population(i).chrom(j)=flip(0.5);  
    end  
end
```

### decode.m

```
%%Decoding procedure
```

```
function decode(popsi,Npara,para_length)
```

```
global population
```

```
for i=1:popsi  
    num=1;  
    final=0;  
    for j=1:Npara  
        ans=0;  
        initial=num;  
        final=final+para_length(j);  
        for k=initial:final  
            temp=population(i).chrom(k)*2^(final-k);  
            ans=ans+temp;  
            num=num+1;  
        end  
        if j==1  
            population(i).x(j)=(0.6*ans+14)/100;  
        elseif j==2  
            population(i).x(j)=(6*ans+160)/100;  
        elseif j==3  
            population(i).x(j)=(5*ans+130)/100;  
        elseif j==4  
            population(i).x(j)=(4*ans+80)/100;  
        elseif j==5  
            population(i).x(j)=(8*ans+200)/100;  
        else  
            population(i).x(j)=(4*ans+90)/100;  
        end  
    end  
end
```

### objfunction.m

```
%%Evaluation of the objective function and Rank
```

```
function objfunction(popsi,Npara,Coef_penalty)
```

```
global population ID
```

```
ar=0.10; % allowable range of modification within the standard value of parameters, should be less than 15%  
  
s(1)=0.18; % Standard values of given parameter set  
s(2)=2.02;  
s(3)=1.69;  
s(4)=1.1;  
s(5)=2.60;  
s(6)=1.2;
```

```

for i=1:popsiz
    temp=0;
    for j=1:Npara
        if population(i).x(j)<(s(j)-ar*s(j)) | population(i).x(j)>(s(j)+ar*s(j))
            temp=temp+abs((population(i).x(j)-s(j))/s(j));
        end
    end
    population(i).feas=Coef_penalty*temp*10;
end
j=0;
k=0;
for i=1:popsiz
    if population(i).feas==0
        ID=i;
        j=j+1;
        [mag,w,phase_shift,eigenvals,he]=bode_plot;
        individual(j).hee=he;
        individual(j).eigen=eigenvals;
        %%%find the coordinate of second peak%%
        for q=1:99
            diff=mag(100-q)-mag(100-q+1);
            if diff<0
                peak_id=100-q+1;
                break
            end
        end
        sepeak(j).sx=w(peak_id);
        sepeak(j).sy=mag(peak_id);
        population(i).fitness=0;
        population(i).penalty=0;
        success(j)=i;
    else
        population(i).fitness=population(i).feas;
        population(i).penalty=population(i).feas;
        k=k+1;
        fail(k)=i;
    end
end

if j~=0
    minpeak=min([sepeak.sy]);
    minfreq=min([sepeak.sx]);
    for i=1:j
        %%%Peak value comparison--%%
        if (sepeak(i).sy-minpeak)>=50
            peakfitness=50;
        else
            peakfitness=(sepeak(i).sy-minpeak);
        end
        population(success(i)).fitness=population(success(i)).fitness+peakfitness;
        %%%Frequency value comparison%%
        if (sepeak(i).sx-minfreq)>=50
            freqfitness=50;
        else
            freqfitness=(sepeak(i).sx-minfreq);
        end
        population(success(i)).fitness=population(success(i)).fitness+freqfitness;
        %%%Stability Test with eigenvalues%%
        [ro,co]=size(individual(i).eigen);
        penal=0;
        for p=1:co
            R=real(individual(i).eigen(p));
            if R>0
                penal=penal+Coef_penalty*1;
            end
        end
    end
end

```

```

        end
        %%%Heo>0.001 m condition%%
        if individual(i).hee < 0.001
            penal=penal+Coef_penalty*3;
        end
        population(success(i)).penalty=population(success(i)).penalty+penal;
        population(success(i)).fitness=population(success(i)).fitness+population(success(i)).penalty;
    end
end

%% highest rank number is minimum fitness value%%
if j~=0
    p=0;
    for i=1:j
        p=p+1;
        temp_s(p)=population(success(i)).fitness;
    end
    temp1=sort([temp_s]);
    for i=1:j
        for p=1:j
            if population(success(p)).fitness==temp1(i)
                population(success(p)).rank=popsi- i+ 1;
            end
        end
    end
    for i=1:j
        if sepeak(i).sx<=50
            population(success(i)).sx=sepeak(i).sx;
        else
            population(success(i)).sx=50;
        end
        if sepeak(i).sy<=50
            population(success(i)).sy=sepeak(i).sy;
        else
            population(success(i)).sy=50;
        end
    end
end
end

if k~=0
    p=0;
    for i=1:k
        p=p+1;
        temp_f(p)=population(fail(i)).fitness;
    end
    temp2=sort([temp_f]);
    for i=1:k
        for p=1:k
            if population(fail(p)).fitness==temp2(i)
                population(fail(p)).rank=popsi- i- j+ 1;
            end
        end
    end
    for i=1:k
        population(fail(i)).sx=50;
        population(fail(i)).sy=50;
    end
end
end

```

### **srselect.m**

%%Stochastic Remainder selection

function choices = srselect(popsi)

```

global population

i=0; j=0;
while(i<popsiz)
    i=i+1;
    expected=population(i).rank/mean([population.rank]);
    jassign=fix(expected);
    fraction(i)=expected-jassign;
    while(jassign>0)
        j=j+1;
        jassign=jassign-1;
        choices(j)=i;
    end
end
i=0;
while(j<popsiz)
    i=i+1;
    if i>popsiz
        i=1;
    end
    if fraction(i)>0.0
        winner=flip(fraction(i));
        if winner==1
            j=j+1;
            choices(j)=i;
            fraction(i)=fraction(i)-1.0;
        end
    end
end
end

```

### point\_cross.m

```

%%Point crossover

function [child1,child2]=point_cross(parent1,parent2,para_length,Pc)

lchrom=sum([para_length]);
if flip(Pc)==1
    jcross=md(1,lchrom);
else
    jcross=lchrom;
end
for j=1:jcross
    child1(j)=parent1(j);
    child2(j)=parent2(j);
end
if jcross~=lchrom
    for j=jcross+1:lchrom
        child1(j)=parent2(j);
        child2(j)=parent1(j);
    end
end
end

```

### two\_point\_cross.m

```

%%Two Point Crossover

function [child1,child2]=two_point_cross(parent1,parent2,para_length,Pc)

lchrom=sum([para_length]);
if flip(Pc)==1

```

```

a=md(1:lchrom);
b=md(1:lchrom);
while(a==b)
    b=md(1:lchrom);
end
if a<b
    jcross1=a;
    jcross2=b;
else
    jcross1=b;
    jcross2=a;
end
for j=1:jcross1
    child1(j)=parent1(j);
    child2(j)=parent2(j);
end
for j=jcross1+1:jcross2
    child1(j)=parent2(j);
    child2(j)=parent1(j);
end
if jcross2~=lchrom
    for j=jcross2+1:lchrom
        child1(j)=parent1(j);
        child2(j)=parent2(j);
    end
end
else
    child1=parent1;
    child2=parent2;
end
end

```

### **random corss.m**

%%Random Crossover

```
function [child1,child2] = random_cross(parent1,parent2,para_length,Pc)
```

```

lchrom=sum([para_length]);
if flip(Pc)==1
    for i=1:lchrom
        j=rand(1,2);
        if j==1
            child1(i)=parent1(i);
        else
            child1(i)=parent2(i);
        end
        j=rand(1,2);
        if j==1
            child2(i)=parent1(i);
        else
            child2(i)=parent2(i);
        end
    end
else
    for i=1:lchrom
        child1(i)=parent1(i);
        child2(i)=parent2(i);
    end
end
end

```

### **single mut.m**

%%Single bit mutation

```
function newchrom = single_mut(chrom,para_length,Pm);
```

```
lchrom=sum([para_length]);  
for i=1:lchrom  
    if flip(Pm)==1  
        if chrom(i)==1  
            newchrom(i)=0;  
        else  
            newchrom(i)=1;  
        end  
    else  
        newchrom(i)=chrom(i);  
    end  
end
```

### two\_mut.m

```
%%Two bit swapping mutation
```

```
function newchrom = two_mut(chrom,para_length,Pm)  
lchrom=sum([para_length]);  
newchrom=chrom;  
if flip(Pm)==1  
    p1=md(1,lchrom);  
    p2=md(1,lchrom);  
    newchrom(p1)=chrom(p2);  
    newchrom(p2)=chrom(p1);  
end
```

### elitist.m

```
%%Elitist Replacement
```

```
function elitist(popsizе,Npara_n_elit)
```

```
global oldpopulation population
```

```
temp1=sort([oldpopulation.rank]);  
for i=1:n_elit  
    for j=1:popsizе  
        if oldpopulation(j).rank==temp1(popsizе-i+1)  
            true=1;  
            if i==1  
                for k=1:i-1  
                    if elit(k)==j  
                        true=0;  
                    end  
                end  
            end  
            elit(i)=j;  
            if true==1  
                break  
            end  
        end  
    end  
end
```

```
temp2=sort([population.rank]);  
for i=1:n_elit  
    for j=1:popsizе  
        if population(j).rank==temp2(i)  
            true=1;  
            if i==1
```

```

        for k=1:i-1
            if bad(k)==j
                true=0;
            end
        end
        end
        bad(i)=j;
        if true==1
            break
        end
    end
end
end

for i=1:n_elit
    population(bad(i)).chrom=oldpopulation(elit(i)).chrom;
    population(bad(i)).x=oldpopulation(elit(i)).x;
    population(bad(i)).fitness=oldpopulation(elit(i)).fitness;
    population(bad(i)).penalty=oldpopulation(elit(i)).penalty;
    population(bad(i)).rank=oldpopulation(elit(i)).rank;
    population(bad(i)).sx=oldpopulation(elit(i)).sx;
    population(bad(i)).sy=oldpopulation(elit(i)).sy;
    population(bad(i)).feas=oldpopulation(elit(i)).feas;
end

%%%Rank Re-distributor%%%
j=0;
k=0;
for i=1:popsiz
    if population(i).feas==0
        j=j+1;
        success(j)=i;
        population(i).fitness=0;
    else
        k=k+1;
        fail(k)=i;
    end
end

if j~=0
    for i=1:j
        sepeak(i).sx=population(success(i)).sx;
        sepeak(i).sy=population(success(i)).sy;
    end
    minpeak=min([sepeak.sy]);
    minfreq=min([sepeak.sx]);
    for i=1:j
        %%%Peak value comparison---%%%
        if (sepeak(i).sy-minpeak)>=50
            peakfitness=50;
        else
            peakfitness=(sepeak(i).sy-minpeak);
        end
        population(success(i)).fitness=population(success(i)).fitness+peakfitness;
        %%%Frequency value comparison%%%
        if (sepeak(i).sx-minfreq)>=50
            freqfitness=50;
        else
            freqfitness=(sepeak(i).sx-minfreq);
        end
        population(success(i)).fitness=population(success(i)).fitness+freqfitness;

        population(success(i)).fitness=population(success(i)).fitness+population(success(i)).penalty;
    end
end
end

```

```

if j~=0
    for i=1:j
        temps(i)=population(success(i)).fitness;
    end
    tempsl=sort([temps]);
    for i=1:j
        for p=1:j
            if population(success(p)).fitness==tempsl(i)
                population(success(p)).rank=popsi-1;
            end
        end
    end
end
end
end

```

```

if k~=0
    for i=1:k
        tempfl(i)=population(fail(i)).fitness;
    end
    tempfl=sort([tempfl]);
    for i=1:k
        for p=1:k
            if population(fail(p)).fitness==tempfl(i)
                population(fail(p)).rank=popsi-1;
            end
        end
    end
end
end
end

```

### output\_data.m

```
%%Output of the result
```

```
function output_data(popsi)
```

```
global population
```

```

best=max([population.rank]);
for i=1:popsi
    if best==population(i).rank
        best_one=i;
        break
    end
end
disp("");
disp('The best chromosome is');
disp([population(best_one).chrom]);
disp("");
disp("");
disp('Its L1 value is');
disp(population(best_one).x(1));
disp('Its L2 value is');
disp(population(best_one).x(2));
disp('Its L3 value is');
disp(population(best_one).x(3));
disp('Its L4 value is');
disp(population(best_one).x(4));
disp('Its Lob value is');
disp(population(best_one).x(5));
disp('Its Pb/Pc value is');
disp(population(best_one).x(6));
disp("");
disp("");
disp('Its Second peak height is');
disp(population(best_one).sy);

```

```

disp('Its Second frequency (rad/s) is');
disp(population(best_one).sx);
disp('Its penalty is');
disp(population(best_one).penalty);
disp('');

```

### drawing.m

%This file draws the pictures of ACV skirt with original and optimized dimensions

```
global ID
```

```
%Original Dimension
```

```
ID=1;
[Bb,Db,Hb,LD,Lm,Mc,L1,L2,L3,L4,Lob,omega,Ms,LM,Lb,alphao,gammao,Gamma,sigmao,phi,mu,omegaMo,Af0,Aeff,ls,g,rho,C
b,Cc ...
.heo,Bf,Pbo,Pco,Qbo,Qco,hfo,Xso] = input_data;
```

```
height=1/6*Bb;
```

```

P1=[0.0]
P2=[P1(1)-Bb/2,P1(2)+0]
P3=[P2(1)-L1*cos(alphao),P2(2)-L1*sin(alphao)]
P4=[P3(1)-L3*cos(mu),P3(2)-L3*sin(mu)]
P5=[P4(1)-L4*cos(phi+omega-mu),P4(2)+L4*sin(phi+omega-mu)]
P6=[P2(1)-Db,P2(2)+Hb]
P7=[P6(1),P6(2)+1/6*Bb]
P8=[P1(1)+Bb/2,P1(2)+0]
P9=[P8(1)+L1*cos(alphao),P8(2)-L1*sin(alphao)]
P10=[P9(1)+L3*cos(mu),P9(2)-L3*sin(mu)]
P11=[P10(1)+L4*cos(phi+omega-mu),P10(2)+L4*sin(phi+omega-mu)]
P12=[P8(1)+Db,P8(2)+Hb]
P13=[P12(1),P12(2)+1/6*Bb]

```

```
hold on
```

```

h(1)=plot([P1(1),P2(1)],[P1(2),P2(2)]);
h(2)=plot([P2(1),P3(1)],[P2(2),P3(2)]);
h(3)=plot([P3(1),P4(1)],[P3(2),P4(2)]);
h(4)=plot([P4(1),P5(1)],[P4(2),P5(2)]);
h(5)=plot([P2(1),P6(1)],[P2(2),P6(2)]);
h(6)=plot([P6(1),P7(1)],[P6(2),P7(2)]);
h(7)=plot([P1(1),P8(1)],[P1(2),P8(2)]);
h(8)=plot([P8(1),P9(1)],[P8(2),P9(2)]);
h(9)=plot([P9(1),P10(1)],[P9(2),P10(2)]);
h(10)=plot([P10(1),P11(1)],[P10(2),P11(2)]);
h(11)=plot([P8(1),P12(1)],[P8(2),P12(2)]);
h(12)=plot([P12(1),P13(1)],[P12(2),P13(2)]);
h(13)=plot([P7(1),P13(1)],[P7(2),P13(2)]);
h(14)=plot([P3(1),P5(1)],[P3(2),P5(2)]);
h(15)=plot([P9(1),P11(1)],[P9(2),P11(2)]);

```

```
%Optimized Dimension
```

```
ID=2;
[Bb,Db,Hb,LD,Lm,Mc,L1,L2,L3,L4,Lob,omega,Ms,LM,Lb,alphao,gammao,Gamma,sigmao,phi,mu,omegaMo,Af0,Aeff,ls,g,rho,C
b,Cc ...
.heo,Bf,Pbo,Pco,Qbo,Qco,hfo,Xso] = input_data;
```

```

P1=[0.0]
P2=[P1(1)-Bb/2,P1(2)+0]
P3=[P2(1)-L1*cos(alphao),P2(2)-L1*sin(alphao)]
P4=[P3(1)-L3*cos(mu),P3(2)-L3*sin(mu)]
P5=[P4(1)-L4*cos(phi+omega-mu),P4(2)+L4*sin(phi+omega-mu)]
P6=[P2(1)-Db,P2(2)+Hb]

```

```

P7=[P6(1),P6(2)+height]
P8=[P1(1)+Bb/2,P1(2)+0]
P9=[P8(1)+L1*cos(alphao),P8(2)-L1*sin(alphao)]
P10=[P9(1)+L3*cos(muoa),P9(2)-L3*sin(muoa)]
P11=[P10(1)+L4*cos(phi+omega-muoa),P10(2)+L4*sin(phi+omega-muoa)]
P12=[P8(1)+Db,P8(2)+Hb]
P13=[P12(1),P12(2)+height]

```

```

plot([P1(1),P2(1)],[P1(2),P2(2)],'r:');
plot([P2(1),P3(1)],[P2(2),P3(2)],'r:');
plot([P3(1),P4(1)],[P3(2),P4(2)],'r:');
plot([P4(1),P5(1)],[P4(2),P5(2)],'r:');
plot([P2(1),P6(1)],[P2(2),P6(2)],'r:');
plot([P6(1),P7(1)],[P6(2),P7(2)],'r:');
plot([P1(1),P8(1)],[P1(2),P8(2)],'r:');
plot([P8(1),P9(1)],[P8(2),P9(2)],'r:');
plot([P9(1),P10(1)],[P9(2),P10(2)],'r:');
plot([P10(1),P11(1)],[P10(2),P11(2)],'r:');
plot([P8(1),P12(1)],[P8(2),P12(2)],'r:');
plot([P12(1),P13(1)],[P12(2),P13(2)],'r:');
plot([P7(1),P13(1)],[P7(2),P13(2)],'r:');
plot([P3(1),P5(1)],[P3(2),P5(2)],'r:');
plot([P9(1),P11(1)],[P9(2),P11(2)],'r:');

```

```
hold off
```

```
set(h,'LineWidth',2)
axis equal
```

```
title('WABANAKI')
```

## APPENDIX D. Codes for Expert System

### ES.m

%%Expert System for Initial Design of Air Cushion Vehicle%%

[Mc,Vm,Purpose] = input\_file;

[SC] = speed\_category(Vm);

[Lc,Bc,Pc,h\_L,Pt,TE,w1,w2,w3,w4,w5,w6,w7,wL] = inference\_engine1(Mc,Vm);

[eta\_t,Ns,Ds,psi,phi,fc,eta\_ap,St] = inference\_engine2;

output\_file(Mc,Vm,Purpose,SC,Lc,Bc,Pc,h\_L,Pt,TE,w1,w2,w3,w4,w5,w6,w7,wL,eta\_t,Ns,Ds,psi,phi,fc,eta\_ap,St);

### inference\_engine1.m

%%Inference Engine1 ----uses forward chaining%%

function [Lc,Bc,Pc,h\_L,Pt,TE,w1,w2,w3,w4,w5,w6,w7,wL] = inference\_engine1(Mc,Vm)

%%PART I%%

%Vehicle Overall Dimensions [m]%

[Lc,Bc] = OD(Mc);

%Parametric Study%

[Pc,h\_L,Pt,TE] = PS(Mc,Vm,Lc,Bc);

%Weight Distribution%

[w1,w2,w3,w4,w5,w6,w7,wL] = WD(Mc,Lc,Bc,Pc,Pt,TE,Vm);

### inference\_engine2.m

%%Inference Engine2 ----uses forward chaining%%

function [eta\_t,Ns,Ds,psi,phi,fc,eta\_ap,St] = inference\_engine2

%%PART II%%

%Lift System Design%

[eta\_t,Ns,Ds,psi,phi,fc] = LS;

%Propulsion System Design%

[eta\_ap] = ProS;

%Skirt and Cushion System Design%

[St] = SCS;

### input\_file.m

function [Mc,Vm,Purpose] = input\_file

Mc = 36740; % Total craft mass (kg)

Vm = 25.8; % Maximum speed (m/s)

Purpose = 4; % Purpose of ACV: 1 --Commercial, 2 --Military, 3 --Sport, 4 --Utility

## output file.m

%%Output file%%

function output\_file(Mc,Vm,Purpose,SC,Lc,Bc,Pc,h\_L,Pt,TE,w1,w2,w3,w4,w5,w6,w7,wL,eta\_t,Ns,Ds,psi,phi,fc,cta\_ap,St)

```
%Craft mass and maximum velocity%
disp('-----');
disp('<< General Information of ACV >>');
disp(' ');
disp('Craft mass(Kg):');
disp(Mc);
disp('Maximum speed(m/s):');
disp(Vm);
%Purpose of ACV and Speed Category%
disp('Speed category:');
matrix2 = [ ' Low Speed '
            ' Medium Speed '
            ' High Speed ' ];
disp([matrix2(SC,:)]);
disp(' ');
disp('Purpose of ACV:');
matrix1 = [ ' Commercial '
            ' Military '
            ' Sport '
            ' Utility ' ];
disp([matrix1(Purpose,:)]);
disp(' ');
%Overall dimensions of vehicle%
disp('Craft Length(m):');
disp(Lc);
disp('Craft Width(m):');
disp(Bc);
%Cushion Pressure, Nominal airgap, and Total Power%
disp('Cushion Pressure(Pa):');
disp(Pc);
disp('Nominal Airgap:');
disp(h_L);
disp('Total Power(kW):');
disp(Pt);
%Transport Efficiency%
disp('Transport Efficiency:');
disp(TE);
%Weight Distribution%
disp('-----');
disp('<< Weight Distribution >>');
disp(' ');
disp('Structural Weight(Kg):');
disp(w1);
disp('Propulsion System Weight(Kg):');
disp(w2);
disp('Electrical System Weight(Kg):');
disp(w3);
disp('Command and Surveillance Weight(Kg):');
disp(w4);
disp('Auxiliary Weight(Kg):');
disp(w5);
disp('Outfit and Furnishings Weight(Kg):');
disp(w6);
disp('Armament/Equipments(Kg):');
disp(w7);
disp('Load Weight(Kg):');
disp(wL);
%Lift System%
disp('-----');
disp('<< Lift System >>');
```

```

disp(' ');
disp('Fan Efficiency:');
disp(eta_t);
disp('Specific Speed:');
disp(Ns);
disp('Specific Diameter:');
disp(Ds);
disp('Pressure Coefficient:');
disp(psi);
disp('Flow Coefficient:');
disp(phi);
disp('Fan Type:');
matrix3 = [ 'Centrifugal fan '
           'Mixed_Flow fan '
           'Axial_Flow fan ' ];
disp([matrix3(fc,:)]);
disp(' ');
%Propulsion System%
disp('-----');
disp('<< Propulsion System >>');
disp(' ');
disp('Air Propeller System');
disp('Max. Efficiency of Air Propeller:');
disp(eta_ap);
disp('Gas Turbine System');
disp(' ');
disp('In order to proceed further the propulsion system design. ');
disp('more database is required including');
disp('the propeller profile or properties of gas turbine');
disp(' ');
%Skirt and Cushion System%
disp('-----');
disp('<< Skirt and Cushion System >>');
disp(' ');
disp('Skirt Type:');
matrix4 = [ 'Bag and Finger '
           'Loop Segment '
           'Jupe '
           'Pericell ' ];
disp([matrix4(St,:)]);
disp(' ');
disp('Bag and Finger Skirt is the most updated and');
disp('advanced system developed in ACV Industries');
disp(' ');
disp('-----');

```

### **speed\_category.m**

%%ACV is categorized into low, medium, and high speed vehicle%%

```
function [SC] = speed_category(Vm)
```

% SC is speed category: 1 --low speed, 2 --Medium speed, 3 --high speed

% All unit is m/s

```
if Vm <= 13.4
```

```
    SC = 1;
```

```
elseif Vm <= 44.7
```

```
    SC = 2;
```

```
else
```

```
    SC = 3;
```

```
end
```

### **OD.m**

%%Craft Overall dimensions%%

function [Lc,Bc] = OD(Mc)

%Units are in m%

Lc = 0.6503\*(Mc)^0.3334;

Bc = 0.3721\*(Mc)^0.3148;

### WD.m

%%Weight Distributiono%%

function [w1,w2,w3,w4,w5,w6,w7,wL] = WD(Mc,Lc,Bc,Pc,Pt,TE,Vm)

%Structural Weight%

temp=0.0064\*Pc/(Lc\*Bc)^0.5;

if temp <=0.75

w1=(0.28/(Mc/1000)^(1/3)+0.04\*((Mc/1000)^(1/3))/(temp)^(1/3))\*Mc;

elseif temp<=1.5

w1=(0.24+0.007\*((Mc/1000)^(1/3))/(temp)^(1/3))\*Mc;

else

w1=(0.21+0.008\*((Mc/1000)^(1/3))/(temp)^(1/3))\*Mc;

end

%Propulsion System Weight%

temp=1.25+74/(Pt/0.7457)^(0.5);

w2=(temp\*(3.28\*Vm)\*(1/(550\*TE)))\*Mc;

%Electrical System Weight%

w3=(0.00034\*(Mc/1000)^0.5+0.1/(Mc/1000)^0.5)\*Mc;

%Command and Surveillance Weight%

w4=(0.14/(Mc/1000)^(1/3)-w3/Mc)\*Mc;

%Auxiliary System Weight

w5=(0.0024\*(Mc/1000)^(1/3)+0.06/(Mc/1000)^(1/3)+0.044+0.08/(Mc/1000)^(1/3))\*Mc;

%Outfit and Furnishings Weight

w6=(0.003\*(Mc/1000)^(1/3)+0.07/(Mc/1000)^(1/3))\*Mc;

%Armament

w7=(0.5/(Mc/1000)^(1/3))\*Mc;

%Load Weight

wL=Mc-(w1+w2+w3+w4+w5+w6+w7);

### PS.m

%%Parametric Study%%

function [Pc,h\_L,Pt,TE] = PS(Mc,Vm,Lc,Bc)

%Cushion Pressure [Pa]%

Pc = (Mc\*9.81)/(Lc\*Bc);

%Nominal air gap%

h\_L = 0.014/(1.1\*Mc/1000)^(1/3);

%Total Power [kW]%

Pt = 0.269\*(Mc)^0.867;

```
%Transport Efficiency%
TE = (1800*Mc/1000)*(3.28*Vm)/(550*P/0.7457);
```

### LS.m

```
%%Lift System Design%%
```

```
function [eta_t,Ns,Ds,psi,phi,fc] = LS
```

```
%Desired Fan Efficiency%
eta_t = 0.8;
```

```
%Specific Speed%
Ns = 1/0.02*(0.85-eta_t);
```

```
%Specific Diameter%
Ds = 0.9+2/Ns;
```

```
%Pressure Coefficient%
psi = (1/(Ds*Ns))^2;
```

```
%Flow Coefficient%
phi = psi^(3/2)*Ns^2;
```

```
%Choice for fans%
%1 --Centrifugal fan, 2 --Mixed flow fan, 3 --Axial flow fan%
if Ns <= 2.5
    fc = 1;
elseif Ns <= 3.5
    fc = 2;
else
    fc = 3;
end
```

### ProS.m

```
%%Propulsion System Design%%
```

```
function [eta_ap] = ProS
```

```
%Air Propeller System%
eta_ap = 0.65;
```

```
%Gas Turbine System%
```

```
%In order to proceed the propulsion system design, more database is required including
%the propeller profile or properties of gas turbine
```

### SCS.m

```
%%Skirt and Cushion System Design%%
```

```
function [St] = SCS
```

```
%Skirt Type%
%1 --Bag and Finger, 2 --Loop segment, 3 --Jupe, 4 --Pericell
St = 1;
```

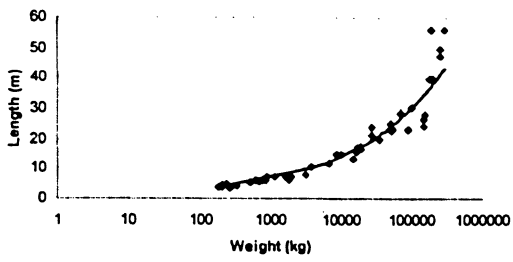
## ACV Database

Name	Builder	Purpose	Power Plant	Length(m)	Beam(m)	Mc(kg)	Vcru(m/s)	Vmax(m/s)	Payl.(kg)	#pass.
Saint-Michel	Ackerman I.	Public Ser.	37kW	5.9	2.3	600	13.9	n/a	600	5
Baroudeur	Ackerman I.	Public Ser.	37kW	3.7	2.2	200	11.1	n/a	n/a	3
Adoc 4	Ackerman I.	Public Ser.	37kW	4.6	2.3	200	13.9	n/a	n/a	4
Adoc 3S	Ackerman I.	Sport/Util.	37kW	3.6	1.8	200	11.1	n/a	n/a	2
Garonne	Ackerman I.	Public Ser.	63kW	7.0	3.0	1100	16.7	n/a	500	5
Canair 300	ACV D.	Sport/Util.	1 Piston engine	3.8	2.2	182	9.7	12.5	182	2
Canair 500	ACV D.	Sport/Util.	1 Piston engine	5.0	2.2	237	11.1	13.3	295	4
AH560P	Airlift H.	Comm.	2 Piston engines, 77kW	6.1	4.0	830	15.3	16.4	550	7
AH560U	Airlift H.	Sport/Util.	2 Piston engines, 77kW	6.1	4.0	759	15.3	16.4	650	2
AH1160	Airlift H.	Comm.	2 Diesel engines, 330kW	12.2	6.0	n/a	19.6	28.4	3000	29
BBV 6	BBV H.	Sport/Util.	99kW	5.3	2.5	495	12.9	n/a	600	4
GH-2006	British H.C.	Comm.	4 Gas turbine, 11334kW	56.4	27.9	195000	25.8	30.9	3000	321
CCGH 045	British H.C.	Public Ser.	1 Gas turbine, 896kW	14.7	7.7	8500	20.6	30.9	n/a	3
CCGH Siyay	GKN W.A.	Public Ser.	4 Diesel engines, 2818kW	28.5	12.0	70000	23.2	30.9	25000	4
375TD	Griffon H.	Sport/Util.	1 Diesel engine, 83kW	6.6	3.4	n/a	n/a	12.9	300	5
450TD	Griffon H.	Military	2 Diesel engines, 112kW	7.6	3.4	n/a	n/a	15.5	380	6
1000TD	Griffon H.	Comm.	1 Diesel engine, 141kW	9.0	4.7	n/a	n/a	13.9	1000	12
2000TD	Griffon H.	Comm.	1 Diesel engine, 265kW	12.7	6.1	n/a	n/a	18.0	2200	26
3000TD	Griffon H.	Comm.	2 Diesel engines, 772kW	18.4	10.1	n/a	n/a	19.1	4000	44
4000TD	Griffon H.	Comm.	2 Diesel engines, 772kW	21.2	10.1	n/a	n/a	18.0	5900	68
8000TD	Griffon H.	Comm.	2 Diesel engines, 1192kW	21.2	11.0	n/a	n/a	20.6	9300	82
Mariah 425	Mariah H.	Sport/Util.	Yamaha Vmax 600cc	4.2	2.0	320	n/a	22.2	480	6
Hovertrek	Neoteric	Sport/Util.	Fuji EC50PM-02, 39kW	4.2	2.5	200	15.6	20.0	272	4
Gepard	Neptun H.	Sport/Util.	1 ZMZ-505, 180kW	6.9	3.2	n/a	n/a	20.8	380	5
Puma	Neptun H.	Comm.	2 ZMZ-53-11, 240kW	12.2	5.2	n/a	n/a	18.1	1350	18
Irbis	Neptun H.	Comm.	2 Diesel engines, 382kW	17.5	6.2	n/a	n/a	18.1	3000	34
Bizon	Neptun H.	Military	3 1D12BMS1, 895kW	18.7	9.1	n/a	n/a	2.8	10000	2
Sobol	Neptun H.	Sport/Util.	1 Rotax-582, 48kW	4.0	2.0	n/a	n/a	18.1	200	2
Alligator	Neptun H.	Comm.	2 VAZ-2112, 119kW	8.5	3.2	n/a	n/a	n/a	n/a	9
Klamath	Oregon H.	Public Ser.	Diesel engine, 75kW	6.1	2.4	n/a	20.6	25.8	n/a	7
Columbia	Oregon H.	Sport/Util.	2 Diesel engines, 225kW	13.4	4.6	n/a	24.2	28.3	n/a	14
Deschutes	Oregon H.	Sport/Util.	Diesel engine, 188kW	11.6	4.3	n/a	22.2	25.8	n/a	14
SF3000	Scat H.	Comm.	2 Diesel engines, 384kW	15.0	4.8	n/a	13.9	n/a	n/a	34
SF2000	Scat H.	Comm.	2 Diesel engines, 262kW	11.6	4.3	n/a	16.7	n/a	n/a	21
SF6000	Scat H.	Comm.	2 Diesel engines, 384kW	18.0	8.0	n/a	18.0	n/a	n/a	63
Sovereign500	Scat H.	Comm.	2 Diesel engines	5.6	2.4	670	12.9	15.5	500	6
Airlift1950A	Scat H.	Public Ser.	2 Diesel engines, 268kW	9.5	4.2	n/a	14.4	18.0	1700	12
Fire T. 1060	Scat H.	Public Ser.	2 Diesel engines, 306kW	10.6	4.6	n/a	14.4	n/a	2000	6
CS700	Scat H.	Public Ser.	2 Gasoline engines, 164kW	8.5	4.2	n/a	n/a	15.5	1000	15
Shuttle	Scat H.	Comm.	2 Diesel engines	7.1	4.0	850	12.9	15.5	600	7
SAH2200	Slingsby	Comm.	Diesel engine, 238kW	10.6	4.2	n/a	16.5	20.6	2200	23
LCAC	Textron	Military	4 Gas turbines, 11930kW	26.8	14.3	149500	20.6	20.6	60000	29
SEAL	West Cost H.	Sport/Util.	Briggs&Stratton, 15kW	4.4	2.2	n/a	14.2	17.8	317	2
SHARK	West Cost H.	Sport/Util.	Automotive, 63kW	5.5	2.4	n/a	15.5	22.2	453	6
SEALION	West Cost H.	Comm.	Automotive, 112kW	6.7	3.0	n/a	20.0	24.4	815	9
SEAWOLF	West Cost H.	Comm.	Automotive, 149kW	8.5	4.3	n/a	20.0	24.4	1178	13
TOURISTER	West Cost H.	Comm.	Diesel engine, 447kW	10.7	4.9	n/a	24.4	27.5	1993	22
Odyssey	Pacific H.	Comm.	Diesel engine, 221kW	10.5	4.5	3750	19.6	n/a	2400	25
Explorer	Pacific H.	Comm.	Toyota 4L V8, 194kW	7.3	3.5	1600	18.5	n/a	1200	12
Slider	Pacific H.	Sport/Util.	Twin cylinder, 34kW	3.5	1.9	265	19.4	n/a	200	2
Viking 7501	Canada		1268kW	13.2	6.7	14700	25.8			
Viking 7505	Canada		1268kW	16.5	6.7	19000	25.8			
Voyageur	Canada		1939kW	20.0	10.0	35000	24.2			
N300	France		2237kW	24.0	10.5	27000	32.0			

N500	France	12677kW	50.0	23.0	265000	36.1
MV.PP5	Japan	783kW	15.4	7.6	16300	28.4
MV.PP5MkII	Japan	783kW	17.6	7.6	19300	26.8
MV.PP15	Japan	3281kW	25.1	11.1	50000	33.5
Aist	Russia	19388kW	47.8	17.5	260000	36.1
Gus	Russia	1745kW	21.3	7.3	27000	25.8
Lebed	Russia	5369kW	23.3	10.2	90000	28.4
BH.7	UK	2834kW	23.1	11.3	50000	30.9
BH.7 Mk5A	UK	2834kW	23.1	11.2	55000	29.9
SH2	UK	149kW	5.9	4.4	1800	23.2
SH2-4	UK	149kW	8.0	4.4	3100	21.6
Skima 12(12)	UK	186kW	7.2	2.8	1900	13.9
SR.N5	UK	671kW	11.8	6.6	6700	30.9
SR.N6	UK	671kW	14.8	6.6	10000	26.8
SR.N4 Mk1	UK	12677kW	39.7	23.2	180000	36.1
SR.N4 Mk2	UK	12677kW	39.7	23.2	200000	36.1
SR.N4 Mk3	UK	13423kW	56.4	23.2	300000	33.5
SR.N6 Mk6	UK	839kW	17.1	6.6	17000	25.8
VT-2	UK	5667kW	30.2	13.3	100000	32.5
Bell AL30	USA	2685kW	23.0	10.0	52000	25.8
JEFF(A)	USA	16778kW	28.0	13.4	157000	30.9
JEFF(B)	USA	16778kW	24.2	13.1	150000	32.0

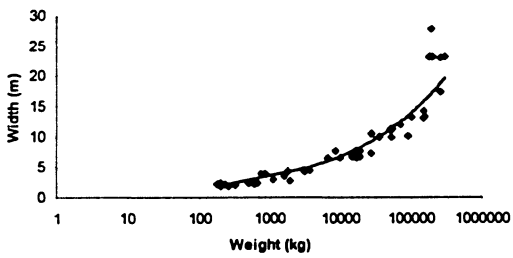
M	L	M	W	M	Pt
600	5.9	600	2.3	600	37
200	3.7	200	2.2	200	37
200	4.6	200	2.3	200	37
200	3.6	200	1.8	200	37
1100	7.0	1100	3.0	1100	63
182	3.8	182	2.2	830	77
237	5.0	237	2.2	759	77
830	6.1	830	4.0	495	99
759	6.1	759	4.0	195000	11334
495	5.3	495	2.5	8500	896
195000	56.4	195000	27.9	70000	2818
8500	14.7	8500	7.7	200	39
70000	28.5	70000	12.0	149500	11930
320	4.2	320	2.0	3750	221
200	4.2	200	2.5	1600	194
670	5.6	670	2.4	265	34
850	7.1	850	4.0	14700	1268
149500	26.8	149500	14.3	19000	1268
3750	10.5	3750	4.5	35000	1939
1600	7.3	1600	3.5	27000	2237
265	3.5	265	1.9	265000	12677
14700	13.2	14700	6.7	16300	783
19000	16.5	19000	6.7	19300	783
35000	20.0	35000	10.0	50000	3281
27000	24.0	27000	10.5	260000	19388
265000	50.0	265000	23.0	27000	1745
16300	15.4	16300	7.6	90000	5369
19300	17.6	19300	7.6	50000	2834
50000	25.1	50000	11.1	55000	2834
260000	47.8	260000	17.5	1800	149
27000	21.3	27000	7.3	3100	149
90000	23.3	90000	10.2	1900	186
50000	23.1	50000	11.3	6700	671
55000	23.1	55000	11.2	10000	671
1800	5.9	1800	4.4	180000	12677
3100	8.0	3100	4.4	200000	12677
1900	7.2	1900	2.8	300000	13423
6700	11.8	6700	6.6	17000	839
10000	14.8	10000	6.6	100000	5667
180000	39.7	180000	23.2	52000	2685
200000	39.7	200000	23.2	157000	16778
300000	56.4	300000	23.2	150000	16778
17000	17.1	17000	6.6	36740	1760
100000	30.2	100000	13.3		
52000	23.0	52000	10.0		
157000	28.0	157000	13.4		
150000	24.2	150000	13.1		

**Weight VS. Length**



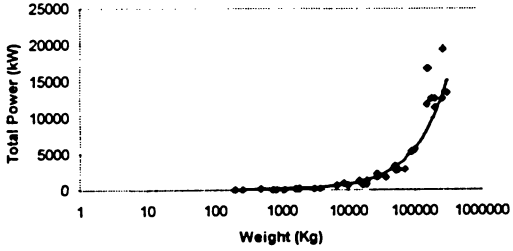
$$y = 0.6503x^{0.3334}$$

**Weight VS. Width**



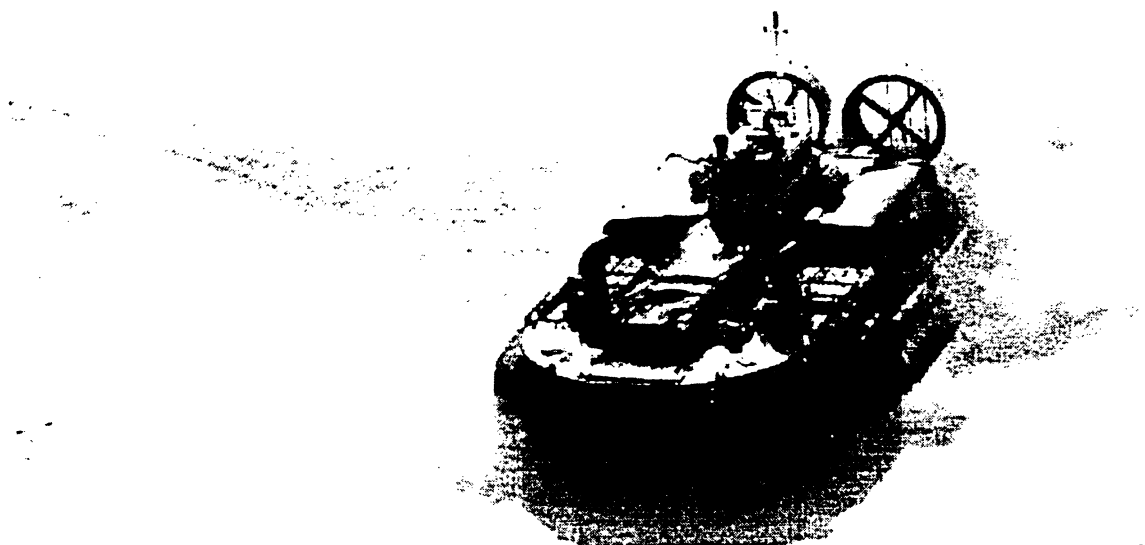
$$y = 0.3721x^{0.3148}$$

**Weight VS. Total Power**



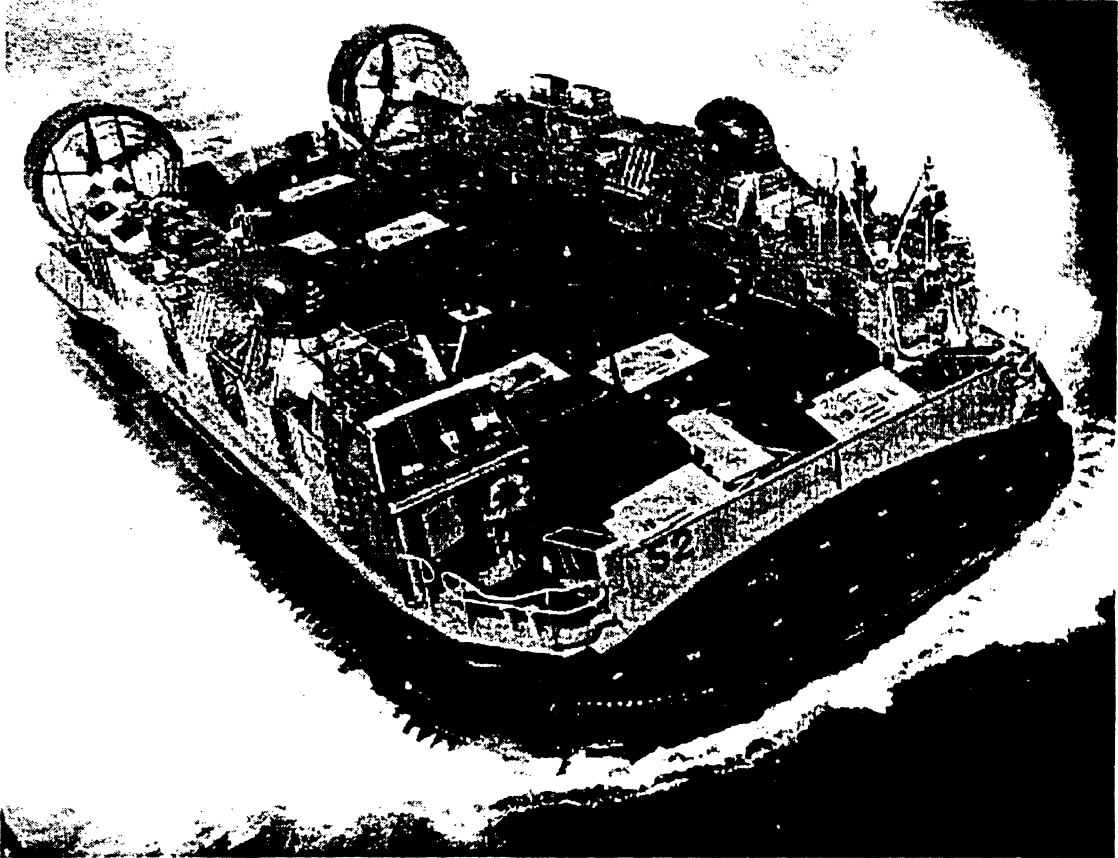
$$y = 0.269x^{0.867}$$

## APPENDIX E. CCG WABAN-AKI



(Source: Canadian Coast Guard. [http://www.vif.com/users/malina/cacts/garde\\_e.htm](http://www.vif.com/users/malina/cacts/garde_e.htm))

APPENDIX F. LCAC



(Source: LCAC. <http://www.rlhenterprises.com/hovercraft/lcac.htm>)

91-123-193